DEVELOPMENT OF A WEB GIS-BASED TSUNAMI INUNDATION MAPPING
SERVICE; A CASE STUDY FOR MARMARA SEA REGION

A THESIS SUBMITTED TO
THE GRADUATE SCHOOL OF NATURAL AND APPLIED SCIENCES OF
MIDDLE EAST TECHNICAL UNIVERSITY

BY

AYKUT AYÇA

IN PARTIAL FULFILLMENT OF THE REQUIREMENTS
FOR
THE DEGREE OF MASTER OF SCIENCE
IN
CIVIL ENGINEERING

JUNE 2012

Approval of the thesis:

DEVELOPMENT OF A WEB GIS-BASED TSUNAMI INUNDATION MAPPING SERVICE; A CASE STUDY FOR MARMARA SEA REGION

submitted by **AYKUT AYÇA** in partial fulfillment of the requirements for the degree of **Master of Science in Civil Engineering Department, Middle East Technical University** by,

Prof. Dr. Canan Özgen   _____
Dean, Graduate School of **Natural and Applied Sciences**

Prof. Dr. Güney Özcebe   _____
Head of Department, **Civil Engineering**

Prof. Dr. Ahmet Cevdet Yalçıner   _____
Supervisor, **Civil Engineering Dept., METU**

Examining Committee Members:

Prof. Dr. Ayşen Egin   _____
Civil Engineering Dept., METU

Prof. Dr. Ahmet Cevdet Yalçıner   _____
Civil Engineering Dept., METU

Assoc. Prof. Dr. Zuhal Akyürek   _____
Civil Engineering Dept., METU

Assoc. Prof. Dr. Utku Kanoğlu   _____
Engineering Sciences, METU

Dr. Işıkhan Güler   _____
Civil Engineering Dept., METU

Date: _____

I hereby declare that all information in this document has been obtained and presented in accordance with academic rules and ethical conduct. I also declare that, as required by these rules and conduct, I have fully cited and referenced all material and results that are not original to this work.

Name, Last Name: AYKUT AYÇA

Signature:

ABSTRACT

DEVELOPMENT OF A WEB GIS-BASED TSUNAMI INUNDATION MAPPING
SERVICE; A CASE STUDY FOR MARMARA SEA REGION

AYÇA, Aykut

M.Sc., Civil Engineering Department
Supervisor: Prof. Dr. Ahmet Cevdet YALÇINER

June 2012, 95 pages

Tsunamis, as the catastrophic disasters, can cause loss of live and property when they come to the shores. Preparation of emergency plans is essential to reduce the damage. Consequently, any initiative in tsunami modeling and inundation mapping is of vital importance for progressing safety surveillance and maintenance.

In an effort to achieve a thorough analysis of effect of tsunami, it is critical to estimate the geographical extent of possibly affected area and to predict tsunami impacts. The inundation mapping system also must serve to manage the simulation data in a scalable environment to reach end-users in the time of event. For this purpose, in this study, the generation of a Web based Geographic Information System (GIS) to serve inundation maps through web.

The research methodology consists of four main stages: (i) simulating tsunamis based on six different scenarios (ii) processing simulation data through a GIS application; (iii) development of web interfaces and implementation of the developed model for Web-GIS application;

(iv) verification of the created model for Marmara Sea Region. The proposed system is expected to be an efficient tool for improving inundation mapping efforts for expected tsunamis in Turkey.

ÖZ

MARMARA DENİZİ İÇİN WEB-CBS TABANLI TSUNAMİ BASKIN
HARİTALARININ HAZIRLANMASI

AYÇA, Aykut
Yüksek Lisans, İnşaat Mühendisliği
Tez Yöneticisi: Prof. Dr. Ahmet Cevdet YALÇINER

Haziran 2012, 95 sayfa

Tsunami gibi büyük deniz afetleri, kıyılara ulaştıklarında büyük miktarda can ve mal kaybına neden olabilmektedir. Ancak, hazırlanacak acil durum planları, oluşacak can ve mal kaybının azalmasında çok önemli bir yer tutmaktadır. Sonuç olarak, tsunami benzetimi ve baskın haritalarının hazırlanmasında yapılacak her yenilikçi girişim, daha sonrasında oluşturulacak eylem planları için büyük öneme sahiptir.

Olası bir tsunaminin etkilerinin araştırılmasında, etkilenmesi muhtemel alanın coğrafi sınırlarının belirlenmesi ve tsunaminin bu alana olan etkilerinin tahmin edilmesi gereklidir. Ayrıca, tsunami baskın haritalama sistemi de acil bir durum esnasında birden fazla son kullanıcıya ulaşıtırılması için ölçeklenebilir bir ortamda benzetim sonuçlarının yönetilmesine olanak sağlamalıdır. Bu çalışmada, bahsedilen hedef doğrultusunda, tsunami baskın haritaları için Web tabanlı bir Coğrafi Bilgi Sistemi (CBS) geliştirilmesi planlanmıştır.

Çalışmada izlenen yol dört ana aşamadan oluşmaktadır: (i) altı farklı olası tsunami senaryosunun benzetimlerinin yapılması; (ii) CBS ortamında elde edilen benzetim sonuçlarının işlenmesi;

(iii) web uygulamasının arayüzünün geliştirilmesi ve hazırlanan modelin Web-CBS uygulaması olarak servis edilmesi; (iv) oluşturulan modelin Marmara Denizi için doğrulanması. Önerilen sistemin, Türkiye kıyılarında yaşanabilecek olası bir tsunami için oluşrulacak baskın haritalarının hazırlanmasında etkin bir araç olması beklenmektedir.

Anahtar Kelimeler: Tsunami benzetimi, baskın haritası, Coğrafi Bilgi Sistemleri (CBS), Web-CBS, NAMI DANCE, Marmara Denizi

family and friends

ACKNOWLEDGEMENT

and lovely family, and to my little sister İpek for her constant love. Every success I acquired is their achievement.

Finally, the presence of Seda Şalap makes everything less burdensome, more amusing and bearable together with her endless motivation, patience and love not only throughout this study but also in my life.

TABLE OF CONTENTS

LIST OF FIGURES

FIGURES

LIST OF TABLES

TABLES

CHAPTER 1

INTRODUCTION

Tsunamis are the huge catastrophic events that should not be ignored. As the mostly seen tsunami type, rupture specific tsunamis possess more energy than tsunamis generated by other sources since the energy released due to rupture occurred in the sea bottom directly-transferred to the water body. These types of tsunamis can travel long distances without losing considerable energy and can cause devastating damage even in far coasts. Two recent earthquake induced tsunami events, hit Sumatra in 2004 and Japan in 2011 caused loss of thousands of lives and property, not mentioning the environmental effects.

Although, for the near future in Japan, an offshore earthquake and a following tsunami was being expected, everybody unfortunately witnessed while tsunami waves were overtopping offshore tsunami breakwaters and 10 meters high tsunami protection walls surrounding the cities, which again proved irresistible power of tsunamis. Japan tsunami underlined an important fact that preparedness does not only mean building protection structures. Even if it is not possible to save property, lives can be saved by preparing applicable emergency plans.

Production of inundation maps based on simulations of possible tsunami sources is the paramount step in preparing emergency plans. Moreover, the prepared inundation maps should be shared with public to reach multiple end-users at the same time and web technology is the best way for publishing those maps.

Tsunamis are more frequently occur at Pacific and Indian Oceans than the other parts of world. Although tsunamis are not frequent for Marmara

Sea Region, there are numerous tsunamis encountered in the region due to earthquakes or/and submarine ground failures throughout the history.

This study is aimed to produce tsunami inundation maps along Marmara Sea Region for different possible rupture specific tsunami scenarios through numerical modeling. NAMI DANCE is used as numerical tsunami modeling software and results are processed and mapped in ArcMAP 10. Subsequently, produced maps are serviced as a Web-GIS based application using ArcGIS Server 10. By the help of this application, managing data from one hand, enabling use of multiple end-users and providing most up-to-date data information are possible on the internet via a web browser. Moreover; incorporation of the information generated from the inundation maps provides geocoding of the potentially affected areas which affords policy makers an additional level of preparedness.

The following chapters define the subject in a comprehensive view. Chapter 2 is devoted to a broad literature survey about the problem statement and the provided solution methods. Chapter 3 focuses on rupture specific tsunami simulation and their results. In this chapter selected tsunami scenarios and estimated rupture parameters are given in detail. In Chapter 4 the data acquisition and pre-processing applied to produce inundation maps in ArcMAP are explained. This chapter also includes knowledge about serving these maps in web environment, and capabilities of web service. Thesis completed with chapter 5 which includes a discussion and concluding remarks and as the final section, recommendations for future studies.

CHAPTER 2

LITERATURE SURVEY

The Marmara Sea Region is the most populated region of Turkey with more than 20 million settled people according to the 2009 census. Seven of eleven cities in this region, including Istanbul, have coasts to the Marmara Sea and the settlement at the coastline is high. In addition, Marmara Region has an important role on Turkish economy. In the fields of industry, trade and agriculture it has the leading position in Turkey. Especially, Kocaeli and Istanbul possess many commercial ports. Besides economic features, Istanbul has an invaluable cultural heritage from different eras, and some of them are located in the coastal areas. Marmara Sea Region is located in a tectonically active zone and catastrophic events like earthquakes or earthquake induced tsunamis that may be occurred in the Marmara Sea basin could cause a great economic and cultural impact in the region and in the country.

To understand the tectonic characteristics and tsunami risk of the Marmara Sea Basin, historical tectonic and tsunami records, earthquake and tsunami catalogues and past tsunami modeling studies are reviewed and summarized below. Moreover, inundation mapping based on Web-based Geographic Information Systems (GIS) are discussed by considering the previously accomplished studies.

2.1 Historical Tsunamis in the Sea of Marmara

Turkey is surrounded by seas and there are many active fault zones around. Throughout the history several tsunamis have occurred and damaged Turkish coasts (Figure 2.1).
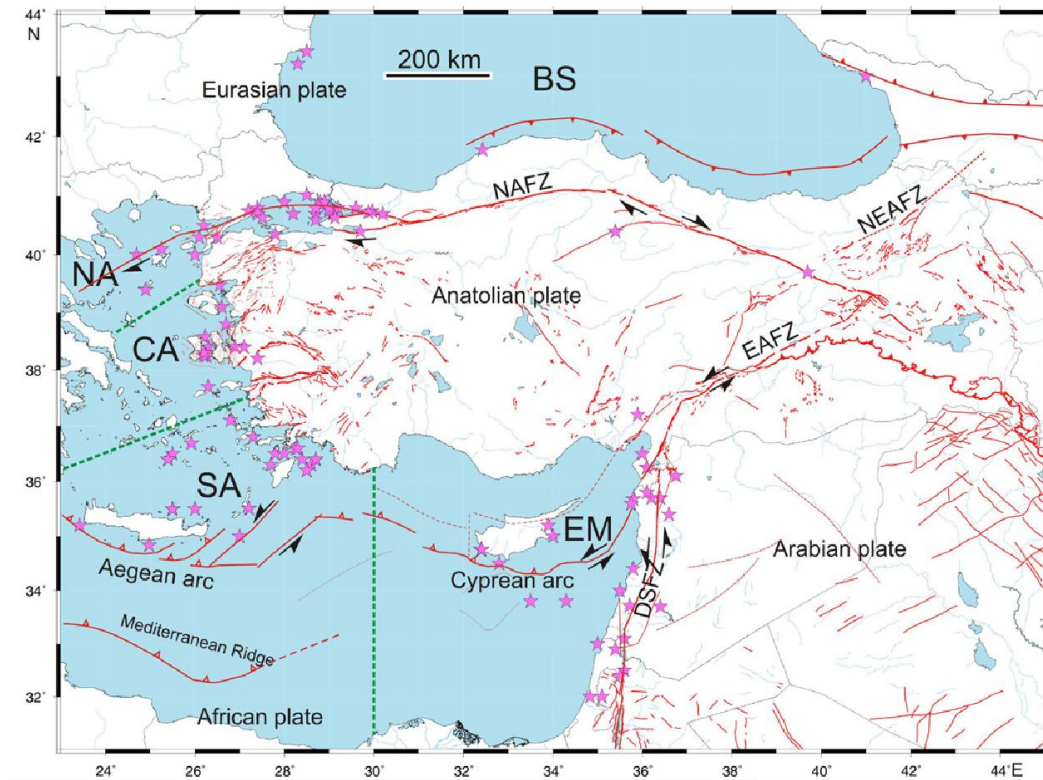
Figure 2.1 The fault systems affecting Turkey and Stars Showing Source Locations of Tsunamis in Altinok's Catalogue (2011)

Especially (specifically), Marmara Sea basin is under the influence of western part of North Anatolian Fault (NAF), which is a major strike-slip fault; forms the boundary between Arabian and Eurasian plates. The crash of these plates, initiates a right-lateral motion of NAF. (Barka & Kandinsky-Cade, 1988). The Arabian Plate drives the Anatolian Plate towards the west with a rate of approximately 24mm/yr. (Straub, Kahle, & Schindler, 1997).

During the 20th century, due to the stress accumulation, NAF system is one of the most seismically active zones in the world. From 1912 to 1999, in the Marmara Sea Basin 9 big earthquakes with Ms > 6.5 have occurred (Ambraseys, 2002). All of these earthquakes including destructive August 1999 Kocaeli earthquake, showed the same kind of

right-lateral strike-slip faulting. The region seismically active throughout the history experienced 31 earthquakes with Ms >7.0, and 55 earthquakes with Ms >6.5 occurred between the years 0 – 1900 (Table 2.1) (Ambraseys, 2002).

Table 2.1 Earthquakes occurred between 0-1900 effected Marmara Sea Region after Ambraseys, 2002

| | Year | Latitude | Longitude | Ms | General Effects | | | | | | | | | | Region |
					1	2	3	4	5	6	7	8	9	10	
1	32	40.5	30.5	7	1	4	2	2	2	0	2	2	0	0	Nicaea
2	68	40.7	30	7.2	1	4	2	2	2	0	2	2	0	0	Nicaea
3	121	40.5	30.1	7.4	1	3	4	3	3	2	2	0	0	0	Nicomedia
4	123	40.3	27.7	7	1	3	1	2	2	0	0	0	0	0	Cyzicus
5	160	40	27.5	7.1	1	3	6	3	2	0	2	2	2	0	Hellespont
6	180	40.6	30.6	7.3	1	4	2	2	3	0	2	0	0	0	Nicomedia
7	268	40.7	29.9	7.3	1	3	3	3	3	0	2	0	0	0	Nicomedia
8	358	40.7	30.2	7.4	1	3	6	3	3	3	2	2	2	2	Izmit
9	362	40.7	30.2	6.8	1	4	3	2	2	0	1	1	0	0	Izmit
10	368	40.5	30.5	6.8	1	4	2	2	2	0	2	1	0	0	Persis
11	368	40.1	27.8	6.8	1	4	1	2	2	0	0	0	0	0	Germe
12	407	40.9	28.7	6.8	2	4	2	2	1	0	1	1	0	0	Hebdomon
13	437	40.8	28.5	6.8	3	4	1	2	1	1	1	1	0	0	Istanbul
14	447	40.7	30.3	7.2	1	3	5	3	3	3	2	2	2	2	Nicomedia
15	460	40.1	27.6	6.9	1	4	3	4	2	2	2	2	2	0	Cyzicus
16	478	40.7	29.8	7.3	2	3	5	3	3	3	2	2	0	1	Helenopolis
17	484	40.5	26.6	7.2	1	3	8	3	3	2	2	2	2	0	Callipolis
18	554	40.7	29.8	6.9	2	4	4	2	2	2	2	1	2	0	Nicomedia
19	557	40.9	28.3	6.9	2	4	3	2	2	2	1	1	0	0	Silivri
20	740	40.7	28.7	7.1	3	4	5	2	3	2	2	2	0	2	Marmara
0	823	0	0	0	0	0	0	0	0	0	0	0	0	0	Panium
21	860	40.8	28.5	6.8	3	4	2	2	1	1	2	1	0	0	Marmara
22	869	40.8	29	7	2	4	1	2	2	1	2	2	0	0	CP

Table 2.1 (Cont'd) Earthquakes occurred between 0-1900 effected Marmara Sea Region after Ambraseys, 2002

| | Year | Latitude | Longitude | Ms | General Effects | | | | | | | | | | Region |
					1	2	3	4	5	6	7	8	9	10	
23	967	40.7	31.5	7.2	1	3	4	3	3	3	2	2	0	0	Bolu
24	989	40.8	28.7	7.2	3	4	3	2	2	2	2	0	0	1	Marmara
25	1063	40.8	27.4	7.4	1	3	5	3	3	3	2	2	0	0	Panio
26	1065	40.4	30	6.8	1	4	2	2	1	0	1	1	0	0	Nicaea
27	1296	40.5	30.5	7	1	4	2	2	2	1	2	2	0	0	Bithynia
28	1343	40.7	27.1	6.9	1	3	6	3	2	2	1	1	0	0	Ganos
29	1343	40.9	28	7	2	4	3	2	2	1	2	0	0	1	Heraclea
30	1354	40.7	27	7.4	1	2	7	3	3	3	2	2	1	0	Hexamili
31	1419	40.4	29.3	7.2	1	4	3	2	3	2	2	0	2	0	Bursa
0	1489	0	0	0	0	0	0	0	0	0	0	0	0	0	Saros?
32	1509	40.9	28.7	7.2	2	2	15	2	2	3	1	2	2	2	CP
33	1556	40.6	28	7.1	1	3	3	3	3	2	0	2	0	0	Gonen
34	1625	40.3	26	7.1	3	4	5	3	0	0	0	2	0	0	Saros
35	1659	40.5	26.4	7.2	2	4	5	2	0	0	0	2	0	0	Saros
36	1672	39.5	26	7	2	4	3	2	2	0	0	2	0	0	Biga
37	1719	40.7	29.8	7.4	1	2	17	3	3	3	2	2	2	0	Izmit
38	1737	40	27	7	1	3	19	3	3	0	1	2	2	0	Biga
39	1752	41.5	26.7	6.8	1	3	17	3	2	2	2	2	2	0	Edirne
40	1754	40.8	29.2	6.8	2	3	9	3	2	2	2	2	0	2	Izmit
41	1766	40.8	29	7.1	2	3	16	2	3	2	2	2	0	1	Marmara
42	1766	40.6	27	7.4	1	2	20	3	3	3	2	2	2	0	Gonas
43	1855	40.1	28.6	7.1	1	2	24	3	3	1	1	2	2	0	Bursa
44	1859	40.3	26.1	6.8	2	3	25	3	1	2	1	2	2	2	Saros
45	1893	40.5	26.2	6.9	2	3	31	3	2	1	1	2	0	1	Saros
46	1894	40.7	29.6	7.3	2	2	81	1	3	3	2	2	2	2	Izmit
47	1912	40.7	27.2	7.3	1	2	99	1	2	2	2	2	1	2	Ganos
48	1912	40.7	27	6.8	1	3	32	1	2	1	1	2	2	0	Ganos
49	1944	39.5	26.5	6.8	2	2	67	1	1	1	1	1	2	0	Edremit
50	1953	40.1	27.4	7.1	1	2	45	1	2	2	2	2	1	0	Gonen

Table 2.1 (Cont'd) Earthquakes occurred between 0-1900 affected Marmara Sea Region after Ambraseys, 2002

| | Year | Latitude | Longitude | Ms | General Effects | | | | | | | | | | Region |
					1	2	3	4	5	6	7	8	9	10	
51	1957	40.7	31	7.1	1	2	81	1	2	2	2	2	1	0	Abant
52	1964	40.1	28.2	6.8	1	2	70	1	1	1	1	1	1	0	Manyas
53	1967	40.7	30.7	7.2	1	2	99	1	3	2	2	2	1	0	Mudurnu
54	1999	40.7	30	7.4	1	1	0	1	3	3	2	2	1	1	Izmit
55	1999	40.8	31.2	7.1	1	1	0	1	2	2	2	1	1	0	Duzce

1, Location: 1, on land; 2, offshore; 3, at sea. **2,** Epicentral region: 1, instrumental; 2, well-defined macroseismic; 3, less well defined; 4, adopted. **3,** Number of sites used. **4,** Magnitude: 1, instrumental; 2, macroseismic Ms _ 0.5; macroseismic _ 0.35. **5,** Maximum effects: 1, considerable damage; 2, heavy damage; 3, destructive, extensive reconstruction, with social and economic repercussions. **6,** Loss of life: 1, small; 2, significant; 3, great. **7,** Extent of damage: 1, local; 2, widespread. **8,** Felt area: 1, small; 2, large. **9,** Ground effects: 1, surface faulting; 2, ground failures and landslides. **10,** Seismic sea waves: 1, damaging; 2, observed.

Herbert et al. (2005) and Altinok et al. (2001) state that the probability of an offshore earthquake in the Marmara Sea is increased when the westward movement of seismic ruptures and 1999 Kocaeli earthquake are considered together. Parsons et al. (2000) draws attention to increase in stress on underwater faults after 1999 Kocaeli shock and calculates the probability of an underwater earthquake as 62 ± 15%. When the tectonic history of the region is taken into account together with the recent researches, the occurrence of a tsunami following an underwater earthquake in the Marmara Sea is possible.

The most recent tsunami catalogue for Turkish Coasts has been prepared by Altinok et al. (2011). In this study, all the available past catalogues and documents were traced and re-evaluated based on the guidelines defined in GITEC (Genesis and Impact of Tsunamis on the European Coasts) and TRANSFER (Tsunami Risk And Strategies For the European Region) projects.

According to this catalogue, from 17th century BC to 1999, 35 tsunamis have been occurred in the Marmara Sea. Locations of some of the remarkable tsunamis in Marmara Sea are given below in Figure 2.2.
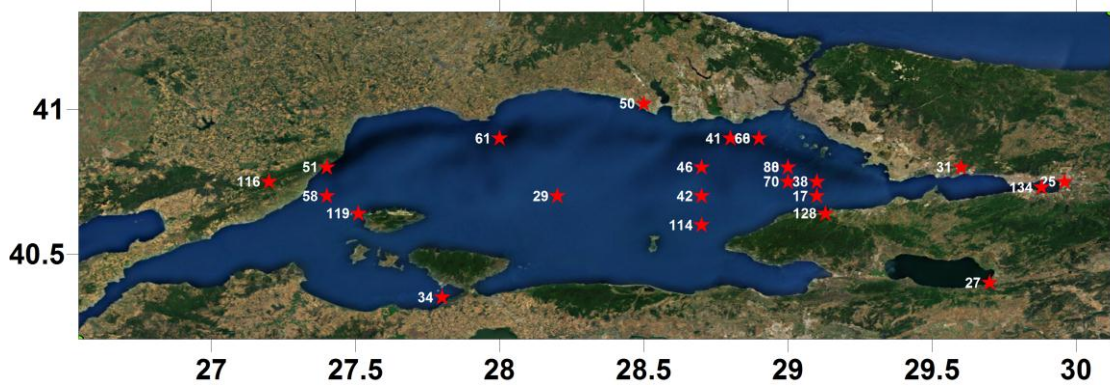
Figure 2.2 Locations of Tsunamigenic Events Occurred in Marmara Sea Region (Redrawn from Altinok, 2011)

After the earthquake in the Marmara Sea with a magnitude of around 7.5 in Sep, 10, 1509, a tsunami was triggered. The waves overtopped the city walls of Istanbul and inundated the land. Archeological researches in Yenikapi reveals that sea penetrated 500-600 meters inland in this region (Altinok et al., 2011). In Izmit castle walls damaged, shipyard collapsed and city was inundated. The maximum wave height is thought to be more than 6 meters (Oztin and Bayulke, 1991).

Another tsunami that effected Istanbul and Izmit was occurred in July, 10, 1894 following the earthquake with Ms=7.3 (Altinok et al., 2011). At the coasts of Istanbul from B.Cekmece to Kartal, maximum 200 meters of water penetration observed. Run-up height at the Istanbul coasts occurred around 2.5 meters (Yalciner et al., 2002)**.**

In August, 9, 1912 an earthquake with Ms = 7.3 occurred near Murefte on Ganos Fault. Approximately 2000 of people died and hundreds of villages damaged (Altinok et al., 2003). According to the past documents yachts, ships and the fishery boats at the bosphorus and Istanbul Coasts damaged because of sea disturbances. In Istanbul, sea level rised up to 3 meters after recedence (Altinok et al., 2003).

An earthquake in August, 17, 1999 of magnitude Mw = 7.4 occurred on the northern strand of the NAF (Altinok, 2001). Vertical displacements up to 3 meters have been observed during detailed field surveys. The international tsunami survey team investigated the area and talked with witnesses. According to their studies, the wave run-up heights measured up to 2.5 meters along the north coast from Tütünçiftlik and Hereke and up to 2.9 meters at Degirmendere and lower values from Degirmendere to Karamursel (Yalciner et al., 2002). More than 300 meters of inundation happened in Kavakli (Altinok et al., 2011).

2.2 Past Attempts of Tsunami Modeling for the Sea of Marmara

Alpar et. al. (2001) and Yalciner et. al. (2002) utilized the model TWO_LAYER, which was created by Tohoku University Disaster Control Research Centre in Japan, for their studies. In this model the non-linear long wave equations are solved by using the finite difference method and the leap-frog solution procedure for two interfacing layers; the water body in the sea and the moving mass at the sea bottom.

Alpar et. al. (2001), as a case study, a scenario of underwater landslides is assumed to occur at the southeast part of Cinarcik Basin, offshore the towns of Yalova and Cinarcik. The results of the simulation; arrival time of tsunami waves are less than 5 min to southeastern coasts and around 10 min to northern coasts. Flow depth on land will exceed 3 m along approximately 15 km of coastline of the northern and southern shores.

Yalciner et. al. (2002) simulates two landslide and one earthquake induced tsunami scenarios. According to the results of these simulations,

the waves reach the near coasts at approximately 5 min and depending on the source and coastal topography 3-6 m of wave heights occur near the shore.

Herbert et. al. (2005) models different scenarios by solving Equation 2.1; conservation of mass and Equation 2.2; conservation of momentum in spherical coordinates using finite difference method with centering in time and using an upwind scheme in space (Heinrich et al., 1998; Hebert et al., 2001a,b).

$$\frac{\partial(\eta+h)}{\partial t} + \nabla\left[\mathbf{v}\left(\eta + h\right)\right] = 0 \qquad \text{(Eqn. 2. 1)}$$

$$\frac{\partial(\mathbf{v})}{\partial t} + \left(\mathbf{v}\,\nabla\right)\mathbf{v} = -g\nabla\eta + \sum \mathbf{f} \qquad \text{(Eqn. 2. 2)}$$

They simulate an earthquake that may be occurred in the Eastern Marmara, Cinarcik Basin, for different rake angles. The maximum waves along the coastline ranges between 0.5 – 1 m for rake angles of 180° and 150°, whereas they reach up to 2 m for rake angles of 120° and 90°. Another scenario is an earthquake in the Western Marmara covering Tekirdag and Central Basins. In this case rake angles differ from 120° to 180°. The maximum waves along the coastline ranges between 0.8 – 1 m for rake angle of 120°. Finally they consider the rupture of whole seismic gap with rake angles 120° - 150° and 150° - 180°. The maximum wave heights vary between 0.5 – 2 m.

2.3 Geographic Information Systems (GIS) and Tsunami Inundation Mapping

A geographic information system (GIS) is a powerful and integrated tool for storing, manipulating, visualizing, and analyzing spatial data. Source data coming from different case scenarios, like tsunami simulation in this study, can be represented as points, lines and polygons in layers with its

attribute data. GIS has the capability of combining several layers in an intelligent map which enables end users to conduct further analysis based on these layers.

Tsunami inundation mapping is aiming at assessing the geographical extent of the tsunami affected area, the intensity of the tsunami impact and the probability of the occurrence (Strunz et al, 2011)

As stated in Strunz et al's study, tsunami inundation mapping consists of five steps:

- Identification of the possible tsunami resources
- Modeling of the tsunami propagation and its inundation on land
- Determination of physical parameters of the inundation (e.g. inundation maximum, run-up height)
- Analysis of the probabilities or return periods of the tsunami events
- Presentation of the results through hazard maps

To accomplish these steps, an information system which is attached to spatial information can be used to guide and monitor land use, delineate transportation routes for potential evacuations, and re-delineate hazard zones based on new knowledge or changes in the natural or human use systems (Greene, 2002).

2.4.1 Advantages of Web - Based Geographic Information Systems

The integration of web technology with GIS has begun during 1990s which enabled distributed and non-expert users to use the power of spatial technology. Several GIS applications have been modified from desktop GIS to Web-based GIS up to date. (Plewe, 1997; Tang and Selwood, 2003; Chang and Park 2004). This change was initiated by the advantages of Web- based GIS over Desktop GIS. The unlimited number of accessible users and scalability are the key forces which drive the usage of web-based applications.

Web-based GIS can support unlimited end-users therefore increase the number of people especially in the decision making process. According to Evans et al. (2004) participants can explore digital maps, reason spatially and express opinions about the problems. This can be applied to the tsunami case scenarios as well. People can see the vulnerability of their houses, be informed about the evacuation areas in case of emergency.

Web-Based application platforms are scalable so that systems can either be deployed on a single machine or can be distributed across multiple servers for supporting enterprise applications (ESRI). Although in its first desktop examples, GIS was mostly centralized and used by professional end user, web technology turned GIS into an open and easily accessible tool for everyone (Dragicevic, 2004). Application done in web environment can be easily accessed by anywhere and anytime. These advantages are the results of efficiently distributed required resources and system of application on the network of web-based systems. Performance and reliability problems are also solved by these advantages. Thus, useful data and information sharing is achieved through the web (Chang and Park, 2004).

The trend from desktop to web also has been introduced in the field of disaster management and risk analysis for catastrophic events like tsunamis (Yang et al,2007). Especially in case of emergency and risk mitigation, Web-based GIS has the power to reach much more people in a very short time. The characteristics of Web-Based GIS such as strong adaptability, wide application, sharing information, powerful real-time performance, easy to use, easy to maintenance are particularly important to the tsunami risk analysis which have attributes of inundation and arrival time of the first and maximum waves.

2.4.2 Use of Web-Based GIS in Tsunami Inundation Mapping

The GIS is well suited for locating the impact of inundation zones, its capability to manage and analyze data from different sources, can be used to perform "what if" scenarios which can be used to evaluate the effects of different planning policies, model impacts of disasters, and suggest mitigation strategies.

GIS and Remote Sensing (RS) technologies are used for detecting tsunami vulnerability areas after the event (Leone et al, 2011), tsunami tracing (Japan Tsunami Trace Database), tsunami risk assessment (Strunz et al, 2011).

In Leone et al's study, main aim is to detect the structural damages by using satellite images and for this purpose every building has been coded depending on its vulnerability and level of damage. This data has been processed in GIS environment to establish magnitude criteria.

In Japan, Tsunami Trace Database is served through their website and available worldwide (Japan Tsunami Trace Database). By using the Japan Tsunami Trace database, users examine vulnerable areas, confidence level and pattern of inundation (Figure 2.3).
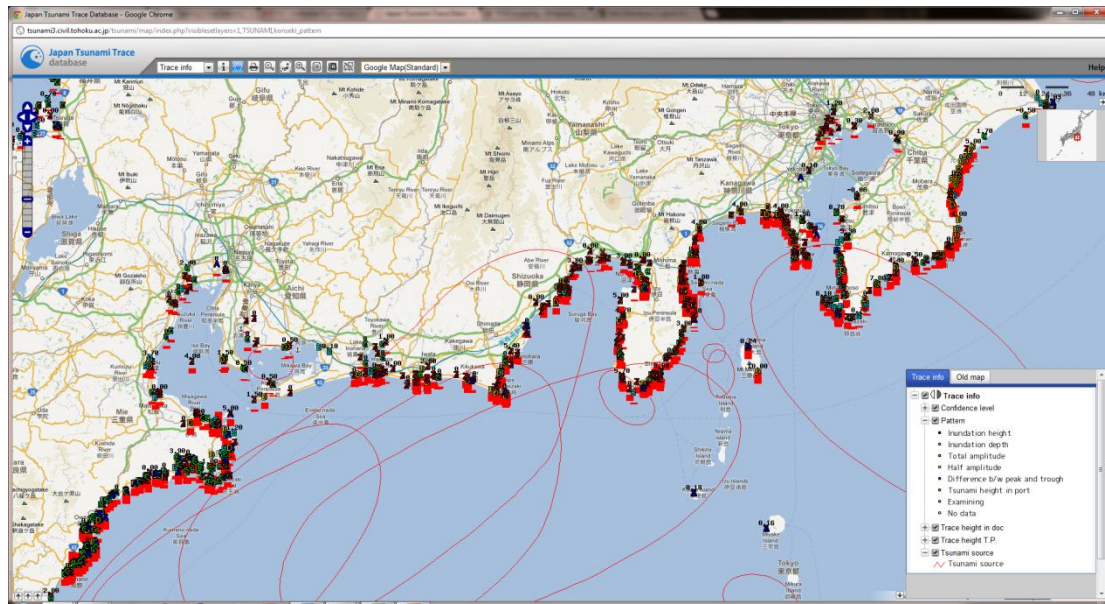
Figure 2.3 Japan Tsunami Trace Database Screenshot (Japan Tsunami Trace Database)

Tsunami risk assessment for Indonesia has been carried out in Strunz et al's research which is based on a mutli-scenario approach for tsunami hazard mapping. The approach integrates pre-calculated tsunami modeling scenarios and takes into account the probabilities of the different scenarios (Figure 2.4).

Figure 2.4 Tsunami Risk Assessment for Indonesia (Strunz et. al., 2011)

2.4 GIS Based Tsunami Risk Analysis in Turkey

So far, no comprehensive GIS based risk assessments have been undertaken that could guide the setting of priorities in national level. Although, there are some efforts to determine or to forecast the inundation distances, in Marmara Sea Region, none of them integrates use of GIS. Alpar et al, (2003) performs tsunami analysis and determines the extent of inundation by Digital Terrain Modeling.

For Turkey, Dilmen (2009), in her MSc thesis, produced GIS based tsunami inundation maps for Fethiye. Salap et. al (2011), conduct a GIS based tsunami risk assessment study for Gocek. In the case of Marmara Sea Region, there are no conducted studies to make GIS based hazard assessments.

A comprehensive literature review has been done in order to gain an overview of research initiatives in Tsunami formation, source characteristics and Inundation mapping by using GIS capabilities. As mentioned above there are several researches which integrates GIS tools in tsunami inundation mapping. However, all these examples are conducted on experienced disasters. This study aims; preparation of Web-GIS based tsunami inundation maps for Marmara Sea Region considering the possible earthquake induced tsunami scenarios. Up to date, this research will be first initiative integrating Web-GIS and tsunami modeling for Turkey.

CHAPTER 3

ESTIMATION OF TSUNAMI SOURCES AND SIMULATIONS

In this chapter, active faults in Marmara Sea region are studied in detail and their rupture parameters are obtained. Bathymetric data used in the simulations are gathered, processed and enhanced to obtain accurate results. Finally, tsunami modeling studies are performed and their results are shown.

Even though still the fundamental knowledge and information are insufficient, a comprehensive approach to tsunami analysis for Marmara Sea has been conducted by simulating earthquake induced tsunamis

3.1 Active Faults and Estimation of Source Parameters

Historically many tsunamis caused by the earthquakes and earthquake triggered submarine landslides have occurred in the Marmara Sea. Coastal cities of the region suffered damages by the tsunami waves repeatedly. The main causes for the tsunami sources occurred in Marmara Sea region are considered as the followings:

- The displacement and deformation of the sea floor by faulting rupture.
- Submarine landslides.

In this study only earthquake triggered tsunami scenarios have been modeled for the study domain. The boundaries of the study domain are given in Table 3.1 and Figure 3.1.

The sources of tsunamis by faulting ruptures are discussed below. For the tsunami simulation, the location of the fault rupture by the earthquake,

the amount of displacement, and the vector of displacement must be estimated.

Table 3.1 Boundaries of study domain

Spatial Reference	GCS_WGS 84	
Longitude	26.539544	30.120357
Latitude	40.20628	41.336956
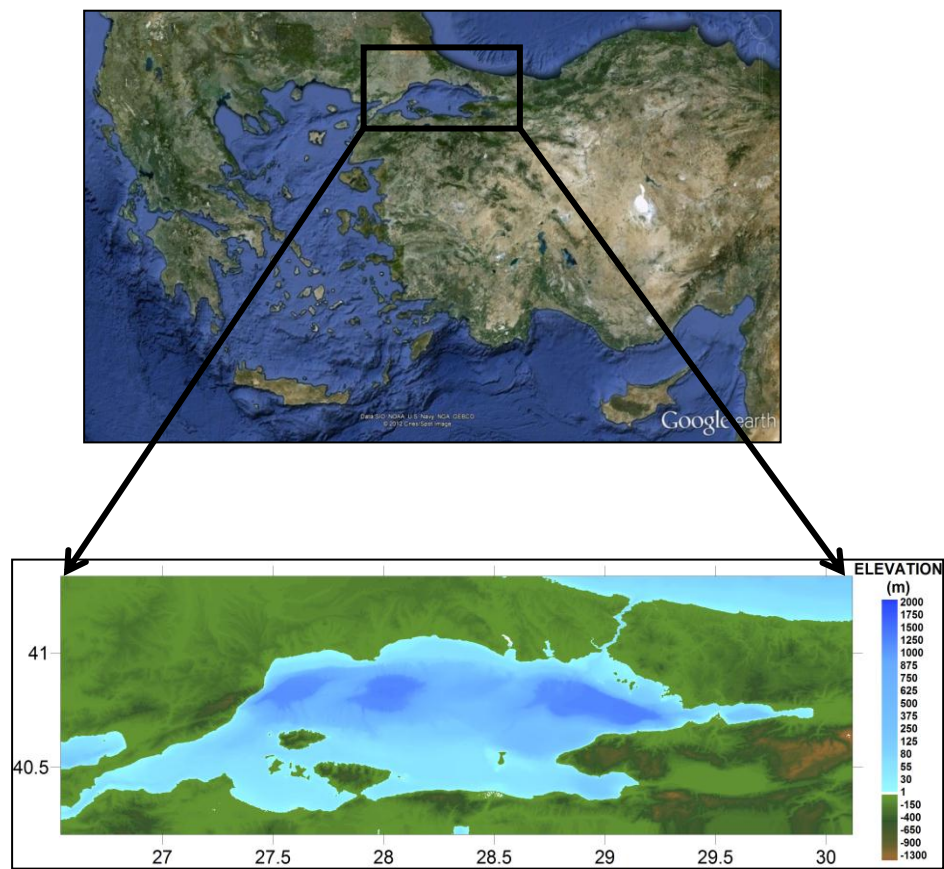
Figure 3.1 Study Domain and Bathymetry

3.1.1 Geological Characteristics of the Marmara Sea

In the northern part of the Marmara Sea, a trough extends from east to west. Along this trough, there are three deep basins called Cinarcik, Central, and Tekirdag basins where maximum depth is more than 1200 m (Yalciner et al., 2002). In addition, there are two highs between these basin; Central and Western Highs.

At the eastern and western end of this trough, Izmit and Ganos faults are located respectively. Macroscopically, it is considered that the Marmara Sea is a pull-apart basin formed by the extensional step-over between these right-lateral faults (Armijo et al., 2005, Figure 3.2). Moreover, the faulting topography showing the various type of fault (right-lateral fault, normal fault and reverse fault) is observed in the sea floor.
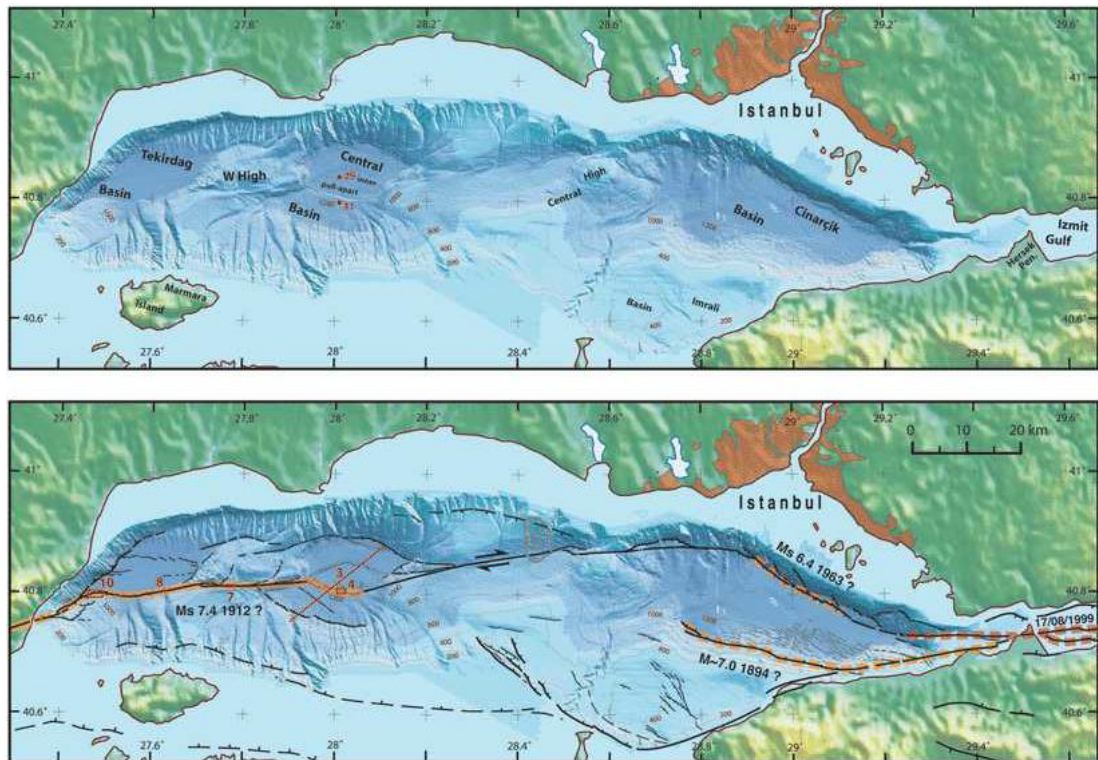
Figure 3.2 The North Anatolian Fault in Marmara Sea (Armijo et al, 2005 and OYO – IMM, 2007)

The extensional step-over between the Izmit and Prince's Islands faults formed the Cinarcik Basin. At the northeastern edge of this basin, Izmit and Prince's Island faults are bonded by a normal fault with a northwest trend.

The Central Basin is surrounded by normal faults along its edges, having a double structure. The young inner basin, which is formed due to the extensional step-over between Prince's Islands and the Ganos faults, is covered by the older one while the older outer basin is bounded by the continental shelf slopes.

Unlike Cinarcik and Central basins, Tekirdag basin does not have a step-over structure. However, the Ganos fault is thru the southern edge of the basin. It is estimated that Ganos fault has a right-lateral characteristics, but there is a normal fault portion at the north side and a reverse fault at the southwest.

Since the western part of the Central High and the Western High prolong straight through the narrow valleys, it can be estimated that the faults in these highs are pure right-lateral faults.

Therefore, as a whole, NAF in the Marmara Sea shows a right-lateral fault having various features according to the tectonics. During the modeling studies, the features of faults in the Marmara Sea should be carefully considered.

3.1.2 Estimation of Probable Tsunami Source Mechanisms for the Marmara Sea

Tsunami source is the area where the initial tsunami wave originated, generally a submarine earthquake, a landslide or any other impulse that can cause rapid displacement of large body of water.

For an earthquake induced tsunami following parameters are used to define the initial tsunami wave;

❖ epicenter

❖ width and length of the fault plane

❖ dip, rake, and strike angles

❖ focal depth

❖ vertical displacement of fault

In this thesis, the sources' parameters are taken from OYO – IMM Report (2007) (Figure 3.3). The critical active faults selected for this study are Princes' Island (PI) fault (strike slip and normal), Ganos (GA) fault, Yalova (YAN) fault (normal) and Central Marmara (CMN) fault (normal). These sources and their parameters are given in Table 3.2.

Table 3.2 Fault Parameters

Fault	Type	Lat_ED50	Lon_ED50	depth from sea bottom	strike	dip	rake	length	width	Displacements in this Study	Displacements in OYO-IMM Report
		degree	degree	m, GL-	degree	degree	degree	m	m	m	m
PI	Right-Lateral	29,47313	40,72793	1968	84,44	90,00	180,00	4717	16000	0,00	0,00
		29,23572	40,73309	946	92,06	90,00	180,00	20066	16000	0,00	0,00
		29,22818	40,73306	805	90,20	90,00	180,00	636	16000	0,00	0,00
	Oblique-Normal	29,12942	40,75691	744	108,15	70,00	195,00	8753	17027	5,00	1,67
		29,06928	40,78610	740	123,15	70,00	195,00	6024	17027	5,00	1,67
		28,99465	40,81653	779	118,85	70,00	195,00	7148	17027	5,00	1,67
		28,90432	40,87251	1210	129,90	70,00	195,00	9834	17027	5,00	1,67
	Oblique-Normal	28,87843	40,87376	1023	94,37	70,00	195,00	2187	17027	5,00	1,67
		28,75089	40,88033	1017	94,66	70,00	195,00	10777	17027	5,00	1,67
		28,70595	40,87843	1131	87,64	70,00	195,00	3795	17027	5,00	1,67
		28,64466	40,87328	1431	84,56	70,00	195,00	5199	17027	5,00	1,67
		28,56006	40,86971	1445	87,73	70,00	195,00	7144	17027	5,00	1,67
	Right-Lateral	28,51766	40,87301	1186	96,80	90,00	180,00	3593	16000	0,00	0,00
		28,47160	40,87298	1219	90,93	90,00	180,00	3884	16000	0,00	0,00
		28,41844	40,86580	1254	80,93	90,00	180,00	4553	16000	0,00	0,00
		28,26801	40,84761	1364	82,03	90,00	180,00	12847	16000	0,00	0,00
		28,06159	40,80420	804	75,73	90,00	180,00	18074	16000	0,00	0,00

22

Table 3.2 (Cont'd) Fault Parameters

Fault	Type	Lat_ED50	Lon_ED50	depth from sea bottom	strike	dip	rake	length	width	Displacements in this study	Displacements in OYO-IMM Report
		degree	degree	m, GL-	degree	degree	degree	m	m	m	m
GA	Oblique-Normal	28,06159	40,80420	804	263,30	70,00	195,00	2143	17027	5,00	1,67
		28,03644	40,80152	775	286,31	70,00	195,00	8664	17027	5,00	1,67
	Right-Lateral	27,93729	40,82170	818	266,61	90,00	180,00	9516	16000	0,00	0,00
		27,82494	40,81458	1197	271,96	90,00	180,00	10494	16000	0,00	0,00
	Oblique-Normal	27,70062	40,81540	1226	260,87	70,00	195,00	12441	17027	5,00	1,67
		27,55582	40,79464	874	278,58	70,00	195,00	5660	17027	5,00	1,67
	Oblique-Reverse	27,48929	40,80081	880	258,14	70,00	165,00	3046	17027	5,00	1,67
		27,45422	40,79441	891	238,95	70,00	165,00	6945	17027	5,00	1,67
	Right-Lateral	27,38506	40,76061	1807	257,18	90,00	180,00	4517	16000	0,00	0,00
YAN	Oblique-Normal	29,47103	40,72115	1978	257,96	70,00	195,00	7058	17027	5,00	1,67
		29,38946	40,70750	1960	261,14	70,00	195,00	6873	17027	5,00	1,67
		29,30920	40,69751	1823	260,98	70,00	195,00	10952	17027	5,00	1,67
	Normal	29,18143	40,68121	1681	262,35	70,00	270,00	4448	17027	5,00	3,00
		29,12936	40,67550	1557	273,96	70,00	270,00	4562	17027	5,00	3,00
		29,07551	40,67791	1252	283,78	70,00	270,00	10021	17027	5,00	3,00
		28,96007	40,69843	1219	294,84	70,00	270,00	3154	17027	5,00	3,00
		28,92602	40,71005	1178	284,90	70,00	270,00	14043	17027	5,00	3,00

Table 3.2 Cont'd Fault Parameters

Fault	Type	Lat_ED50	Lon_ED50	depth from sea bottom	strike	dip	rake	length	width	Displacements in this study	Displacements in OYO-IMM Report
		degree	degree	m, GL-	degree	degree	degree	m	m	m	m
PIN	Normal	29,12942	40,75691	744	108,15	70,00	270,00	8753	17027	5,00	3,00
		29,06928	40,78610	740	123,15	70,00	270,00	6024	17027	5,00	3,00
		28,99465	40,81653	779	118,85	70,00	270,00	7148	17027	5,00	3,00
		28,90432	40,87251	1210	129,90	70,00	270,00	9834	17027	5,00	3,00
CMN	Normal	28,19394	40,61261	1924	276,59	70,00	270,00	9505	17027	5,00	2,00
		28,08215	40,62063	1922	279,18	70,00	270,00	7069	17027	5,00	2,00
		27,99943	40,62938	1917	299,07	70,00	270,00	10705	17027	5,00	2,00
		27,88744	40,67421	1598	283,92	70,00	270,00	7850	17027	5,00	2,00
		27,79683	40,68952	1637	291,38	70,00	270,00	7269	17027	5,00	2,00
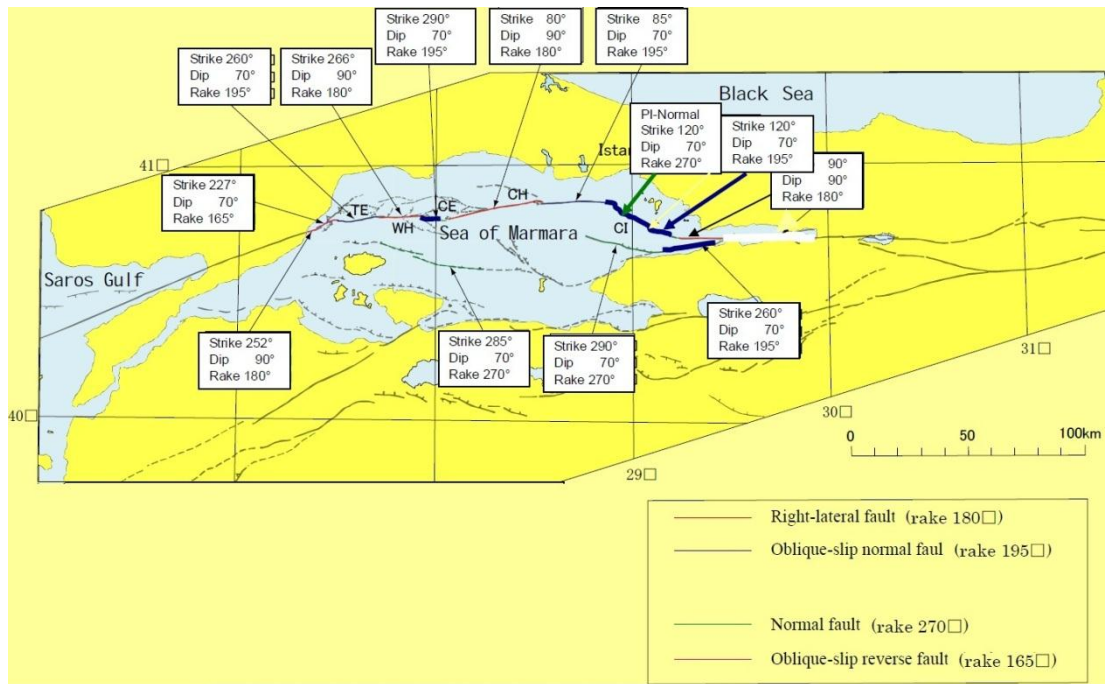
Figure 3.3 Selected Tsunami Sources (OYO-IMM Report, 2007)

In OYO – IMM report, the vertical displacements were selected as 1.67 m for oblique segments and 2 -3 m for normal segments according to the surface deformation investigations (Table 3.2). However, uncertainty in estimating these parameters may affect the results and according decisions. For example, in 2011 Great East Japan Tsunami, vertical displacement occurred almost was twice the expected. Therefore, in this study, to obtain the maximum extent of tsunami inundation, vertical displacements are selected as 5m.

3.2 Tsunami Simulations for Marmara Sea Region

The tsunami simulations can model tsunami generation, propagation, coastal amplification and inundation and the simulation results can be visualized. The accurate and reliable applications in tsunami simulation need tsunami model, which was validated and verified with high

resolution reliable tsunamigenic data (tsunami source parameters) and accurate bathymetric - topographic data.

Even though still the fundamental knowledge and information on rupture characteristics based on limited data, a comprehensive and partly conservative approach is necessary in determination of rupture parameters as input. While selecting input parameters for tsunami simulations this approach is followed.

Tsunami numerical code Nami Dance is used in simulations.

3.2.1 Tsunami Numerical Modeling Code NAMI DANCE

Tsunami numerical models generally solve similar equations; however approach to the problem with different techniques. The main equations in tsunami numerical modeling are non-linear form of shallow water equations with friction term which requires less computer memory decreases computation duration. Moreover, it provides the results in acceptable error limit. The non-linear shallow water equations are given below;

$$\frac{\partial \eta}{\partial t} + \frac{\partial M}{\partial x} + \frac{\partial N}{\partial y} = 0$$

$$\frac{\partial M}{\partial t} + \frac{\partial}{\partial x}\left(\frac{M^2}{D}\right) + \frac{\partial}{\partial y}\left(\frac{MN}{D}\right) + gD\frac{\partial \eta}{\partial x} + \frac{k}{2gD^2}\, M\sqrt{(M^2 + N^2)} = 0$$

$$\frac{\partial N}{\partial t} + \frac{\partial}{\partial x}\left(\frac{MN}{D}\right) + \frac{\partial}{\partial y}\left(\frac{N^2}{D}\right) + gD\frac{\partial \eta}{\partial y} + \frac{k}{2gD^2}\, N\sqrt{(M^2 + N^2)} = 0$$

Where;

η = water surface fluctuation

M and N = discharge fluxes in X and Y directions

D = total water depth

h = undisturbed basin

k = bottom friction coefficient

In this study, the computational tool NAMI DANCE is used in numerical modeling based on the solution of nonlinear form of the long wave equations with respect to related initial and boundary conditions (ESRI Online Help). It was developed by Zaytsev, Yalciner, Pelinovsky, Chernov in C++ programming language by following leap frog scheme numerical solution procedures of Shuto et al., 1990.

3.2.2 Simulations of Co-Seismic Tsunamis in the Sea of Marmara

The simulations are performed using seismic sources. The tsunami source (initial form of tsunami wave) is assumed to be the similar as the sea bottom deformation which is computed by using the relations given in Okada, (1985) by using the rupture parameters. The tsunami sources of selected scenarios used in this study are computed by the code NAMI DANCE by following the similar approach.

In scope of this thesis six scenarios are simulated in single domain, based on the selection of main active faults, setting rupture parameters, and bathymetric data with sufficient resolution. The selected scenarios due to the main active faults are listed below;

- PI: Prince's Islands Fault (Oblique-Normal)
- PIN: Prince's Islands Fault (Normal)
- GA: Ganos Fault (Oblique-Normal and Oblique Reverse)
- YAN: Yalova Fault (Oblique-Normal and Normal)
- CMN: Central Marmara Fault (Normal)
- PI + GA

Bathymetric data used in the simulations is adapted from the data used in OYO - IMM report (2007). The spatial reference of original data was ED_1950_3_Degree_GK_Zone_9. However, to be input in NAMI DANCE,

it is projected into geographic coordinates (WGS 84) by using ArcMap10's project tool. The grid size of the bathymetry is90m, which yields a gridded structure with 3350 grid nodes in x-direction and 1058 grid nodes in y-direction.

Numerical gauge points are placed along Marmara Sea Coasts considering settlements, ports and other important structures. Numerical gauge points are used to observe the water level fluctuations in the sea at a certain coordinate and depth during the simulation time. Since at shallow depths, the tsunami wave rises significantly with the sea bottom effect, numerical gauge points are placed at depths between 5m to 10m to observe this effect. The locations of gauge points are shown in Figure 3.4.
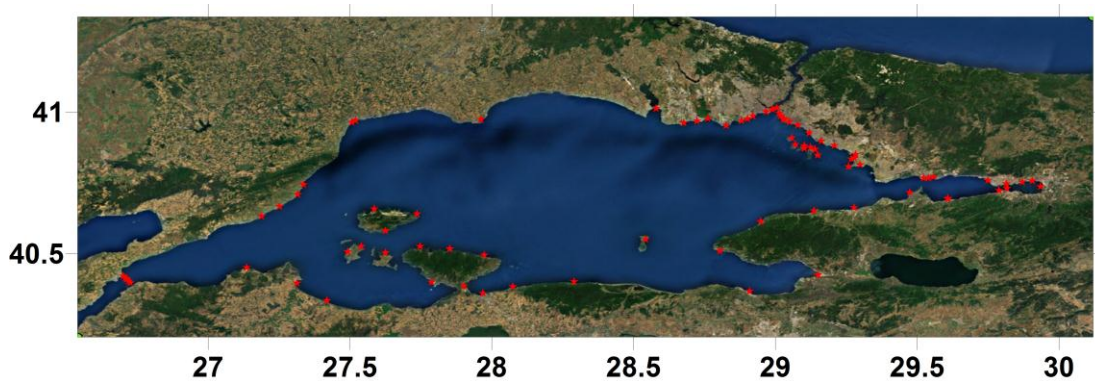
Figure 3.4 Locations of gauge points

Each scenario was simulated with the duration of 180 min. Before deciding the duration of the simulations, 120 min, 180 min and 240 min simulations have been performed and it was understood that 180 min was sufficient to see the effects of the probable tsunamis. As the result of simulations, following outputs were created, and plotted by using softwares GRAPHER 6.0 and SURFER 8.0.

28

- Source parameters and drawings.
- Sea states at 10th, 30th, 60th, and 90th minutes of simulation
- Maximum positive and negative tsunami wave amplitudes at each grid node.
- Arrival time of the first wave (time when water surface elevation exceeds ± 15 cm)
- Water surface fluctuations at selected gauge points.

Simulation of each scenario is given in the following sections.

3.2.2.1 Simulation of Source PI

In the simulation of source PI, it is assumed that, along the North Marmara branch of the North Anatolian Fault, entire PI fault has been ruptured, i.e. all 17 segments are broken (Figure 3.5). Eight of these segments are right-lateral faults (green lines in Figure 3.5); therefore the waves generated due to these segments have relatively small amplifications. In addition to rupture parameters, the initial maximum and minimum wave amplitudes produced by 9 oblique-normal segments are given in Table 3.3 for the rupture along PI.

Table 3.3 Estimated Rupture Parameters and Initial Wave Amplifications for Tsunami Source PI (OYO-IMM, 2007)

Lat	Lon	depth	strike	dip	rake	length	width	Vertical Disp.	Initial Wave Amplitude (m)	
deg.	deg.	m	deg	deg	deg	m	m	m	Max (+)	Min (-)
29.47313	40.72793	1968	84.44	90.00	180.00	4717	16000	0.00	0	0
29.23572	40.73309	946	92.06	90.00	180.00	20066	16000	0.00	0	0
29.22818	40.73306	805	90.20	90.00	180.00	636	16000	0.00	0	0
29.12942	40.75691	744	108.15	70.00	195.00	8753	17027	5.00	0.41	-1.08
29.06928	40.78610	740	123.15	70.00	195.00	6024	17027	5.00	0.37	-1.02
28.99465	40.81653	779	118.85	70.00	195.00	7148	17027	5.00	0.38	-1.04
28.90432	40.87251	1210	129.90	70.00	195.00	9834	17027	5.00	0.37	-1.00

Table 3.3 (Cont'd) Estimated Rupture Parameters and Initial Wave Amplifications for Tsunami Source PI (OYO-IMM, 2007)

28.87843	40.87376	1023	94.37	70.00	195.00	2187	17027	5.00	0.20	-0.61
28.75089	40.88033	1017	94.66	70.00	195.00	10777	17027	5.00	0.39	-1.04
28.70595	40.87843	1131	87.64	70.00	195.00	3795	17027	5.00	0.26	-0.77
28.64466	40.87328	1431	84.56	70.00	195.00	5199	17027	5.00	0.28	-0.79
28.56006	40.86971	1445	87.73	70.00	195.00	7144	17027	5.00	0.31	-0.88
28.51766	40.87301	1186	96.80	90.00	180.00	3593	16000	0.00	0	0
28.47160	40.87298	1219	90.93	90.00	180.00	3884	16000	0.00	0	0
28.41844	40.86580	1254	80.93	90.00	180.00	4553	16000	0.00	0	0
28.26801	40.84761	1364	82.03	90.00	180.00	12847	16000	0.00	0	0
28.06159	40.80420	804	75.73	90.00	180.00	18074	16000	0.00	0	0

Figure 3.5 Tsunami Source PI

The sea states at t=10, 30, 60, 90 min are given in Figure 3.6 for tsunami source PI. In addition to these, distribution of computed maximum positive and maximum negative tsunami wave amplitudes in the study domain throughout the simulation time (3 hour) are given in Figure 3.7. It should be noted here that, their values are +5.0 m and -4.3 m respectively (Figure 3.7)
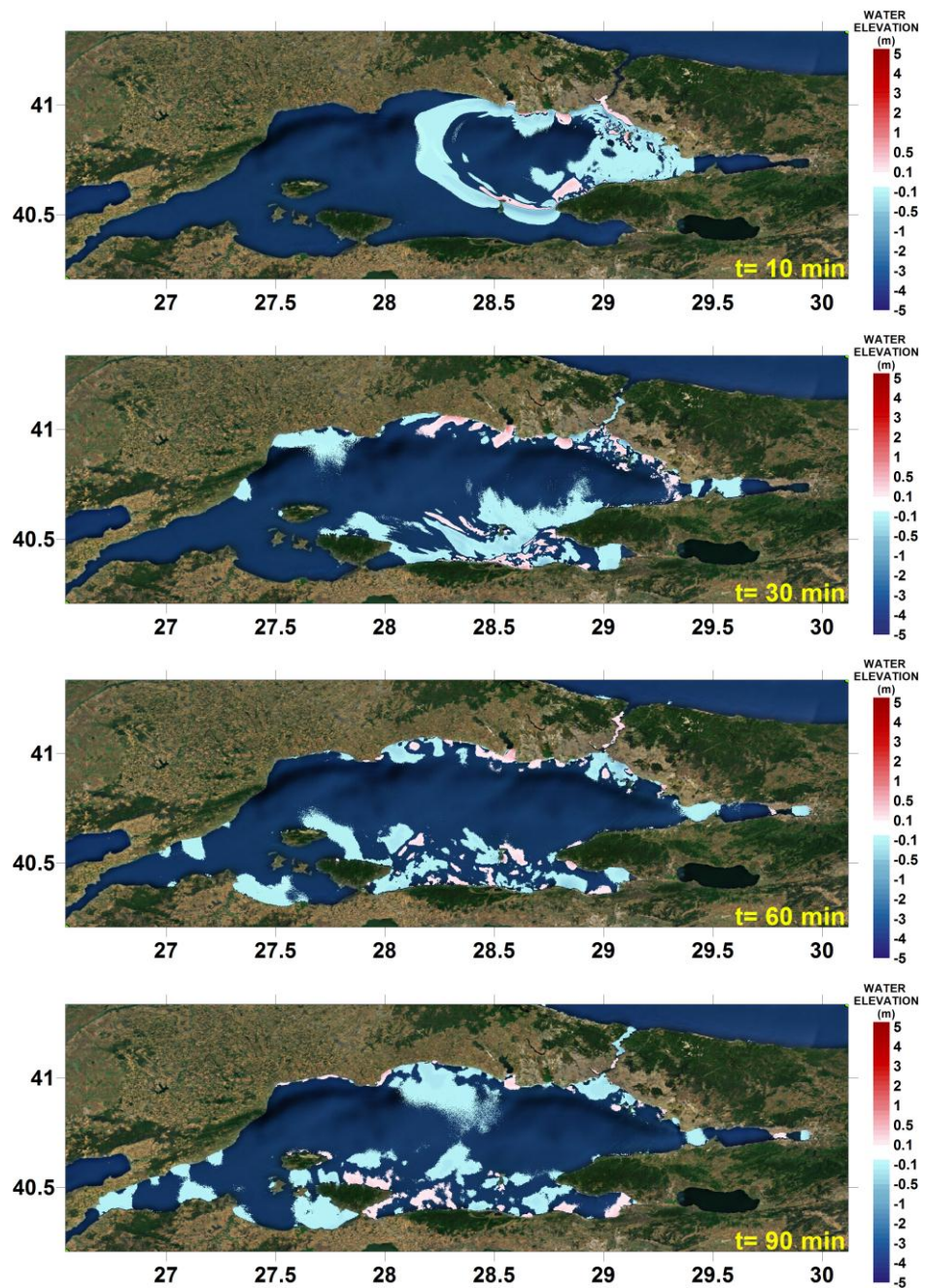
Figure 3.6 Sea states at t=10, 30, 60, and 90 min respectively according to the tsunami source PI
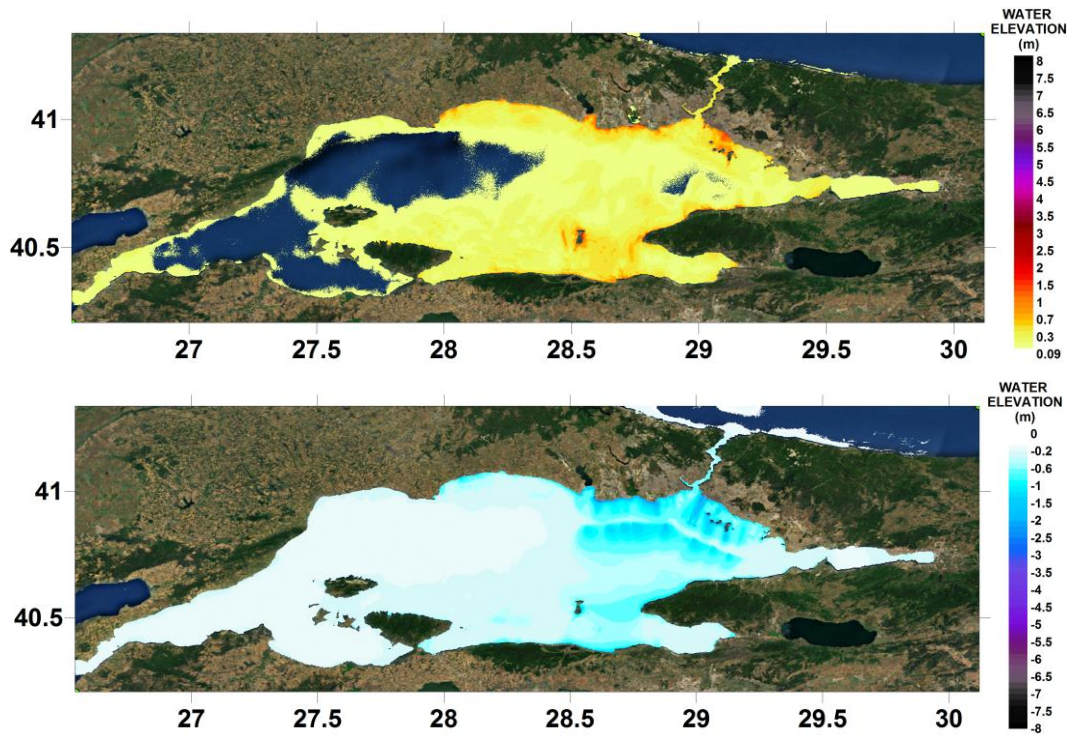
Figure 3.7 Maximum (+) wave amplitude (top) and minimum (-) wave amplitude

In Table 3.4 the summary sheet of selected gauge points are given. Additionally, selected gauge points and water surface fluctuations, arrival times of first and maximum waves, measured at that gauges during simulation are shown in Figure 3.8.

Table 3.4 Summary Sheet of Main Tsunami Parameters at Selected Gauges for Source PI

Name of gauge pt.	Depth of gauge	XCoord	YCoord	Arrival time first wave	Arrival time max.wave	Max(+) wave amp.	Max (-) wave amp.
	m	deg.	deg.	min	min	m	m
Tekirdag1	8.4	27.5068	40.9643	24	173	0.3	-0.3
Mudanya	7.6	28.9089	40.3675	19	29	0.3	-0.4
Izmit3	7.8	29.8707	40.754	46	115	0.2	-0.3
Tuzla4	9.9	29.2828	40.8504	0.0	34	0.6	-0.8
Hpasa1	9.8	29.0787	40.954	0.0	34	1.1	-1.0
Zburnu2	8.9	28.9016	40.9771	1	15	0.7	-1.4
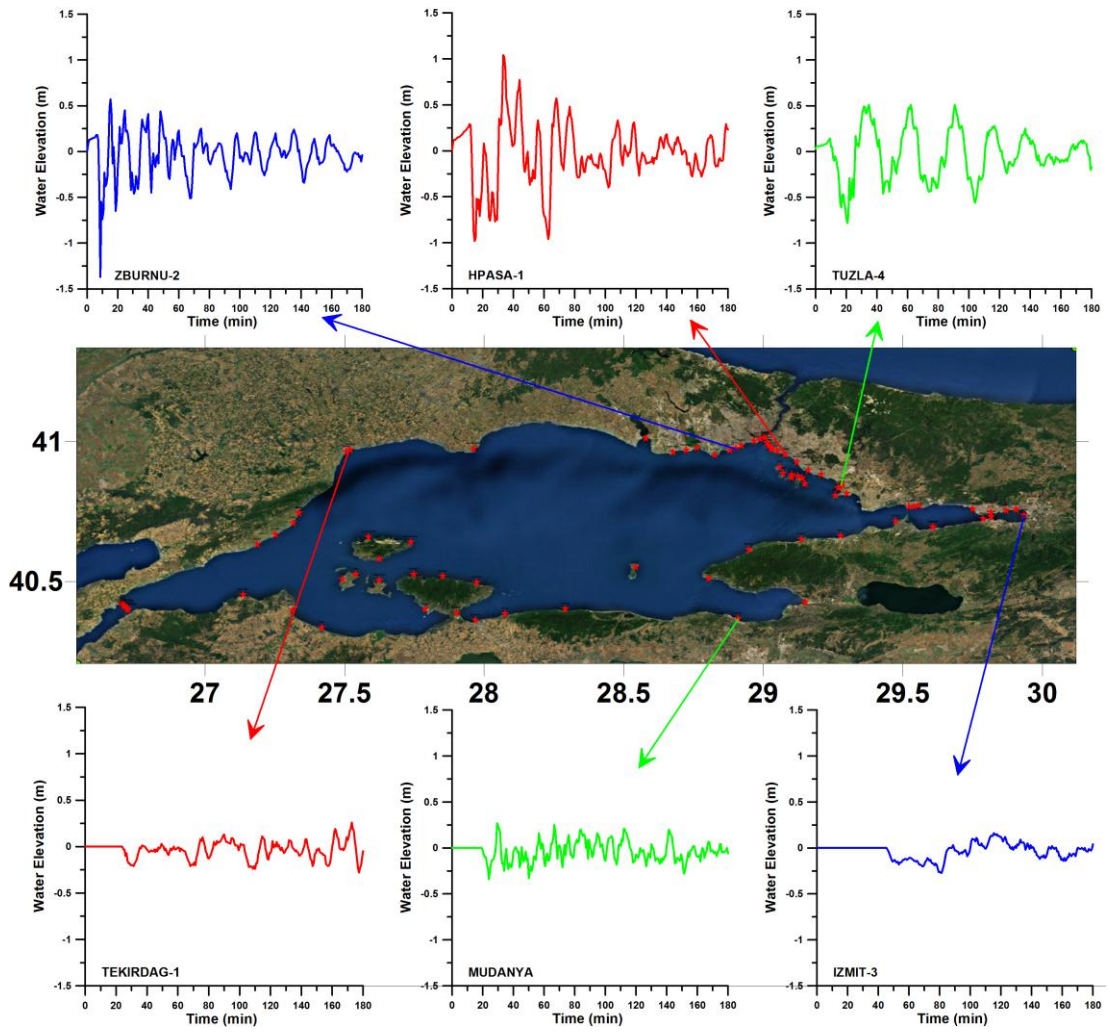
Figure 3.8 Locations of Selected Gauges and Time Histories of Water surface fluctuations for source PI

It is seen from in Figure 3.7 and Figure 3.8, and Table 3.4, the first wave arrives to Istanbul coasts immediately with amplitude less than of 0.5 m, and maximum positive and negative wave amplitudes are up to 1.1m, and -1.4m respectively.

Moreover, source PI cause rather small wave amplitudes in eastern, western and southern coasts of Marmara Sea. Maximum positive wave occurred at Tekirdag and Mudanya is 0.3 for both and maximum negative wave amplitudes are

33

-0.3 m and -0.4 m respectively. Izmit Gulf is protected due to its geographic conditions for this scenario. However, wave agitation and resonance oscillations may be observed (Figure 3.8).

3.2.2.2   Simulation of Source PIN

Tsunami source PIN is the normal form of the first four oblique-normal segments of tsunami source PI. In the simulation of source PIN, as the worst case scenario, it is assumed that entire fault has been ruptured, i.e. all four segments are broken (Figure 3.9). In addition to rupture parameters, the initial maximum and the minimum wave amplitudes produced by four normal segments are given in Table 3.5.

Table 3.5 Estimated Rupture Parameters and Initial Wave Amplitudes for Tsunami Source PIN (OYO-IMM, 2007)

Lat	Lon	depth	strike	dip	rake	length	width	Vertical Disp.	Initial Wave Amplitude (m)	
deg	deg	m	deg	deg	deg	m	m	m	Max (+)	Min (-)
29.12942	40.75691	744	108.15	70.00	270.00	8753	17027	5.00	1.05	-2.57
29.06928	40.78610	740	123.15	70.00	270.00	6024	17027	5.00	0.94	-2.41
28.99465	40.81653	779	118.85	70.00	270.00	7148	17027	5.00	0.98	-2.47
28.90432	40.87251	1210	129.90	70.00	270.00	9834	17027	5.00	0.92	-2.36
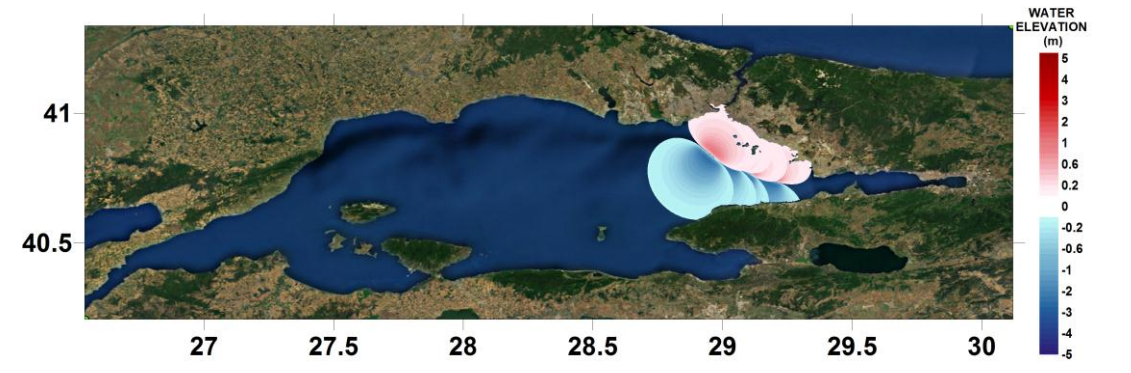
Figure 3.9 Tsunami Source PIN

The sea states at t=10, 30, 60, 90 min are given in Figure 3.11 for source PIN. In addition to these, distribution of maximum positive and maximum negative tsunami wave amplitudes in the study domain throughout the simulation time (3 hour) are given in Figure 3.12. Their values are +8.5 m and -10.1 m respectively (Figure 3.12).
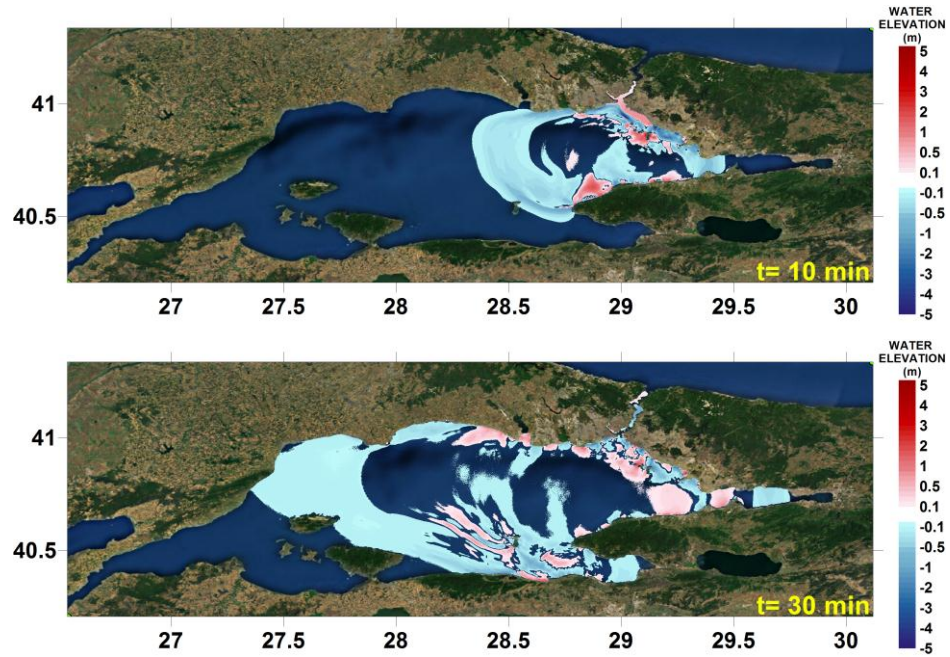

Figure 3.10 Sea states at t=10, 30, 60, and 90 min respectively according to the tsunami source PIN
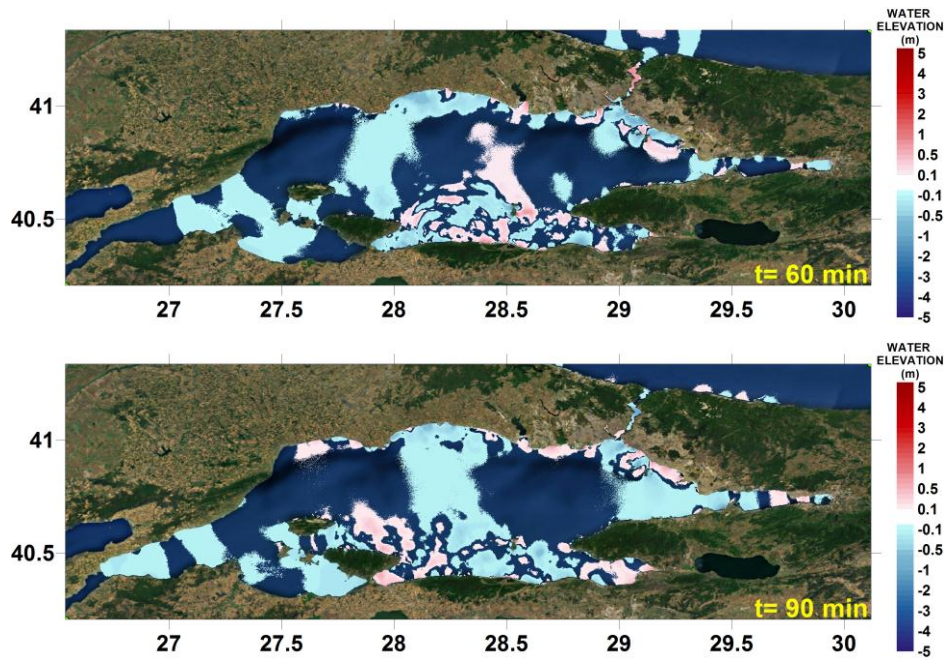
Figure 3.11 (Cont'd) Sea states at t=10, 30, 60, and 90 min respectively according to the tsunami source PIN
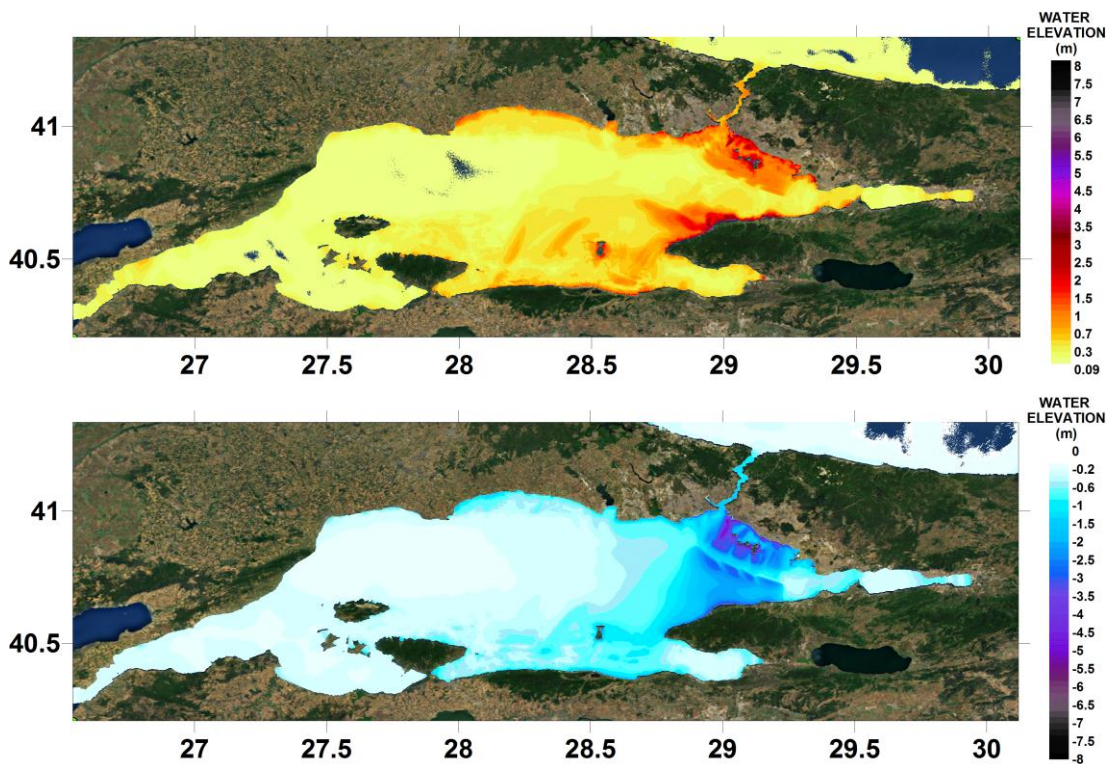
Figure 3.12 Maximum (+) wave amplitude (top) and minimum (-) wave amplitude

In Table 3.6, the summary sheet of selected gauge locations is given. Additionally, selected gauge points and water surface fluctuations, arrival times of first and maximum waves, measured at that gauges during simulation are given in Figure 3.12.

Table 3.6 Summary sheet of main tsunami parameters at selected gauges for Source PIN

Name of gauge pt.	Depth of gauge pt.	XCoord	YCoord	Arrival time of initial wave	Arrival time of max.wave	Max(+) wave amp.	Max (-) wave amp.
	m	deg.	deg.	min	min	m	m
Tekirdag1	8.4	27.5068	40.9643	30	87	0.4	-0.6
Mudanya	7.6	28.9089	40.3675	3	115	0.6	-0.6
Izmit3	7.8	29.8707	40.7540	42	120	0.4	-0.6
Tuzla4	9.8	29.0787	40.9540	0.0	34	2.1	-3.2
Hpasa1	9.7	29.0186	40.9863	0.0	43	1.4	-4.5
Zburnu2	8.9	28.9016	40.9771	0.0	22	2.1	-2.6
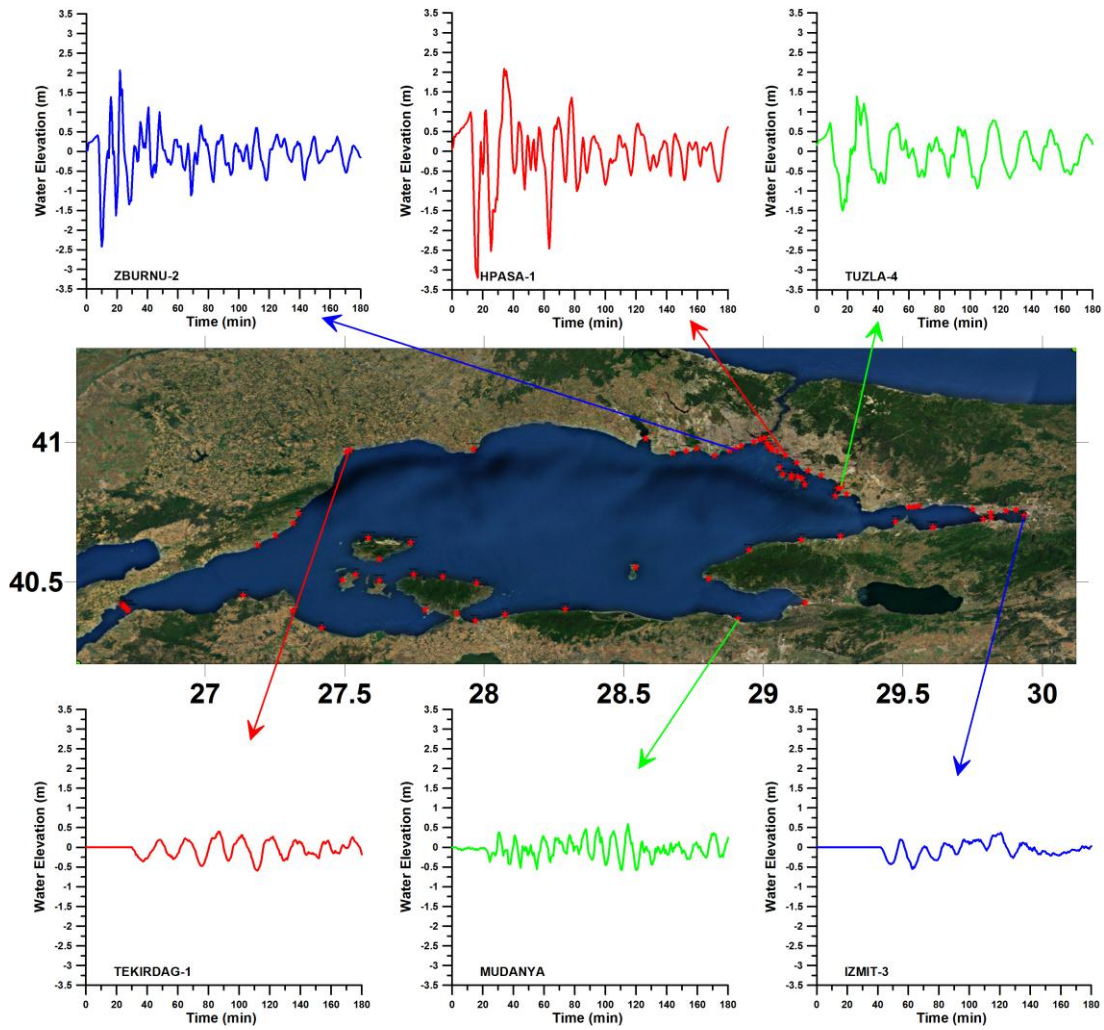
Figure 3.13 Locations of Selected Gauges and Time Histories of the Water surface fluctuations for Source PIN

It is seen in Figure 3.12 and Figure 3.13, and Table 3.6, the tsunami source PIN is mostly critical for Istanbul. First wave arrives to Istanbul coasts immediately with an amplitude of more than 1m, and maximum positive and negative wave amplitudes reach up to 2.1m and -4.5m respectively.

As well as source PI, source PIN did not cause considerable impacts in eastern and western coasts of Marmara Sea. Maximum positive wave occurred at Tekirdag and Mudanya is 0.4m and 0.6m, and maximum

negative wave is -0.6 m for each. Izmit Gulf is protected due to its geographic conditions. However wave agitation and resonance oscillations may be observed.

3.2.2.3   Simulation of Source PI+GA

In this tsunami scenario, it is assumed that entire north trough has been ruptured, i.e. all 28 segments are broken (Figure 3.14). Eleven of these segments are right-lateral faults (green lines in Figure 3.14); therefore the waves generated due to these segments have relatively small amplitudes. In addition to rupture parameters, the initial maximum and minimum wave amplitudes produced by 13 oblique-normal and 2 oblique-reverse segments are given in Table 3.7 for the rupture along PI-GA.
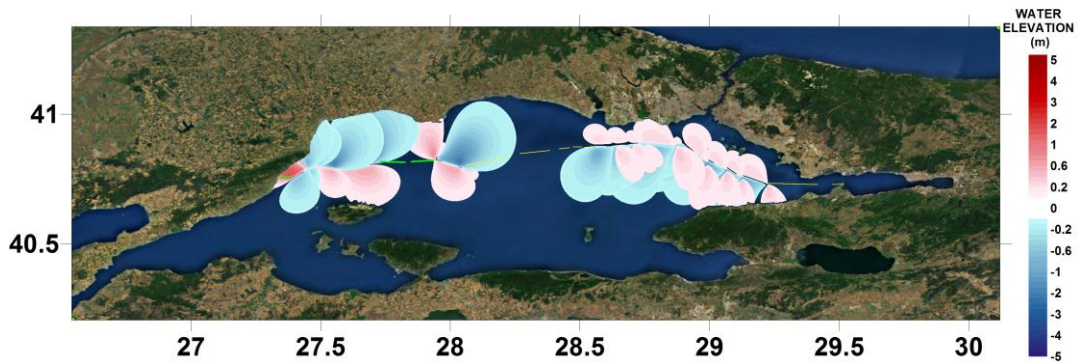
Table 3.7 Estimated Rupture Parameters and Initial Wave Amplitudes for Tsunami Source PI+GA (OYO-IMM, 2007)

Lat	Lon	depth	strike	dip	rake	length	width	Vertical Disp.	Initial Wave Amplitude (m)	
deg.	deg.	m	deg	deg	deg	m	m	m	Max (+)	Min (-)
29.47313	40.72793	1968	84.44	90.00	180.00	4717	16000	0.00	0	0
29.23572	40.73309	946	92.06	90.00	180.00	20066	16000	0.00	0	0
29.22818	40.73306	805	90.20	90.00	180.00	636	16000	0.00	0	0
29.12942	40.75691	744	108.15	70.00	195.00	8753	17027	5.00	0.41	-1.08
29.06928	40.78610	740	123.15	70.00	195.00	6024	17027	5.00	0.37	-1.02
28.99465	40.81653	779	118.85	70.00	195.00	7148	17027	5.00	0.38	-1.04
28.90432	40.87251	1210	129.90	70.00	195.00	9834	17027	5.00	0.37	-1.00
28.87843	40.87376	1023	94.37	70.00	195.00	2187	17027	5.00	0.20	-0.61
28.75089	40.88033	1017	94.66	70.00	195.00	10777	17027	5.00	0.39	-1.04
28.70595	40.87843	1131	87.64	70.00	195.00	3795	17027	5.00	0.26	-0.77
28.64466	40.87328	1431	84.56	70.00	195.00	5199	17027	5.00	0.28	-0.79
28.56006	40.86971	1445	87.73	70.00	195.00	7144	17027	5.00	0.31	-0.88
28.51766	40.87301	1186	96.80	90.00	180.00	3593	16000	0.00	0	0
28.47160	40.87298	1219	90.93	90.00	180.00	3884	16000	0.00	0	0
28.41844	40.86580	1254	80.93	90.00	180.00	4553	16000	0.00	0	0
28.26801	40.84761	1364	82.03	90.00	180.00	12847	16000	0.00	0	0

Table 3.7 (Cont'd)Estimated Rupture Parameters and Initial Wave Amplitudes for Tsunami Source PI+GA (OYO-IMM, 2007)

28.06159	40.80420	804	75.73	90.00	180.00	18074	16000	0.00	0	0
28.06159	40.80420	804	263.30	70.00	195.00	2143	17027	5.00	0.45	-1.38
28.03644	40.80152	775	286.31	70.00	195.00	8664	17027	5.00	0.80	-2.13
27.93729	40.82170	818	266.61	90.00	180.00	9516	16000	0.00	0	0
27.82494	40.81458	1197	271.96	90.00	180.00	10494	16000	0.00	0	0
27.70062	40.81540	1226	260.87	70.00	195.00	12441	17027	5.00	0.78	-2.05
27.55582	40.79464	874	278.58	70.00	195.00	5660	17027	5.00	0.69	-1.92
27.48929	40.80081	880	258.14	70.00	165.00	3046	17027	5.00	1.61	-0.50
27.45422	40.79441	891	238.95	70.00	165.00	6945	17027	5.00	2.05	-0.69
27.38506	40.76061	1807	257.18	90.00	180.00	4517	16000	0.00	0	0

Figure 3.14 Tsunami Source PI+GA

The sea states at t=10, 30, 60, 90 min are given in Figure 3.15 and in for source PI+GA. In addition to these, distribution of maximum positive and maximum negative tsunami wave amplitudes in the study domain throughout the simulation time (3 hour) are given in Figure 3.16. Their values are +5.5 m and -6.2 m respectively (Figure 3.16).
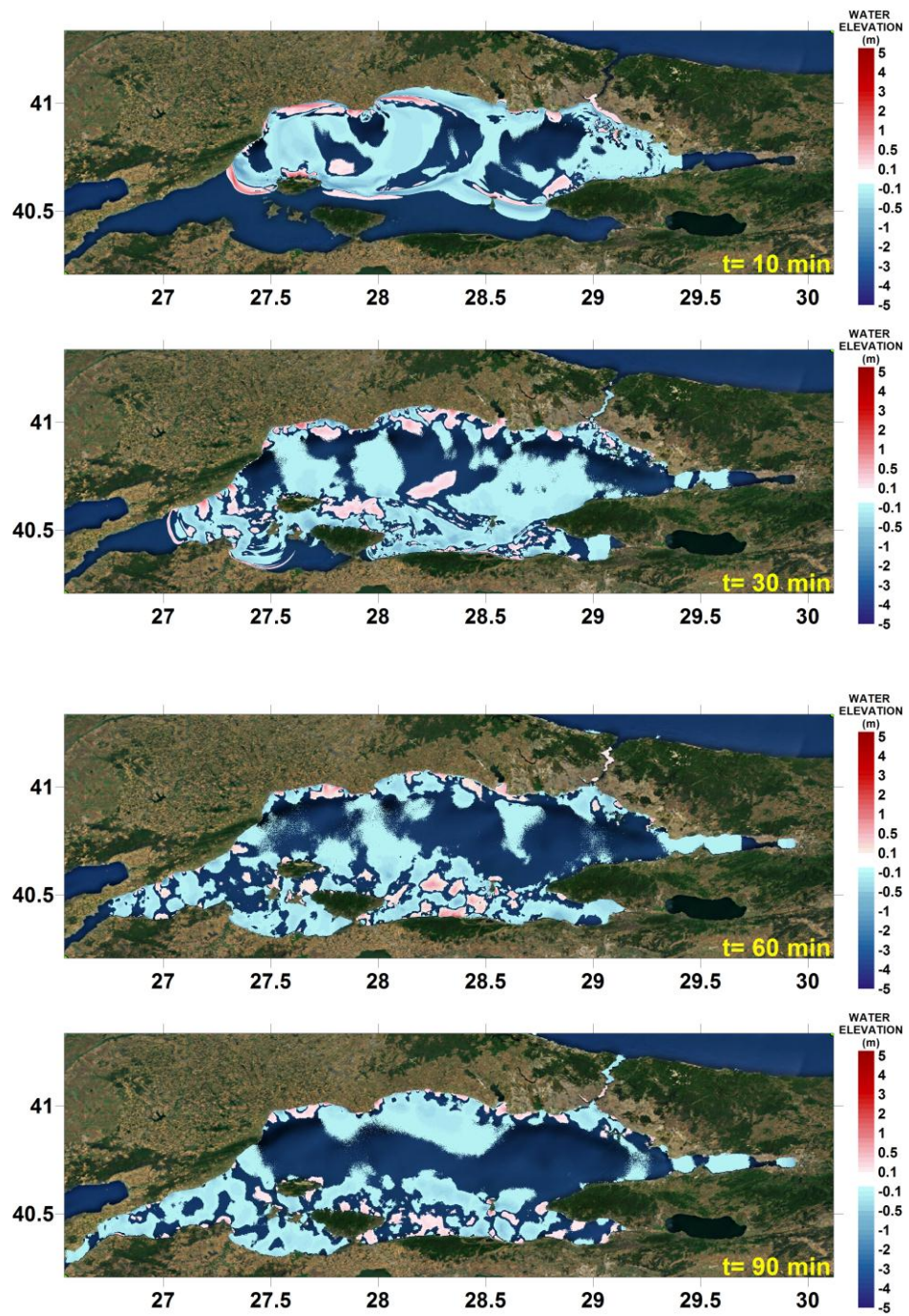
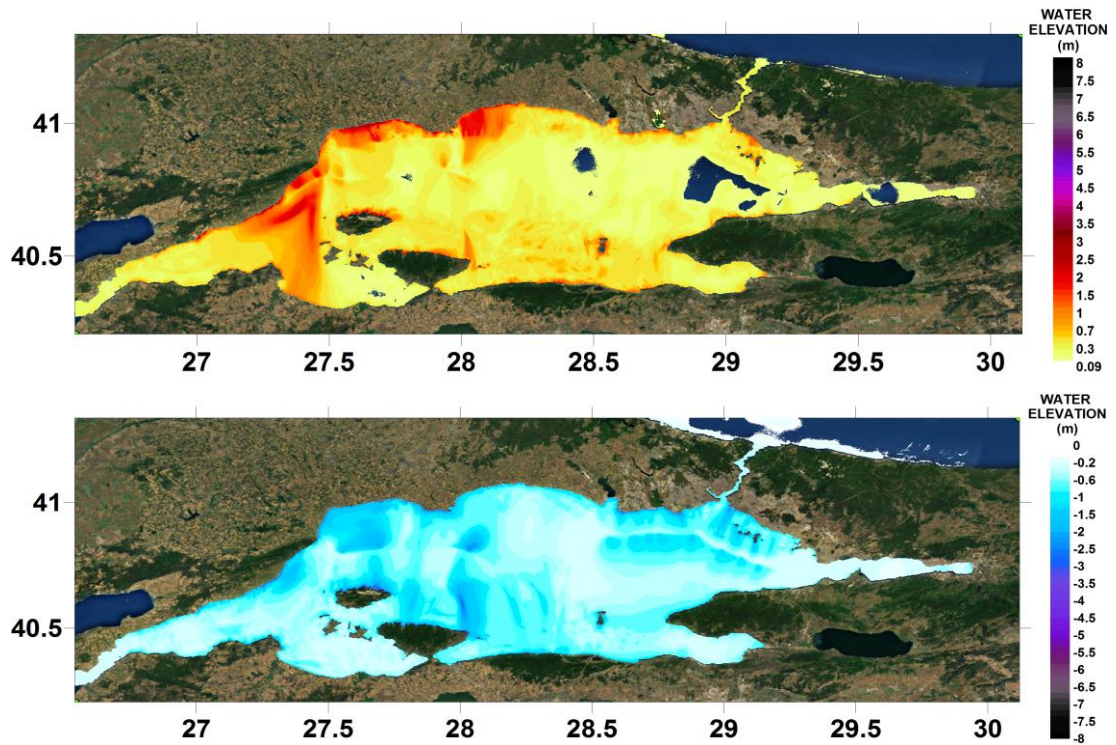**Figure 3.15 Sea states at t=10, 30, 60 and 90 min respectively**

Figure 3.16 Maximum (+) wave amplitude (top) and minimum (-) wave amplitude

In and Table 3.8 the summary sheet of selected gauge locations is given. Additionally, in Figure 3.17 selected gauge points and water surface fluctuations, arrival times of first and maximum waves, measured at that gauges during simulation are given.

Table 3.8 Summary Sheet of Main Tsunami Parameters at selected gauge for Source PI-GA

| Name of gauge pt.	Depth of gauge pt.	XCoord	YCoord	Arrival time of initial wave	Arrival time of max.wave	Max(+) wave amp.	Max (-) wave amp.
	m	deg.	deg.	min	min	m	m
Tekirdag1	8.4	27.5068	40.9643	2	17	1.0	-1.7
Mudanya	7.6	28.9089	40.3675	19	114	0.4	-0.5
Izmit3	7.8	29.8707	40.754	45	140	0.1	-0.4

Table 3.8 (Cont'd) Summary Sheet of Main Tsunami Parameters at selected gauge for Source PI-GA

Name of gauge pt.	Depth of gauge pt.	XCoord	YCoord	Arrival time of initial wave	Arrival time of max.wave	Max(+) wave amp.	Max (-) wave amp.
	m	deg.	deg.	min	min	m	m
Tuzla4	9.9	29.2828	40.8504	0.0	61	0.6	-0.8
Hpasa1	9.8	29.0787	40.954	0.0	34	1.1	-1.0
Zburnu2	8.9	28.9016	40.9771	1	15	0.7	-1.4
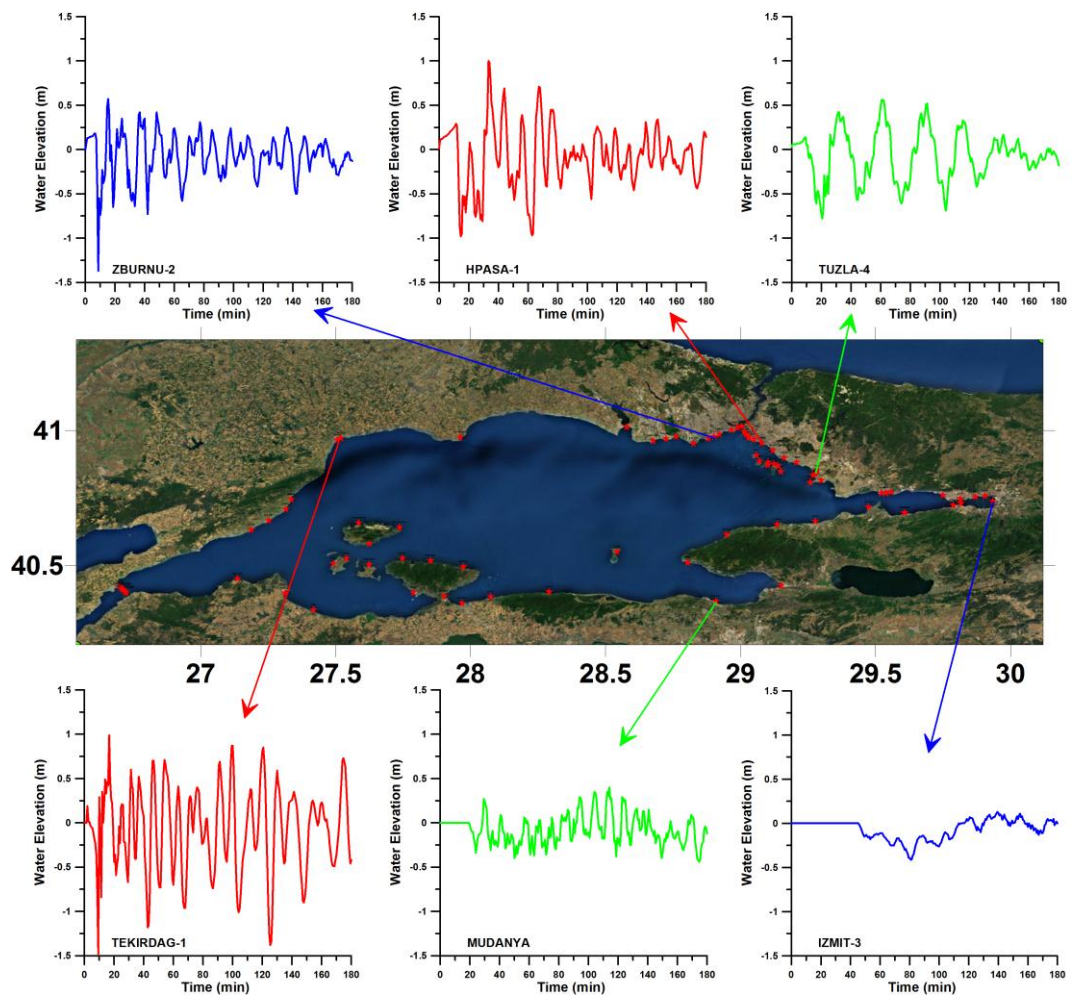
Figure 3.17 Locations of Selected Gauges and Time Histories of Water Surface Fluctuations for Source PI-GA

As can be seen in Figure 3.16 and Figure 3.17, and Table 3.8, the tsunami source PI+GA is critical for Istanbul and Northwestern Marmara Sea Region. First wave arrives to Istanbul and Tekirdag coasts immediately with a magnitude of 0.5 m, and maximum positive and negative wave amplitudes are up to 1m and -1.5m for Istanbul. For Tekirdag, maximum positive and negative wave amplitudes are 1m and -1.5m respectively.

Tsunami source PI+GA did not cause considerable impacts in southern, southeastern and eastern coasts of Marmara Sea. Maximum positive wave occurred at southern coasts is in between 0.4m and 0.6m, and maximum negative wave is -0.6 m. Inside the Izmit Gulf, Maximum positive wave is below 0.5m while, maximum negative wave is around -0.5 m.

3.2.2.4   *Simulation of Source GA*

Tsunami source GA has 9 segments and it is assumed that in the simulation all of them have been ruptured as well as other scenarios (Figure 3.18). The effects of 3 right-lateral segments were neglected and estimated rupture parameters with the initial maximum and the minimum wave amplitudes produced by four normal segments are given in Table 3.9.

Table 3.9 Estimated Rupture Parameters for Tsunami Source GA (OYO-IMM, 2007)

Lat	Lon	depth	strike	dip	rake	length	width	Vertical Disp.	Initial Wave Amplitude (m)	
deg	deg	m	deg	deg	deg	m	m	m	Max (+)	Min (-)
28.06159	40.80420	804	263.30	70.00	195.00	2143	17027	5.00	0.45	-1.38
28.03644	40.80152	775	286.31	70.00	195.00	8664	17027	5.00	0.80	-2.13
27.93729	40.82170	818	266.61	90.00	180.00	9516	16000	0.00	0	0
27.82494	40.81458	1197	271.96	90.00	180.00	10494	16000	0.00	0	0
27.70062	40.81540	1226	260.87	70.00	195.00	12441	17027	5.00	0.78	-2.05

27.55582	40.79464	874	278.58	70.00	195.00	5660	17027	5.00	0.69	-1.92
27.48929	40.80081	880	258.14	70.00	165.00	3046	17027	5.00	1.61	-0.50
27.45422	40.79441	891	238.95	70.00	165.00	6945	17027	5.00	2.05	-0.69
27.38506	40.76061	1807	257.18	90.00	180.00	4517	16000	0.00	0	0
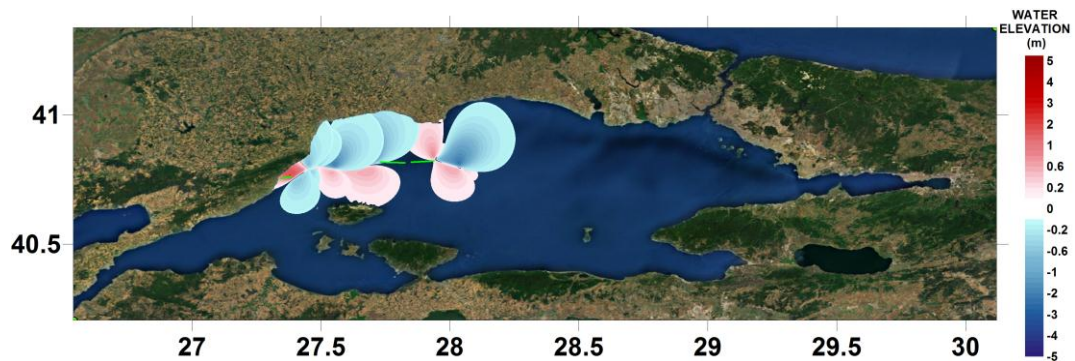
Figure 3.18 Tsunami Source GA

The sea states at t=10, 30, 60, 90 min are given in Figure 3.19 and for source GA. In addition to these, the distribution of computed maximum positive and maximum negative tsunami wave amplitudes in the study domain throughout the simulation time (3 hour) are given in Figure 3.20. Their values are +5.5 m and -7.4 m respectively (Figure 3.20).
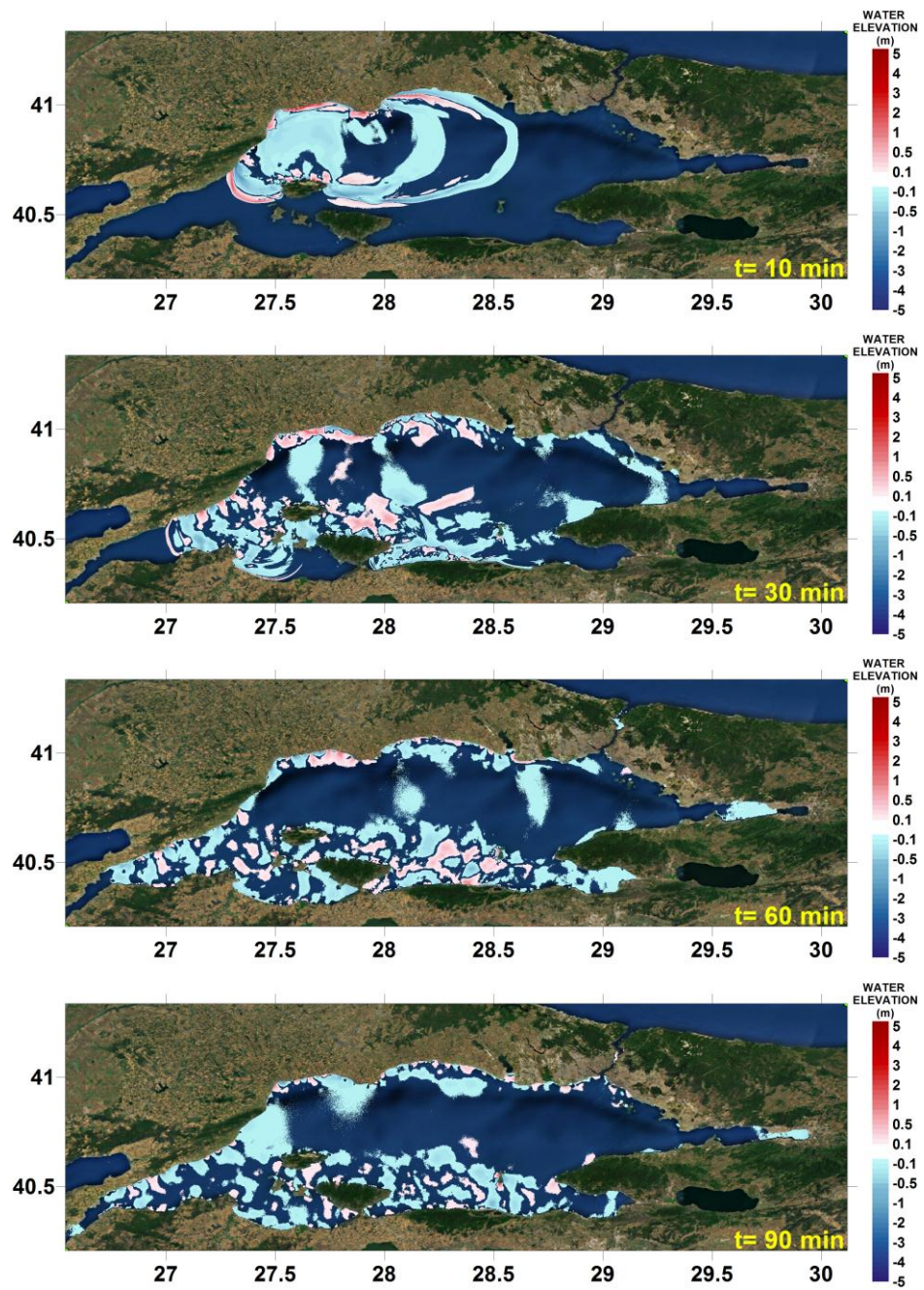
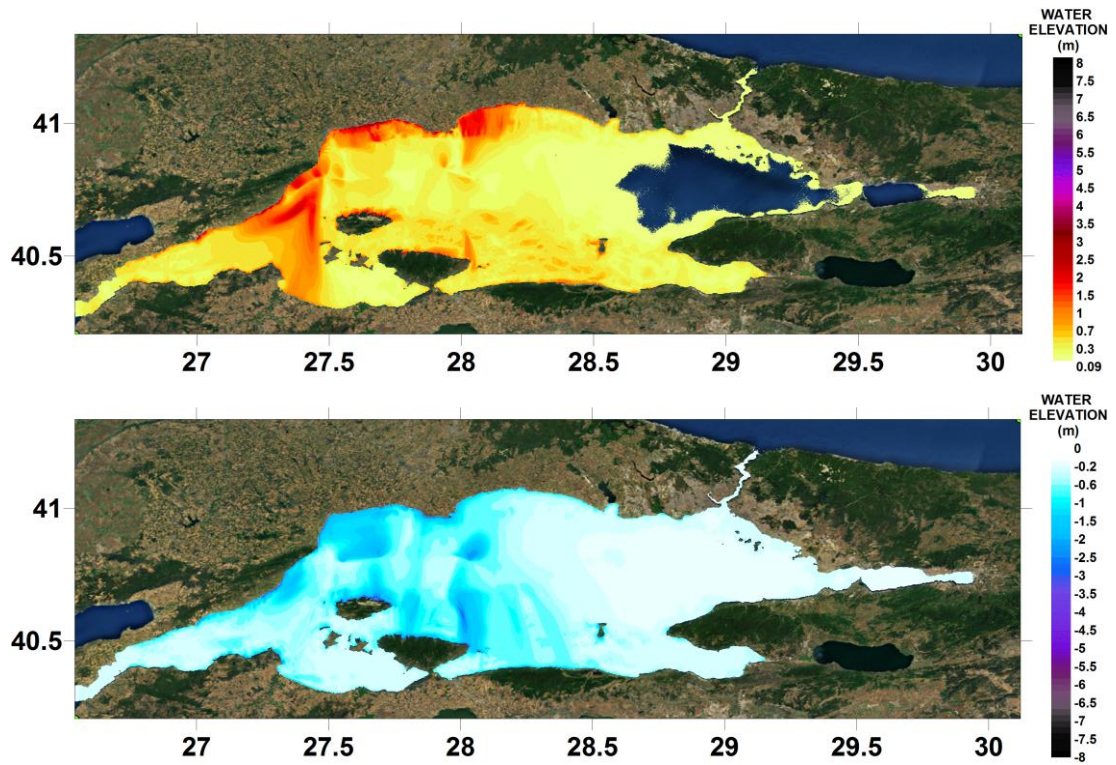**Figure 3.19 Sea states at t=10, 30, 60 and 90min respectively**

Figure 3.20 Maximum (+) wave amplitude (top) and minimum (-) wave amplitude

In Table 3.10, summary sheet of selected gauge points is given. Additionally, in Figure 3.21 and selected gauge points and water surface fluctuations, arrival times of first and maximum waves, measured at that gauges during simulation are given.

Table 3.10 Summary Sheet of Main Tsunami Parameters at Selected Gauges for Source GA

| Name of gauge pt.	Depth of gauge pt.	XCoord	YCoord	Arrival time of initial wave	Arrival time of max.wave	Max(+) wave amp.	Max (-) wave amp.
	m	deg.	deg.	min	min	m	m
Tekirdag1	8.4	27.5068	40.9643	1	15	1.0	-1.7
Mudanya	7.6	28.9089	40.3675	32	103	0.4	-0.4
Izmit3	7.8	29.8707	40.7540	66	161	0.1	-0.3

Table 3.10 (Cont'd) Summary Sheet of Main Tsunami Parameters at Selected Gauges for Source GA

Name of gauge pt.	Depth of gauge pt.	XCoord	YCoord	Arrival time of initial wave	Arrival time of max.wave	Max(+) wave amp.	Max (-) wave amp.
	m	deg.	deg.	min	min	m	m
Tuzla4	9.9	29.2828	40.8504	29	84	0.3	-0.3
Hpasa1	9.8	29.0787	40.9540	28	154	0.3	-0.3
Zburnu2	8.9	28.9016	40.9771	20	76	0.3	-0.3
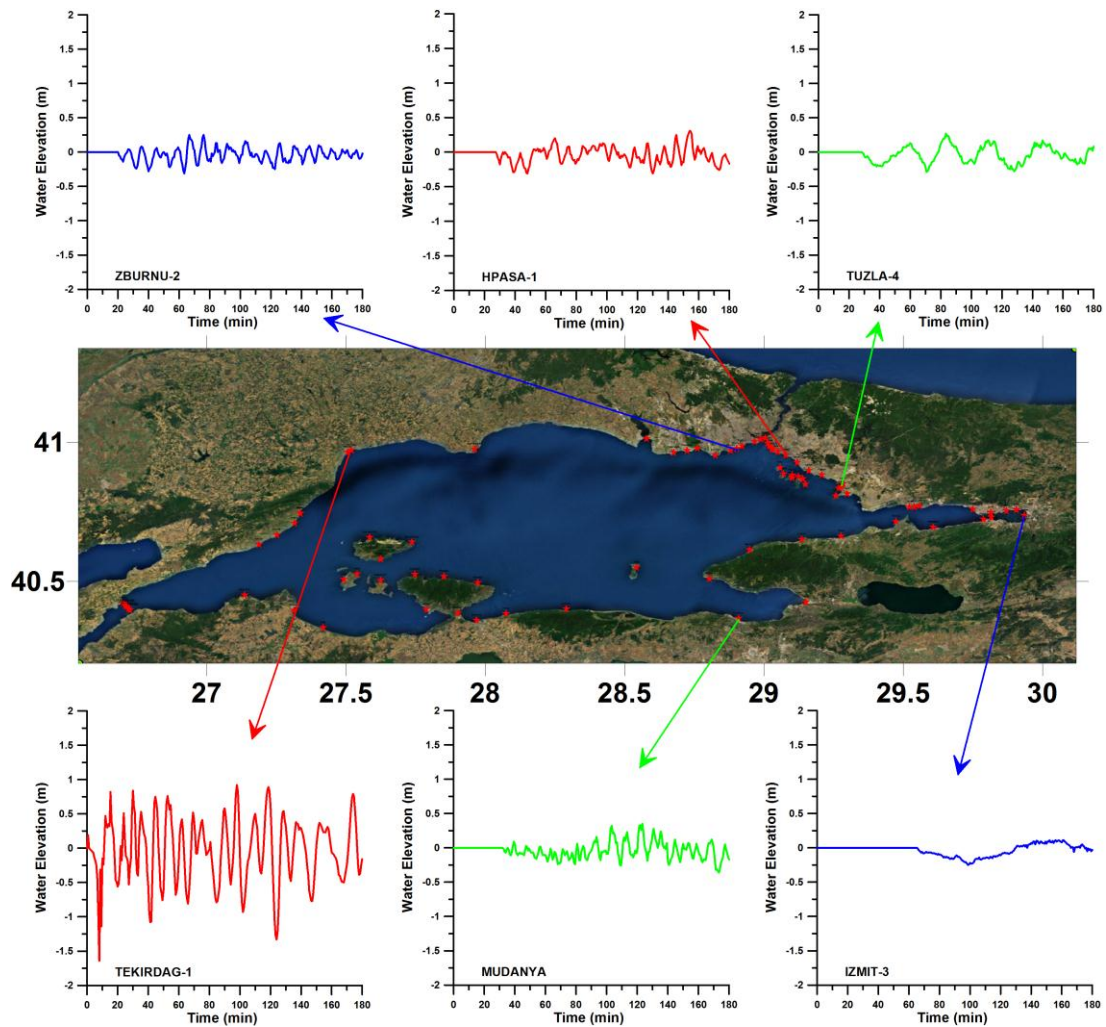
Figure 3.21 Locations of Selected Gauges and Time Histories of Water surface Fluctuations for Source GA

48

As can be seen in Figure 3.20 and Figure 3.21, and Table 3.10, the impacts of tsunami source GA is serious for Northeast Marmara Sea Region. First wave arrives to Tekirdag coasts immediately with amplitude of 0.5 m and, and maximum positive wave is around 1m and maximum negative wave amplitude is -1.5m. However at the coasts at the north and south of the Tekirdag maximum positive wave amplitude reach to 3m.

Tsunami source GA did not cause considerable impacts in eastern coasts of Marmara Sea. Maximum positive wave occurred is around 0.4m and and maximum negative wave is -0.3m at these locations.

3.2.2.5   *Simulation of Source YAN*

In the simulation of source YAN, as the worst case scenario, it is assumed that entire fault has been ruptured, i.e. all 8 segments are broken (Figure 3.22). Three of these segments are oblique-normal and five of them are normal faults. In addition to rupture parameters, the initial maximum and minimum wave amplitudes produced by 8 segments are given in Table 3.11 for the rupture along YAN

Table 3.11 Estimated Rupture Parameters and Initial Wave Amplitudes for Tsunami Source Yan (OYO-IMM, 2007)

| Lat	Lon	depth	strike	dip	rake	length	width	Vertical Disp.	Initial Wave Amplitude (m)	
deg	deg	m	deg	deg	deg	m	m	m	Max (+)	Min (-)
29.47103	40.72115	1978	257.96	70.00	195.00	7058	17027	5.00	0.49	-1.56
29.38946	40.70750	1960	261.14	70.00	195.00	6873	17027	5.00	0.60	-1.65
29.30920	40.69751	1823	260.98	70.00	195.00	10952	17027	5.00	0.92	-2.35
29.18143	40.68121	1681	262.35	70.00	270.00	4448	17027	5.00	0.52	-1.55
29.12936	40.67550	1557	273.96	70.00	270.00	4562	17027	5.00	1.03	-2.51
29.07551	40.67791	1252	283.78	70.00	270.00	10021	17027	5.00	0.53	-1.79
28.96007	40.69843	1219	294.84	70.00	270.00	3154	17027	5.00	0.56	-1,77
28.92602	40.71005	1178	284.90	70.00	270.00	14043	17027	5.00	0.78	-2.15
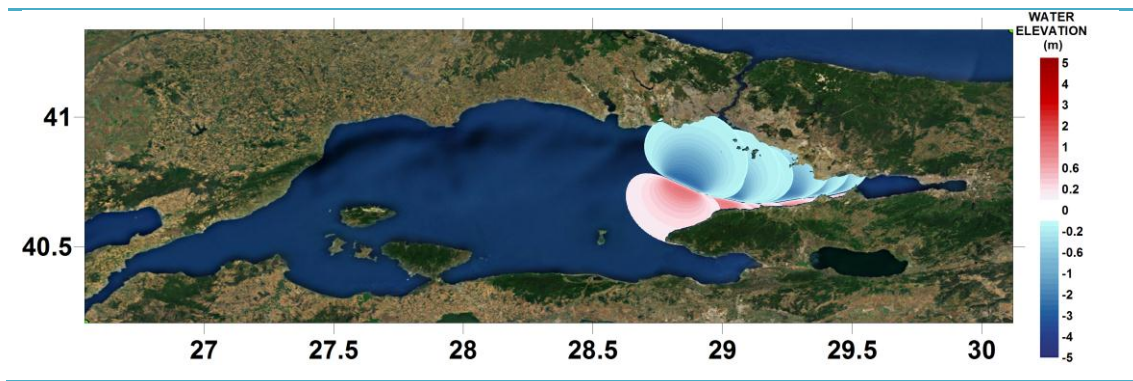
Figure 3.22 Tsunami Source YAN

The sea states at t=10, 30, 60, 90 min are given in Figure 3.22 for source YAN. In addition to these, distribution of maximum positive and maximum negative tsunami wave amplitudes in the study domain throughout the simulation time (3 hour) are given in Figure 3.25. Their values are +12.9 m and -10.9 m respectively (Figure 3.25)
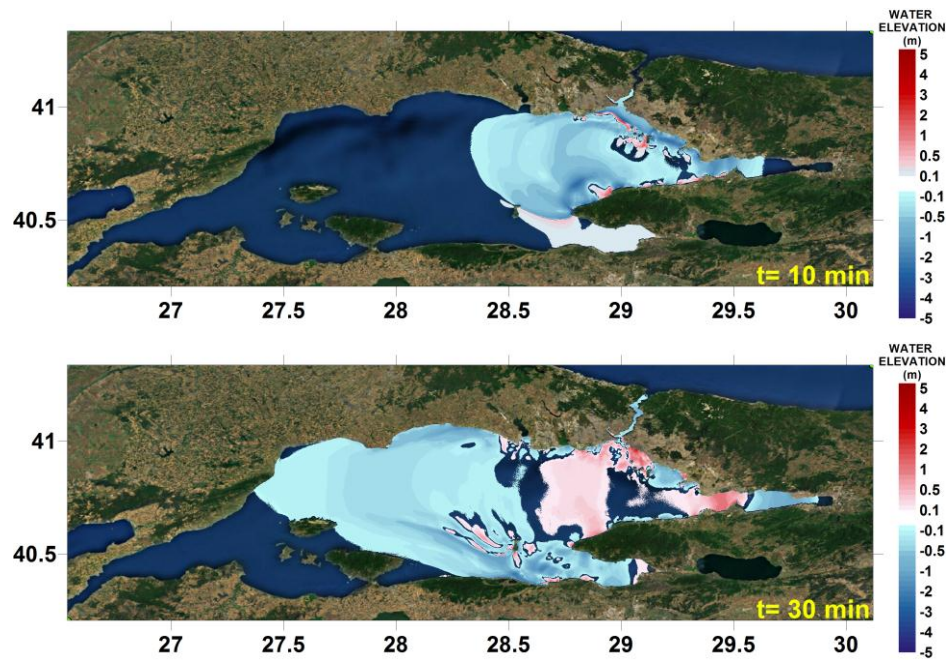

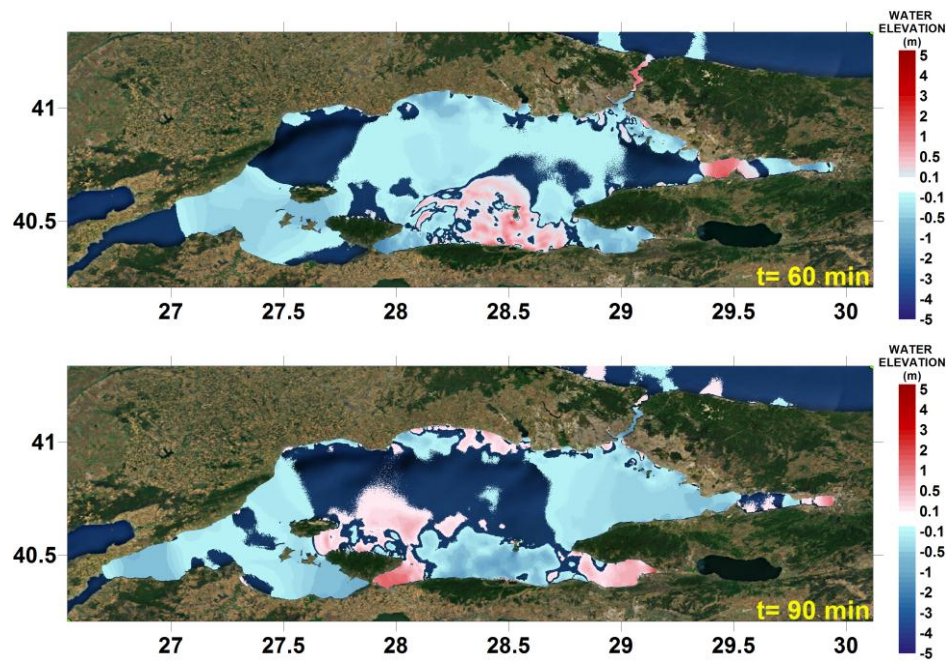**Figure 3.23 Sea states at t=10, 30, 60, and 90 min respectively**

50

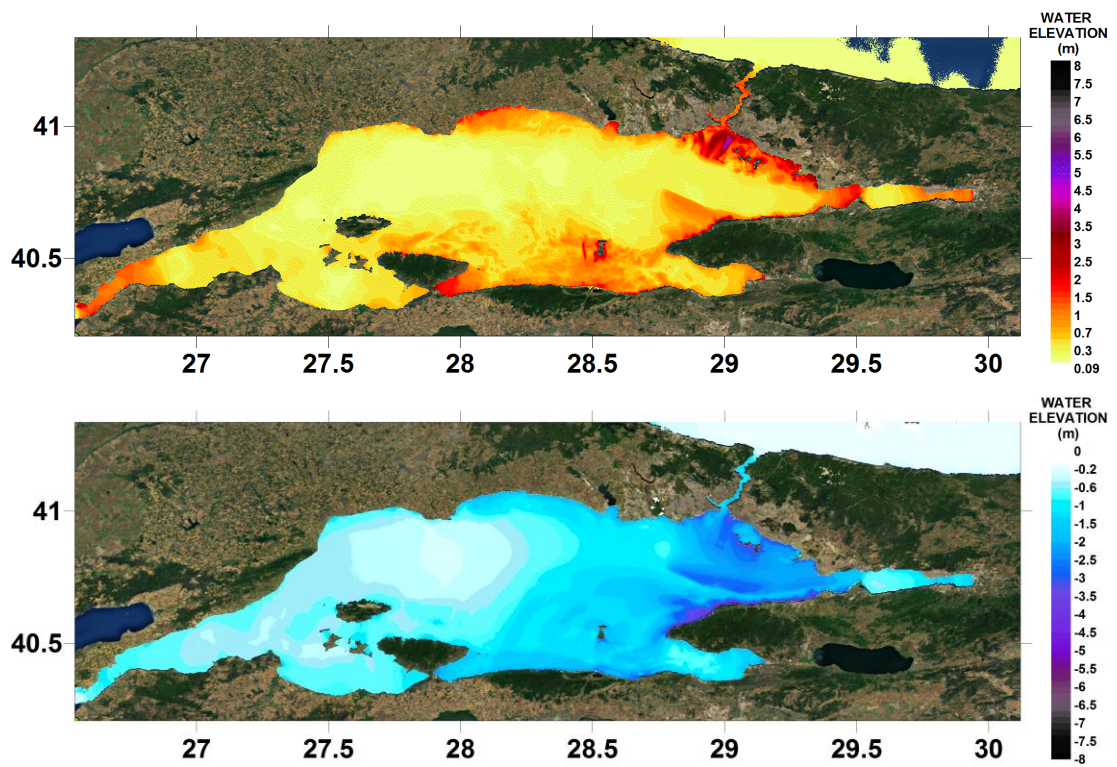**Figure 3.24 (Cont'd)Sea states at t=10, 30, 60, and 90 min respectively**

Figure 3.25 Maximum (+) wave amplitude (top) and minimum (-) wave amplitude

In Table 3.12, summary sheet of selected gauge points are given. Additionally, in Figure 3.26 selected gauge points and water surface fluctuations, arrival times of first and maximum waves, measured at that gauges during simulation are given.

Table 3.12 Summary Sheet of Main Tsunami Parameters at selected gauges for Source YAN

Name of gauge pt.	Depth of gauge pt.	XCoord	YCoord	Arrival time of initial wave	Arrival time of max.wave	Max(+) wave amp.	Max (-) wave amp.
	m	deg.	deg.	min	min	m	m
Tekirdag1	8.4	27.5068	40.9643	31	103	0.7	-1.1
Mudanya	7.6	28.9089	40.3675	1	87	0.9	-1.2
Izmit3	7.8	29.8707	40.754	24	97	1.2	-1.1
Tuzla4	9.9	29.2828	40.8504	0.0	26	2.4	-2.0
Hpasa1	9.8	29.0787	40.954	0.0	31	2.3	-2.6
Zburnu2	8.9	28.9016	40.9771	1	11	1.9	-3.3
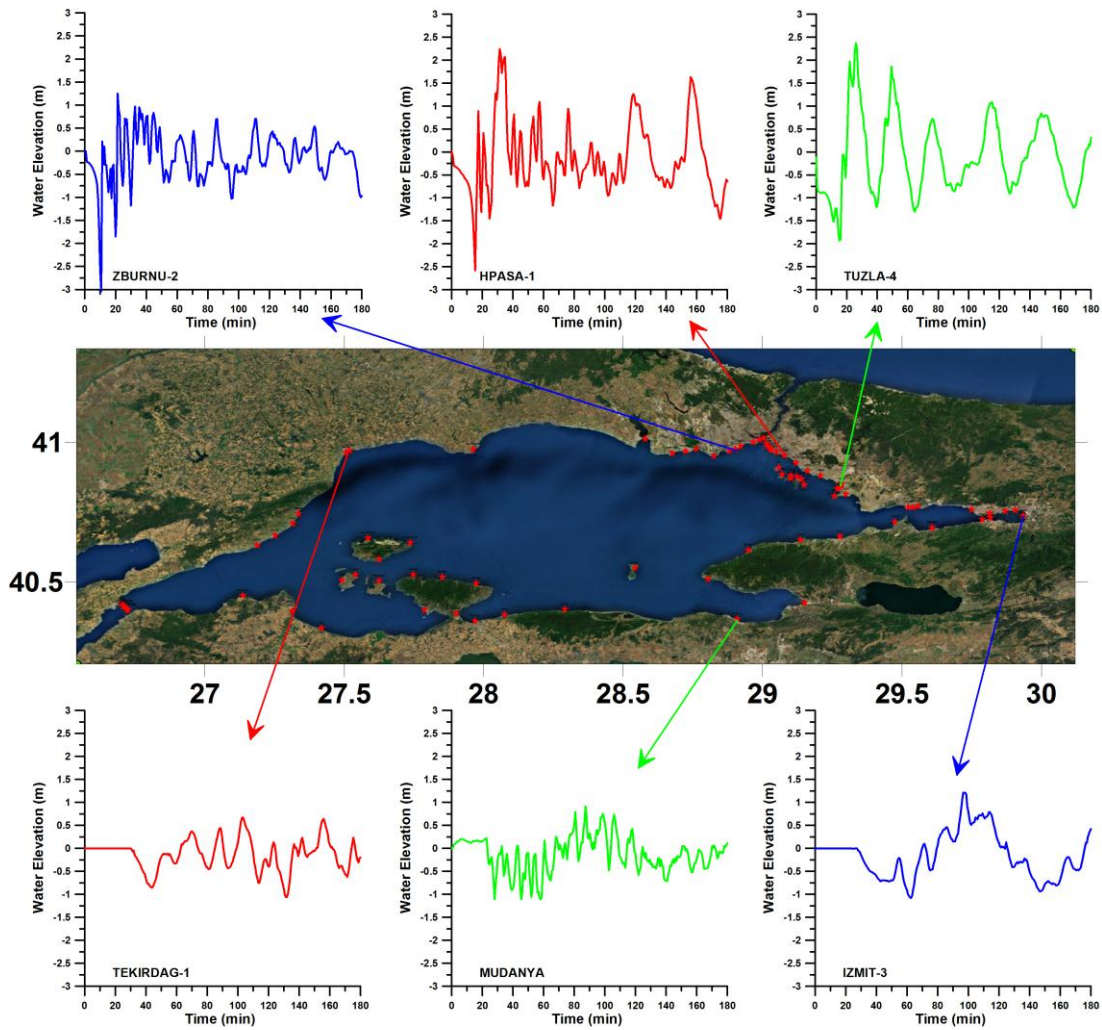
Figure 3.26 Locations of Selected Gauges and Time Histories of Water surface Fluctuations for Source YAN

As can be seen in Figure 3.25 and Figure 3.26, Table 3.12, first wave arrives to Istanbul coasts immediately with an amplitude of 0.5m, and maximum positive wave amplitude reaches up to 2.5m in Tuzla and Haydarpasa. In Zeytinburnu maximum negative wave amplitude is the highest with -3m.

On the other hand, unlike other sources, source YAN has a noteworthy impact on Izmit Gulf.

Maximum positive wave occurred at Izmit Gulf is more than 1m and maximum negative wave amplitude is -1m. These values are same also same for Mudanya and Tekirdag. It can be inferred from these results that scenario YAN is critical for entire Marmara Sea Region.

3.2.2.6   Simulation of Source CMN

In the simulation of source CMN, as the worst case scenario, it is assumed that entire fault has been ruptured, i.e. all 5 segments which are normal faults are broken (Figure 3.27). In addition to rupture parameters, the initial maximum and minimum wave amplitudes produced by 5 segments are given in Table 4.13 for rupture of source CMN

Table 3.13 Estimated Rupture Parameters and Initial Wave Amplitudes for Tsunami Source CMN (OYO-IMM, 2007)

Lat	Lon	depth	strike	dip	rake	length	width	Vertical Disp.	Initial Wave Amplitude (m)	
deg	deg	m	deg	deg	deg	m	m	m	Max (+)	Min (-)
28.19394	40.61261	1924	276.59	70.00	270.00	9505	17027	5.00	0.74	-2.02
28.08215	40.62063	1922	279.18	70.00	270.00	7069	17027	5.00	0.64	-1.81
27.99943	40.62938	1917	299.07	70.00	270.00	10705	17027	5.00	0.78	-2.10
27.88744	40.67421	1598	283.92	70.00	270.00	7850	17027	5.00	0.75	-2.04
27.79683	40.68952	1637	291.38	70.00	270.00	7269	17027	5.00	0.71	-1.97

Figure 3.27 Tsunami Source CMN

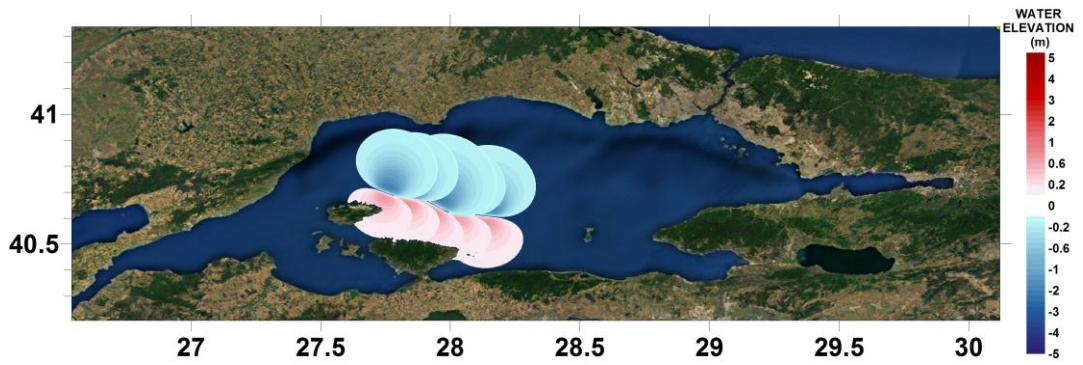The sea states at t=10, 30, 60, 90 min are given in Figure 3.29 for source CMN. In addition to these, distribution of maximum positive and maximum negative tsunami wave amplitudes in the study domain throughout the simulation time (3 hour) are given in Figure 3.30. Their values are +10.7m and -10.3 m respectively (Figure 3.30)
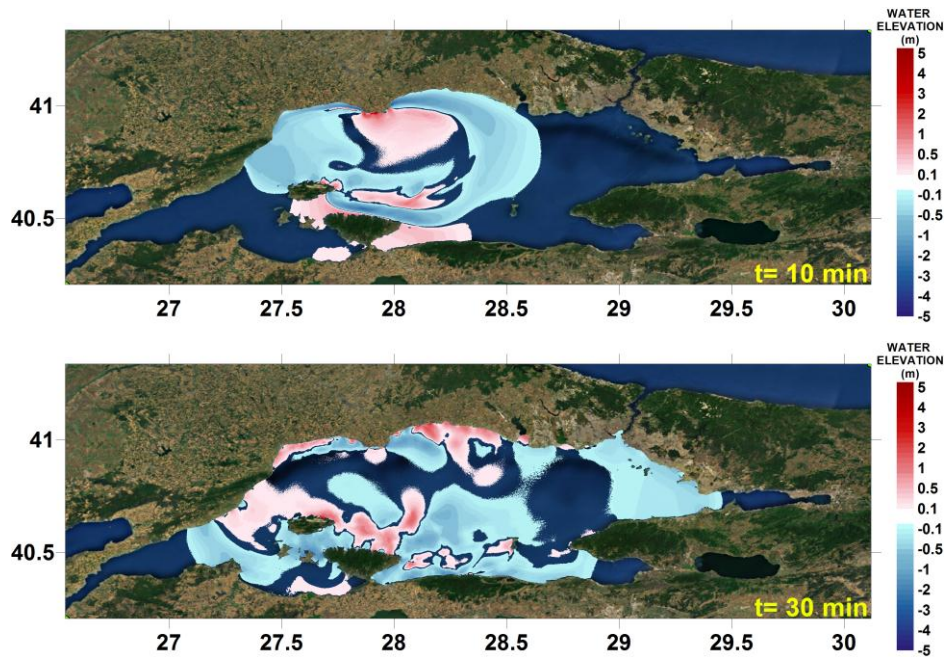

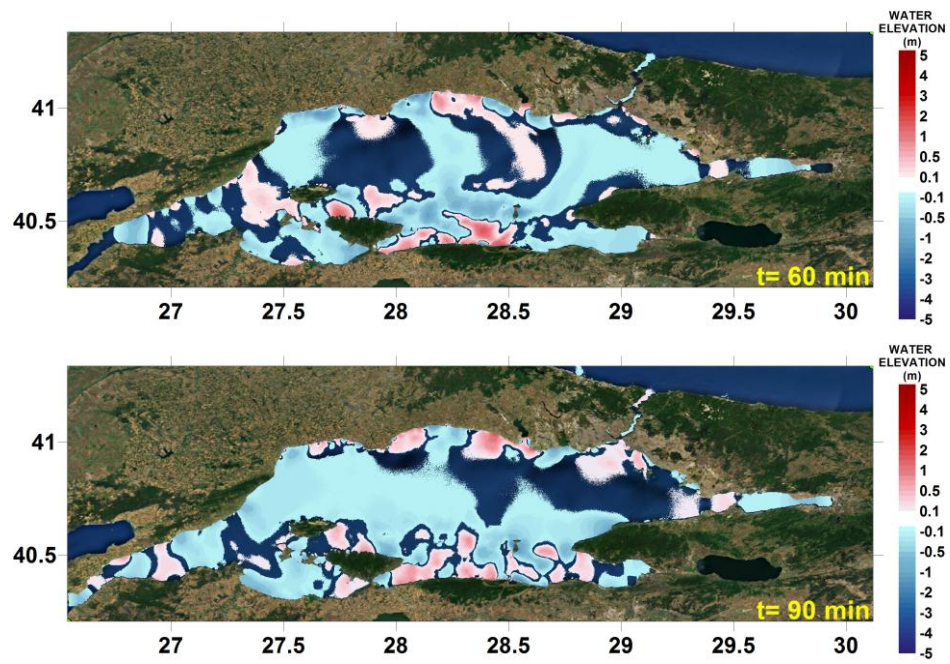**Figure 3.28 Sea states at t=10, 30, 60, and 90 min respectively**

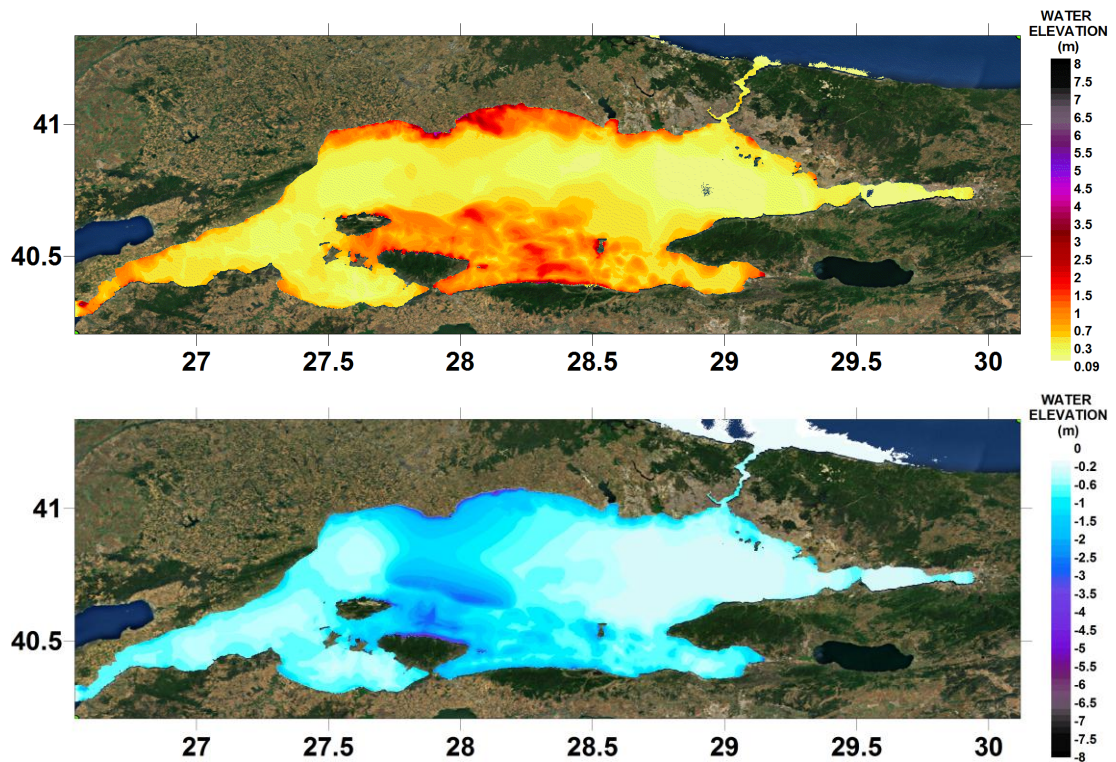**Figure 3.29 (Cont'd) Sea states at t=10, 30, 60, and 90 min respectively**

Figure 3.30 Maximum (+) wave amplitude (top) and minimum (-) wave amplitude

In Table 3.14 summary sheet of selected gauge points is given. Additionally, in Figure 3.31 selected gauge points and water surface fluctuations, arrival times of first and maximum waves, measured at that gauges during simulation are given.

Table 3.14 Summary Sheet of Main Tsunami Parameters at selected gauges for Source CMN

Name of gauge pt.	Depth of gauge pt.	XCoord	YCoord	Arrival time of initial wave	Arrival time of max.wave	Max(+) wave amp.	Max (-) wave amp.
	m	deg.	deg.	min	min	m	m
Tekirdag1	8.4	27.5068	40.9643	31	103	0.7	-1.1
Mudanya	7.6	28.9089	40.3675	1	87	0.9	-1.2
Izmit3	7.8	29.8707	40.7540	24	97	1.2	-1.1
Tuzla4	9.9	29.2828	40.8504	0.0	26	2.4	-2.0
Hpasa1	9.8	29.0787	40.9540	0.0	31	2.3	-2.6
Zburnu2	8.9	28.9016	40.9771	1	11	1.9	-3.3
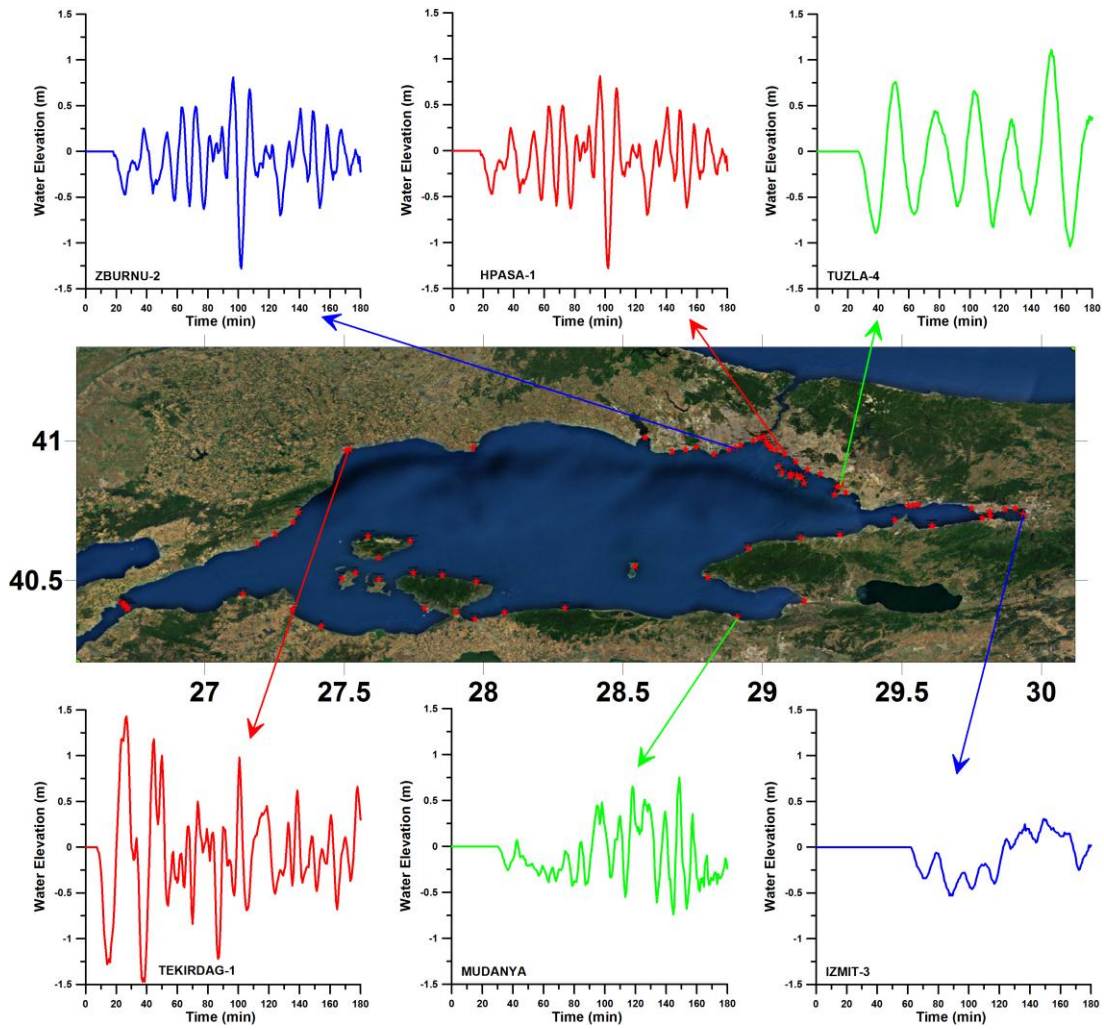
Figure 3.31 Locations of Selected Gauges and Time Histories of Water surface Fluctuations for Source CMN

Tsunami source CMN, like tsunami source YAN, has major importance for Marmara Sea Region. As can be seen in Figure 3.30 and Figure 3.31, maximum positive exceed 1m and maximum negative wave amplitudes -1m at most of the Marmara Sea coasts. In Tekirdag their values arrive at 1.5m and -1.5 respectively.

However, extent of source CMN does not reach significant amounts for Izmit Gulf. However, wave agitation and resonance oscillations may be observed.

3.3 Effect of Fault Rupture Velocity

Rupture velocity is the speed at which a rupture front moves across the surface of the fault during an earthquake.

In this research, the rupture velocities of faults used in tsunami simulations assumed as 1 km/s, which can be considered as slow rupture. In order to observe the effect of rupture velocity on tsunami inundation, scenario PIN is re-simulated with a rupture velocity of 5 km/s. When the results of two cases are compared, it is seen that flow-depths on-land and the tsunami inundation distances are almost the same. Then it can be concluded that, for this study, rupture velocity has negligible influence on tsunami inundation values.

CHAPTER 4

WEB-BASED GIS TSUNAMI INUNDATION MAPPING FOR MARMARA SEA REGION

This chapter focuses on the data used in the preparation of the tsunami inundation mapping, the data formats and characteristics. This chapter also includes the details about monitoring system used in the study domain and the existing operations.

4.1 Data Production and Processing

4.1.1 Data Production

During preparation of an inundation map, the necessary data are; the maximum positive and negative tsunami wave amplitudes, maximum flow depths on land occurred at each grid node throughout the simulation. Additionally propagation time of first wave and summary of results at numerical gauge points which are important also obtained as a result of this study. In Figure 4.1, the mentioned tsunami parameters are shown to clarify definitions.
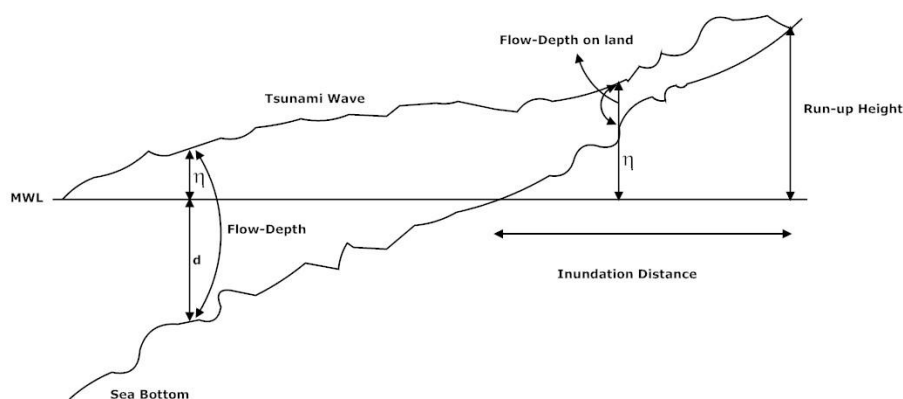

Figure 4.1 Sectional View of a Coastal Area and Main Tsunami Parameters

Tsunami modeling software NAMI DANCE, used in this study, produces all the above mentioned outputs that can be employed to interpret and understand simulation results which further be used to prepare inundation maps. The abbreviations given to these output files and their output data formats are given in Table 4.1.

Table 4.1 Outputs Obtained from NAMI DANCE

OUTPUT FILE	ABBREVIATIONS	FILE FORMAT
Maximum (+) Wave Amplitude	OUT-ZMAX	ASCII GRD
Maximum (-) Wave Amplitude	OUT-ZMIN	ASCII GRD
Maximum Flow Depth on Land	FLOWDEPTHMAXLAND	ASCII GRD
Summary of Results at Gauge Points	OUT-SUMMARY-RESULT	Golden Software Data (.dat)
Propagation Time Curves of First Wave	OUT-TIME-FIRST-WAVE	ASCII GRD

4.1.2 Data Processing

Data processing is an essential procedure because output data gathered from simulations cannot be directly integrated to the GIS environment. Therefore, the data given in Table 4.1 was processed using ArcCatalog 10 and ArcMap 10.

The coordinates of the outputs were in longitudes and latitudes, and they are lack of spatial reference information. Initially, their spatial references were set as GCS_WGS 84 in ArcCatalog.

The grid sizes of output files were same with the input bathymetric map, which is 90m. Each .grd file has 3350 nodes in x-direction and 1058 nodes in y-direction, results in 3.5 million grid nodes in study domain. This quite loaded data cause slow rendering of surfaces both in desktop and web applications. To decrease rendering time, the raster data has to be represented in a series of reduced/increased resolutions. For that reason as a resampling method, pyramids could be built for that particular raster. With pyramids, a lower-resolution copy of the data displays quickly when drawing the entire dataset. Levels with finer resolutions are drawn as zoomed in; performance is maintained because successively smaller areas are being drawn (Figure 4.2). ASCII GRD files, OUT-ZMAX, OUT-ZMIN, and FLOWDETPHMAXLAND were converted into ESRI Grid Raster format in ArcCatalog. With this conversion, pyramids were built for raster data, data size shrank as well as rendering time was decreased.
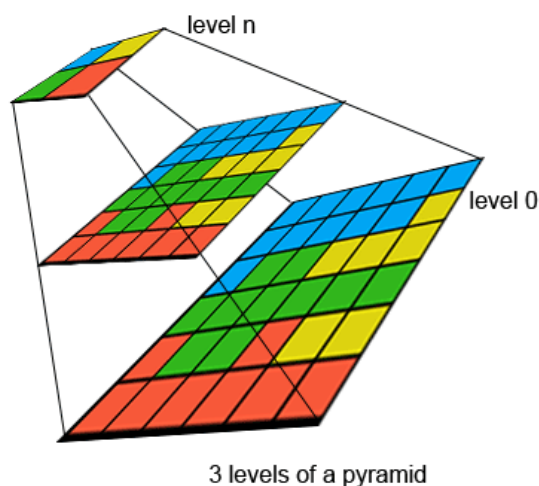
Figure 4.2 Sample Pyramid Structure (ESRI Online Help)

FLOWDEPTHMAXLAND files were added to the system in two different formats. One was in raster format explained above, whereas the other was in shapefile containing point features. Gridded data structure was converted into .dbf file having three columns, each possess x, y and z values respectively. By using this .dbf table, point features were created in ArcCatalog.

OUT-SUMMARY-RESULT file keeps data about arrival time of first and maximum wave, maximum positive and minimum positive wave amplitudes as attributes at gauge points. It was exported to shapefile as point features for each tsunami scenarios. In Figure 4.3, it can be seen an example of an attribute table of OUT-SUMMARY-RESULT file.

Figure 4.3 Out-Summary-Result Table and Its Attributes

OUT-TIME-FIRST-WAVE files store the information about the propagation velocity of initial tsunami wave. The original data format was converted into contour data with 10 minutes interval representing the propagation curves.

As the base map for this study, Esri World Imagery 2D map was used. It includes 15m satellite imagery for the world and high-resolution (1m or better) imagery for the United States, Great Britain, and other metropolitan areas of world including Istanbul and hosted by Esri freely (ArcMap 10 Desktop Help, 2010)

4.1.3 Data Preparation for Arc Server

Before publishing inundation maps as a web service via ArcGIS Server, first they have to be prepared in ArcMAP. In that manner, all input (bathymetry and tsunami sources) and output (such as OUT-ZMAX, OUT-ZMIN) data was mapped in ArcMAP.

A file geodatabase was formed containing all data used (Raster and vector). As a database management system (DBMS), geodatabase provides central data container for spatial data storage and management. It can also be used in server environments allowing to store GIS data in a central location for easy access and management by multiple users.

All source segments used in tsunami scenarios were digitized and their input parameters were entered as attributes of feature class. From Figure 4.4, sources layer and its attributes can be seen. Since in any data analysis, an essential requirement is the ability to be able to see the data being analyzed, for each fault, different color and different line types were selected.
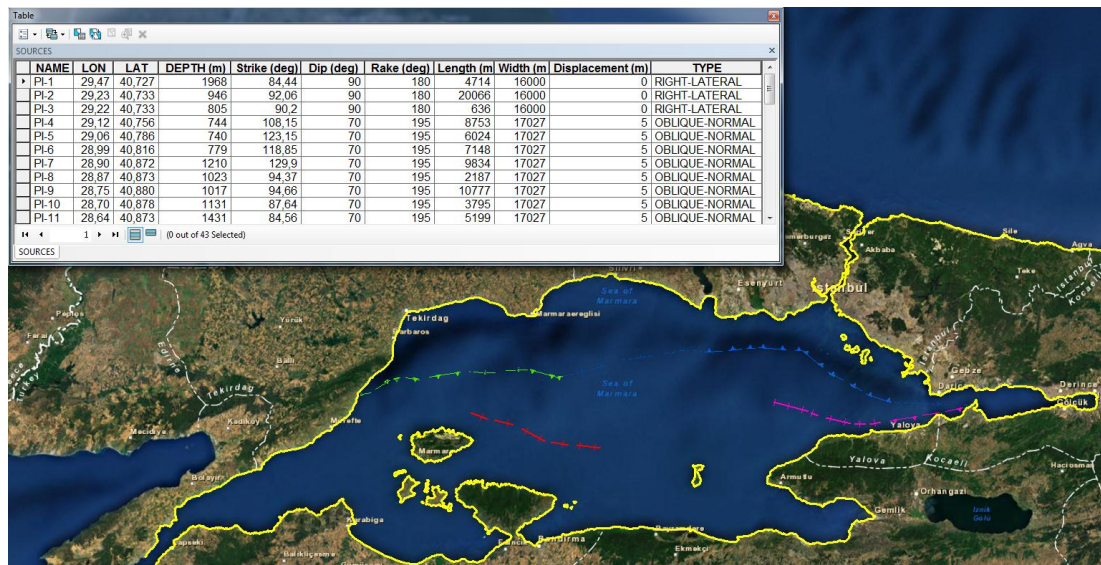
Figure 4.4 Source Layer and Its Attributes

Shoreline data has a paramount importance in inundation mapping studies. If the results are visualized on an online base map, like in this study, the compatibility of shoreline data and base map increases the accuracy of published results. The shoreline data extracted from the bathymetry used and added to geodatabase as polyline features (Figure 4.4– yellow line). As it is seen in Figure 4.4, shoreline data fits on to the base map for most of the area.

To categorize each data set, a data group was formed for each tsunami scenario and each output file was added to the belonging group.

4.2 System Development for Web Application

This section covers the development of inundation maps in ArcMap using processed data of simulation results as a desktop application. This section also includes the process of servicing prepared inundation maps in web environment using ArcGIS Server.

65

4.2.1 System Architecture

The initial point of system development is to select appropriate hardware and software. In this study hardware were selected as in Table .4.2.

Table 4.2 System Properties

System Requirements		System Used
Hardware	2 GB Rams	4 GB Rams
Software	ISS Python 2.6.X Numerical Python 1.3.0	ISS Python 2.6 Numerical Python 1.3.0

As Fu and Sun (2010) mentioned in their book, Web GIS is a type of distributed information system. A Web GIS service basically a client/server architecture. The client may be a Web browser, a desktop application, or a mobile application and the server is a Web application server (Figure 4.5). A user sends a request to connect to the Web server by entering an URL in the browser via Web client. Web server responds back to this request in HTML format by locating corresponding document or script. Finally, the Web client (web browser, mobile, desktop) receives this response and presents it to the user (Figure 4.6). In this study, ArcGIS Server 10 was used as an application map server and Microsoft Internet Information Services (IIS) as web server together performing online mapping operations.
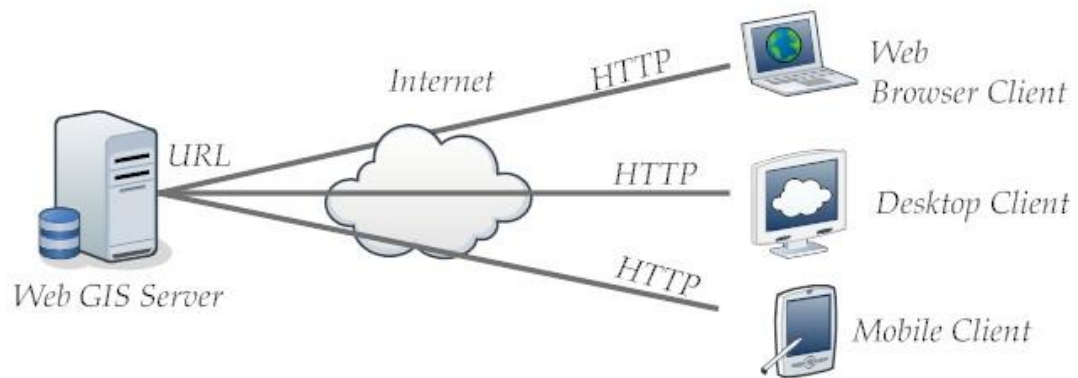
Figure 4.5 Elements of a Web-GIS Application
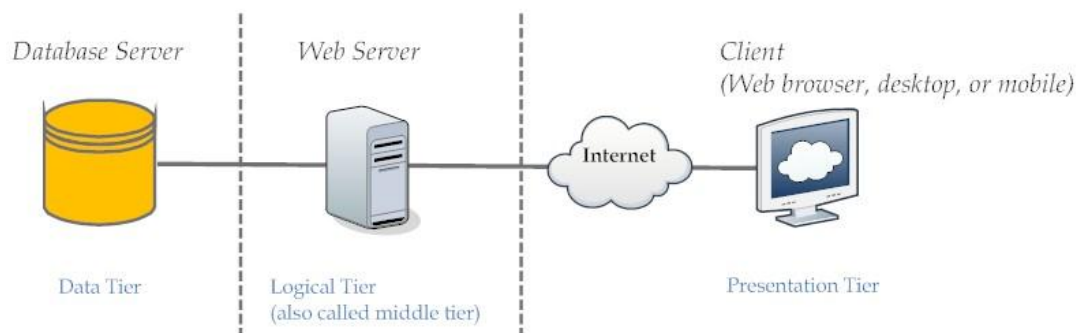
Figure 4.6 Logical Architecture and Workflow of a Basic Web-GIS

ArcGIS Server allows users to share their GIS based desktop applications across the Web. These applications may be maps, address locators, geodatabases and tools.

An ArcGIS Server system is made up of some of the following components:

GIS server—The GIS server hosts GIS resources, such as maps, globes, and address locators, and exposes them as services to client applications.

Web server—The Web server hosts Web applications and services those use the resources running on the GIS server.

Clients—Clients are Web, mobile, and desktop applications that connect to ArcGIS Server Internet services or ArcGIS Server local services.

Data server—The data server contains the GIS resources that have been published as services on the GIS server. These resources can be map documents, address locators, globe documents, geodatabases, and toolboxes.

Manager and ArcCatalog administrators—ArcGIS Server administrators can use either Manager or ArcCatalog to publish their GIS resources as services.

Manager is a Web application that supports publishing GIS resources as services, administering the GIS server, and creating Web applications on the server.

In order to work on map services, .NET, Java, Simple Object Access Protocol (SOAP), and Representational State Transfer (REST) interfaces are provided by Esri. Advanced modifications on map server can be made using these APIs.

4.2.2 Creation of Web Service

ArcGIS Server Manager allows users to create and edit Web mapping applications that showcase the geographic information running on the Web server. The Web application created in Manager can be opened and edited in Visual Studio for further customization. By default, applications are created in C#.

Before a map service is created, first it should have been created as an ArcMap map document (.mxd) that resides in a shared location visible to all Server Object Container (SOC) machines in your GIS server which was

explained. Preparation of .mxd document explained in detail in previous sections of this chapter.

Configuration of the GIS server has been conducted under the system administrator privilege on the server machine. First, operating system tools are granted for access and privilege on the server's output directories for users and administrators (ArcGIS Server Developer Guide, 2004). The SOC account created during postinstallation must also have permissions to read the map document and all the data that the map document references. Screenshot of a started map service in ArcGIS Server Manager is given in Figure 4.7.
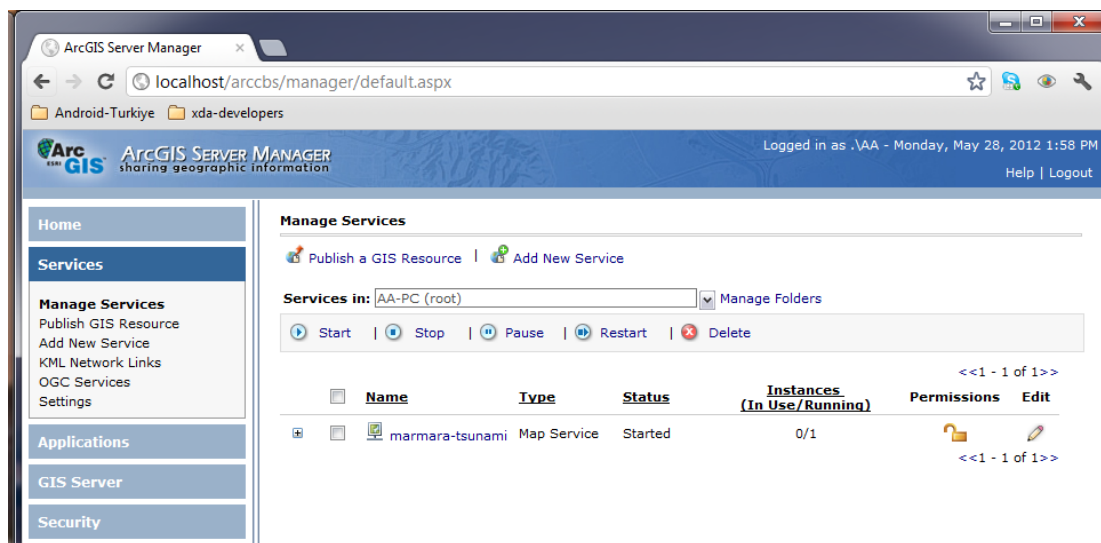
Figure 4.7 Screenshot of ArcGIS Server Manager with a Running Map Service

Once the map service is started, a new web application can be created using that. While creating the web application, the layers wished to be available should be added.

4.2.3 System Components

The visibility of a map is the first thing that attracts the attention of the user. Moreover, the map visually helps user to where those features are and what they represent. Thus, basic map controls are the primary tool to be reflected. Basic mapping operations conducted in this study are operations related with navigation of the GIS map. Since the system is map based, the navigation on the map becomes a necessity. Therefore centering the map to its original position, zooming, and panning operations were added to the web page to make the map usage flexible. The basic mapping tools, their symbols shown on the toolbar, and operations are given in the Table 4.3.

Table 4.3 Navigation Tools and Definitions

Symbol	Name	Operation
	Zoom In	The Zoom In button gets the user a closer area view of your map.
	Zoom Out	The Zoom Out button gets the user a wider area view of your map.
	Pan	The Pan button helps to reposition your map without changing the zoom level.
	Full Extent	Returns the Map to the starting extent of the map
	Back – Forward Extent	Returns the map to the previous zoom levels
	Go to XY	Navigates to desired point in x,y coordinates
	Magnifier	Keeps map display same but show things in greater detail
	Identify	Views attribute values for a feature

Table 4.4 (Cont'd) Navigation Tools and Definitions

Symbol	Name	Operation
	Measure	Allows to measure lines and areas on the map
	Overview	Shows the initial map layers
1:1,873,140 Go	Zoom Level	Changes zoom extent

Identify tool, which is an essential tool for GIS map applications, retrieves the attributes of an object in a vector layer, or a pixel value of a pixel in a raster layer. For the Web-GIS based tsunami inundation mapping applications, tsunami simulation results are crucial information for end-users. To enable the end-users to reach the information such as estimated tsunami source parameters of any fault segment or out summary results at a selected gauge point, identify tool was added to the application to acquire the requested information. When the end-user clicks on the object using identify tool, query first accesses the layer information and then it retrieves all the columns of the attribute table of the object. Use of identify tool on different layers are shown in Figure 4.8.
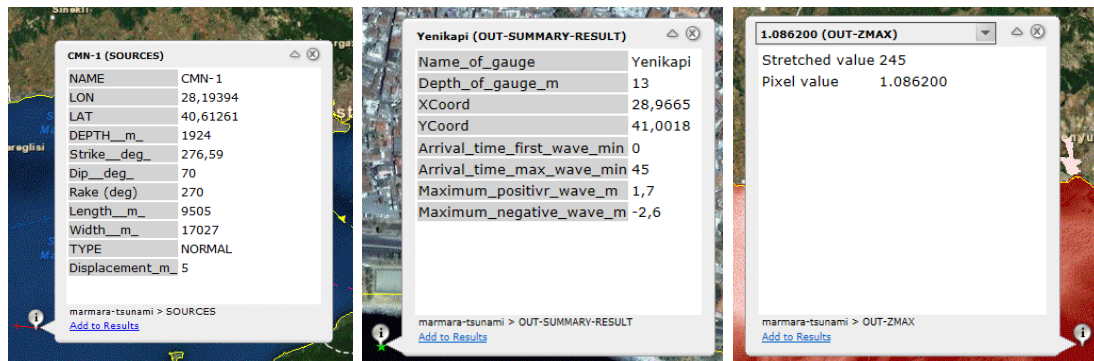
Figure 4.8 Use of Identify Tool

The Measure tool lets user measure lines and areas on the map. Using this smart tool, extent of inundation area can be measured by drawing lines or the inundated area can be measured by drawing polygons. In Figure 4.9 use of measure tool can be seen.
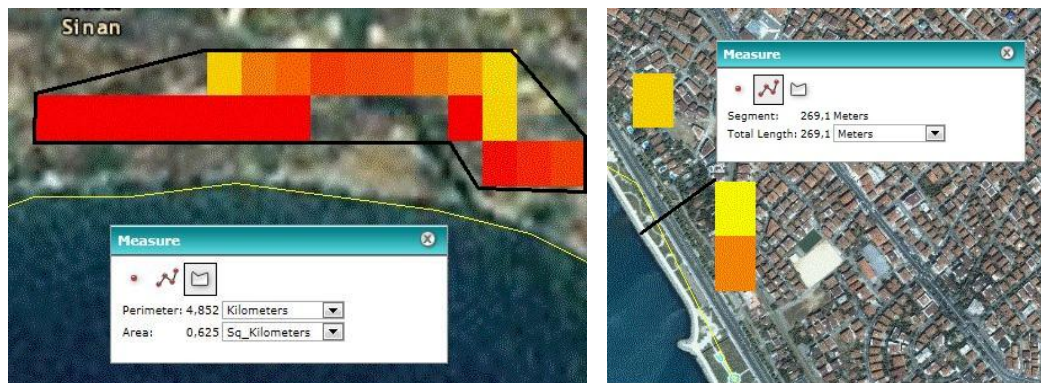
Figure 4.9 Use of Measure Tool

The Search Attributes task allows a user to enter some text that will be used to search the attributes of the layers on the map. This kind of search is similar to the simple Web search that web-sites such as Yahoo!

and Google provide. After searching for something, the user can then select, zoom to, or pan to any features in the list of results

The Print task allows the user to print the map along with any task results they choose. When invoked from the Web application, the task displays a printing dialog box that allows the user to enter a title for their map, set the map size and quality, and choose any task results to print under the map. Clicking the button to create the printed page opens a new browser window with a preview of the printed page. The user can then print to any available printer.

An overview of Web application can be seen in Figure 4.10.
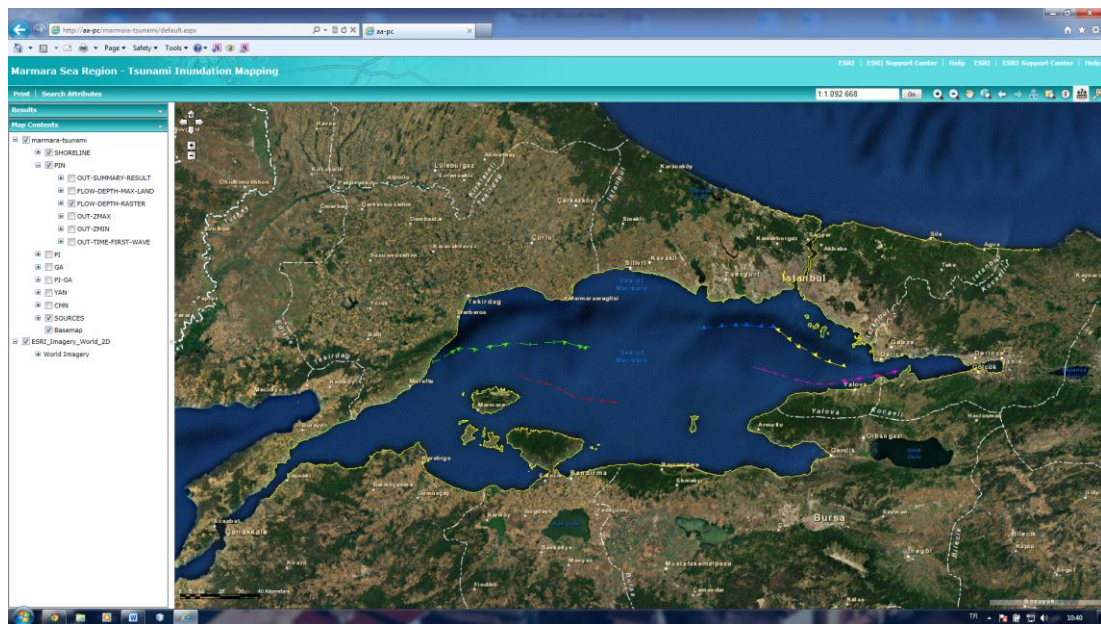
Figure 4.10 General View of Web Page

4.3 The Possible Use Areas of Developed System

This study aimed to establish a user-friendly and widely, easily accessible Web-GIS base inundation map service for Sea of Marmara. This developed service can be both used for public welfare as well as commercial purposes by private sector.

Emergency policy makers can contribute to the data management, updating and publishing procedures as well as decision making process from different places by using this system.

Public people can easily access to this system via their web browsers with an internet connection and see the vulnerable areas regarding different tsunami scenarios. No additional software installation is needed.

Finally, insurance companies can use this system while deciding the amount of insurance of a building against a possible tsunami. For this purpose more detailed analysis can be performed on demand to get the inundation distances more accurately.

CHAPTER 5

CONCLUSIONS and RECOMMENDATIONS

The aim of this research is to build a user-friendly Web-GIS based application on the visualization of tsunami inundation maps. As the case study area, the most important region Marmara Sea Region is chosen due to its economic, cultural and social importance for Turkey. Several tsunami scenarios have been conducted for region, and the results of these simulations discussed first in this chapter. Besides simulation results, properties and capabilities of web application are also reviewed.

In this chapter, main outcomes obtained from this research study and recommendations for the future work are discussed.

5.1 Conclusion on Tsunami Simulations

There is no formal procedure to estimate magnitudes and return periods of tsunami sources, since the knowledge in this area is still emerging. Therefore, in this study a deterministic approach is followed to find the possible maximum extent of tsunami inundations. Following results are obtained from the tsunami simulations for Sea of Marmara;

1. Six different tsunami scenario simulations, namely Prince's Islands (PI), Prince's Islands Normal (PIN), Ganos Fault (GA), Yalova Fault Normal (YAN), Central Marmara Fault Normal (CMN), and Prince's Island and Ganos Fault (PI+GA) were performed,

2. Scenario PIN is the most critical among other scenarios for Istanbul and Yalova. The wave run-up heights are around 8 m for these coasts.

3. It is found that, scenario YAN is critical for entire Marmara Sea Region. It mostly affects Istanbul and Yalova with run-up height values between 6-8 m. Southern coasts of Marmara Sea, Eastern

Kapidag and entrance of Izmit Gulf are also affected by this source. Average run-up values are 2-4 m.

4. GA and PI+GA scenarios are crucial for northwestern and western coasts from Marmara Eregli to Gelibolu. In GA scenario, run-up heights reach up to 6 m around Tekirdag.

5. Scenario CMN affects entire region. Waves with run-up height between 3-5 m occurs at an area from West Istanbul to Tekirdag, Southern coasts, Northern Kapidag and Eastern Marmara Island.

6. Scenario PI is only effective at Prince's Islands and some portion of Istanbul.

7. It is also found out that, Izmit Gulf is protected against possible tsunami waves, only tsunami source YAN creates considerable waves in the gulf.

Run-up and flow depth values occurred at selected locations along Sea of Marmara is given in Table 5.1 and 5.2. These results are parallel with OYO-IMM Report (2007), regarding the difference in displacement values. In this study, fault displacements are taken as almost twice of the displacements estimated in OYO-IMM Report. Since OYO-IMM Report only focuses at Istanbul Coasts, only results obtained for Istanbul Coasts from this research are compared. Consequently, run-up and flow-depth values in Istanbul Coasts calculated as 1.5-2 times of values reported in OYO-IMM as expected.

Table 5.1 Tsunami Flow Depth Values Occurred at Selected Locations along Marmara Sea Region

Area Fault	ISTANBUL COASTS						OTHER MARMARA SEA COASTS				
	Avcilar	Yeşilköy	Yenikapı	Haydarpaşa	Kadıköy	Tuzla	İzmit Gulf	Mudanya	Bandırma	Tekirdağ	Gelibolu
PIN	1.5	2.5	3.9	2.2	5.4	2.7	0.9	0.8	1.2	0.5	0.3
PI	2.2	1.7	1.2	1.1	1.8	1.3	0.4	0.7	0.5	0.2	0.2
PI-GA	1.6	1.7	1.2	1.4	1.9	0.8	0.4	0.7	0.7	2.2	0.2
GA	0.9	1	0.4	0.3	0.7	0.4	0.2	0.5	0.7	2.3	0.2
YAN	1.4	2.5	2.4	3	3.9	3.9	1.7	1.3	2.5	1	0.4
CMN	2	2.1	0.6	1.2	1	1.4	0.6	1	2.4	2	0.3

Table 5.2 Tsunami Run-Up Values Occurred at Selected Locations along Marmara Sea Region

Area Fault	ISTANBUL COASTS						OTHER MARMARA SEA COASTS				
	Avcilar	Yeşilköy	Yenikapı	Haydarpaşa	Kadıköy	Tuzla	İzmit Gulf	Mudanya	Bandırma	Tekirdağ	Gelibolu
PIN	3.8	6.2	7.3	7	7.2	5.4	0.3	2.1	2	1	0.4
PI	2	1.8	2.3	2.4	2.2	1.4	0.2	0.9	0.9	0.4	0.2
PI-GA	2	1.9	1.5	1.3	1.2	1	0.2	0.9	0.8	4.1	2
GA	0.5	0	0	0.3	0.3	0.1	0	0.9	0.9	4.2	2.2
YAN	3.5	5.2	6.1	5.9	5.2	4.1	1.5	3.1	2.5	0	1.8
CMN	1.9	1.7	0.9	0.7	0.5	0.4	0	2.1	2	2.5	1.3

5.2 Conclusions on Web-GIS Application

The main conclusions drawn from this research on Web-GIS application are;

i. Navigation tools enable users to use the map provided by the web page easily. The buttons existing in the navigation panel are the first steps to introduce the GIS map to the end-user thus their contribution to the system is necessary.

ii. Info tool works for all open layers in the web page. When the user clicks on any item on the map it initializes and retrieves the related information of the object. This information is taken from the server and it is taken as tabular form and printed on the screen as information table.

iii. Measure tools enable end-users to measure distances between selected to points, to calculate areas and perimeters of drawn polygons and obtain the coordinates of any point in the map.

Since the application is web based it has some constraints through the stage from server to end user. Before integrating the system on the internet some considerations ought to be taken about the questions such as how many users going to use this application or what details change from one user to another.

5.3 Recommended Future Studies

In this study, six different tsunami scenarios have been studied. In the future, a wider database can be formed by simulating more scenarios. While deciding new scenarios different fault segment combinations, including possible landslide prone slopes may be considered. So, for each fault, one inundation map can be produced by weighted analysis.

Furthermore, more detailed bathymetric data may be produced for vulnerable areas.

Different manning roughness can be selected for sea bottom, land and on-land structures to obtain more accurate geographic extent of tsunami flooding.

Geoprocessing tools may be added to the web application to make risk assessment as the next step by gathering digital building and population data. Therefore, number of buildings, road segments, and amount of population likely to be affected after a probable tsunami can be determined and published via Web.

For future studies, development of mobile application of this study can be considered. In the case of an emergency, the expected extent of tsunami inundation and areas under risk can be forwarded to rescue teams via mobile devices, which may result in a more orderly rescue operation.

REFERENCES

Alpar, B., Gazioglu, C., Altinok, Y., Yucel, Z. Y., & Dengiz, S. (2004). Tsunamı Hazard Assessment In Istanbul Usıng By High Resolution Satellite Data (Ikonos) and Dtm. 4 pages.

Altinok, Y., Alpar, B., Ozer, N., & Akyurt, H. (2011). Revision of the Tsunami Catalogue Affecting Turkish Coasts and Surrounding Regions. *Natural Hazards and Earth System Sciences, 11*, 273-291.

Altinok, Y., Ersoy, S., Yalciner, A. C., Alpar, B., & Kuran, U. (2001). Historical Tsunamis in the Sea of Marmara. *ITS 2001 , Session 4*, pp. 527-534.

Ambraseys, N. N. (2002). The Seismic Activity of the Marmara Sea Region over the Last 2000 Years. *Bulletin of the Seismology Society of America, 92*(1), 1-18.

Armijo, R. N., Pondard, B., Meyer, B., Ucarkus, G., Lepinay, B. m., Malavieille, J., et al. (2005). Submarine Fault Scarps in the Sea of Marmara Pull-Apart (North Anatolian Fault): Implications for Seismic Hazard in Istanbul. *An Electronic Journal of the Earth Sciences, 6*(6), 1-29.

Barka, A. A., & Kandinsky-Cade, K. (1988). Strike-Slip Fault Geometry In Turkey and Its Influence on Earthquake Activity. *Tectonics, 7*(3), 663-684.

Borrero, J. C., Sieh, K., Chlieh, M., & Synolakis, C. E. (2006). Tsunami Inundation Modeling for Western Sumatra. *PNAS, 103*, 19673-19677.

Chang, Y. S., & Park, H. D. (2004). Development of A Web-Based Geographic Information System for The Management of Borehole and Geological Data. *Computer & Geosciences, 6*, 887-897.

Dilmen, D. I. (2009). GIS Based Tsunami Inundation Maps; Case Studies. *MSc Thesis*, 149.

Dragicevic, S. (2004). The potential of Web-based GIS. *Journal of Geographical Systems, 6*, 79-81.

Evans, A. J., Kingston, R., & Carver S. (2004). Democratic Input Into The Nuclear Waste Disposal Problem: The Influence of Geographical Data on Decision Making Examined Through A Web-Based Gis. *Journal of Geographic Systems, 6*, 117-132.

Green, R. W. (2002). Confronting Catastrophe: A GIS Handbook. In R. W. Green, *Confronting Catastrophe: A GIS Handbook.* ESRI Press.

Hebert, H., Schindele, F., Altinok, Y., Alpar, B., & Gazioglu, C. (2005). "Tsunami Hazard in the Marmara Sea (Turkey): a Numerical Approach to Discuss Active Faulting and Impact on the Istanbul Coastal Areas. *Marine Geology, 215*, 23-43.

IMM, O. a. (2007). *Project report on simulation and vulnerability analysis of Tsunamis affecting the Istanbul Coasts.* Istanbul: OYO Int. Co (Japan) for Istanbul Metropolitan Municipality (IMM).

Leone, F., Lavigne, F., Paris, R., Denain, J.-C., & Vinet, F. (2011). A Spatial Analysis of The December 26th, 2004 Tsunami-Induced Damages: Lessons Learned For A Better Risk Assessment Integrating Buildings Vulnerability. *Applied Geography, 31*, 363-375.

Okada, Y. (1985). Surface Deformation Due To Shear and Tensile Faults in a Half-Space. *Bulletin of the Seismology Society of America, 75*(4), 150-173.

Oztin, F., & Bayulke, N. (1990). Historical Earthquakes of Istanbul, Kayseri, Elazig. *Proceedings of the Workshop on Historical Seismicity and Seismotectonics of the Mediterranean Region, Turkish Atomic Energy Authority*, (pp. 150-173).

Parsons, T., Toda, S., Stein, R. S., Barka, A., & Dieterich, J. H. (2000). Heightened odds of large earthquakes near Istanbul: an interaction-based probability calculation. *Science, 288*, 661-665.

Plewe, P. (1997). GIS Online: Information Retrieval, Mapping, and the Internet. Santa Fe, New Mexico: OnWord Press.

Salap, S., Ayca, A., Akyurek, Z., & Yalciner, A. C. (2011). Tsunami Risk Analysis and Disaster Management. *AGILE.*

Shuto, N., Goto, C., & Imamura, F. (1990). Numerical simulation as a means of warning for near field tsunamis. *Coastal Engineering in Japan, 33*(2), 173-193.

Straub, C., Kahle, H. G., & Schindler, C. (1997). GPS and geological estimates of the tectonic activity in the Marmara Sea region, NW Anatolia. *Journal of Geophysical Research, 102*(B12), 27,587-27,601.

Strunz, G., Post, J., Zosseder, K., Wegscheider, S., Mück, M., Reidlinger, T., et al. (2011). Tsunami Risk Assessment in Indonesia. *Natural Hazards and Earth Sciences, 11*, 67-82.

Synolakis, C. E., Borrero, J., & Eisner, R. (2002). Developing Inundation Maps for Southern California. *Coastal Disasters*.

Tang, W., & Selwood, J. (2003). *Connecting Our World: GIS Web Services.* Redlands, California: ESRI Press.

ESRI, http://www.esri.com/software/arcgis/arcgisserver/index.html, Retrieved 24 05, 2012

Japan Tsunami Trace Database,
http://tsunami3.civil.tohoku.ac.jp/tsunami/map/index.php?visibles
etlayers=1,TSUNAMI,konseki_pattern, Retrieved 05 24, 2012

ESRI Onlie Help,
http://edndoc.esri.com/arcsde/9.2/concepts/rasters/basicprinciples
/pyramids.htm, Retrieved 05 28, 2012

User Manual of Numerical Code NAMI DANCE,
http://namidance.ce.metu.edu.tr, Retrieved 05 31, 2012,

Wood, N. J., & Good, J. W. (2003). Vulnerability of Port and Harbor
Communities to Earthquake and Tsunami Hazards. *The use of GIS
in Community Hazard Planning, 32*, 243-269.

Yalciner, A. C., Alpar, B., Altinok, Y., Ozbay, I., & Imamura, F. (2002).
Tsunamis In The Sea Of Marmara. Historical Documents For The
Past, Models For The Future. *Marine Geology, 190*, 445-463.

Yalciner, A. C., Alpar, B., Özbay, I., Altinok, Y., & Imamura, F. (2001).
Tsunami Generation and Coastal Amplification in the Sea of
Marmara. *NATO ARW Underwater Ground Failures on Tsunami
Generation, Modeling Risk and Mitigation, 1*, 138-146.

Yalciner, A. C., Synolakis , C. E., Alpar, B., Borrero, J., Altinok, Y.,
Imamura, F., et al. (2001). Field Surveys and Modeling 1999 İzmit
Tsunami. *International Tsunami Symposium*, *Session 4* , pp. 557-
563. Seattle.

Yalciner, A. C., Synolakis, C. E., Borrero, J., Altinok, Y., Watts, P.,
Imamura, F., et al. (1999). Tsunami Generation in İzmit Bay by
the İzmit Earthquake. *ITU-IAHS International Conference on the
Kocaeli Earthquake 17 August 1999*, (pp. 217-221). İstanbul.

Yang, M. D., Lin, C. C., & Su, T. C. (2007). A Web-GIs Disaster
Management System Applied in Central Taiwan. *2nd International
Conference on Urban Disaster Reduction.* Taiwan.

APPENDIX A

TSUNAMI CATALOGUE FOR TURKEY COASTS

Historical Tsunamis Occurred in Eastern Mediterranean according to the current version of the database contains the data on 134 tsunamigenic events that have occurred on and near the Turkish coasts (Altinok et al, 2011)

Table A.1 Tsunamis Occurred on and Near Turkish Coasts (Altinok, 2011)

1.	1410±100 BC: 1700–1380 BC (54), 1600–1500 BC (56); SA; VA; 36.5_ N–25.5_ E (55); I0: X–XII (55); TI1: 6? (11), Rel: 3. Earthquakes and a tsunami accompanied the eruption of the Santorini volcano. The Minoan Kingdom ceased to exist on the Aegean islands (2, 17, 41, 53, 54, 56).
2.	1365±5 BC: _1365 BC (52), 1356BC (23); EM; ER; 35.68_ N–35.8_ E (23); I : VIII–IX in Ugharit (52, 67); AA: half of the Ugharit burnt (52); Rel: 2. Tsunami at Syrian coast (23).
3.	1300 BC: NA; ER; TI1: 6? (11, 41), 5 (54); Rel: 2. Tsunami along the shore of the Ionian Sea and in Asia Minor, Dardanelles, Troy (2, 11, 17, 41, 56).
4.	590 BC: EM; EA; I: Tyre VII? (52); ML: 6.8 (67); Rel: 2. Tsunami at Tyre and on the Lebanese coast (52, 67).
5.	525 BC: EM; EA; I: Tyre VIII-IX (52); ML: 7.5 (67); Rel: 2. Tsunami at Bisri and on the Lebanese coast (52, 67).
6.	330 BC: NA; ER; 40.1_ N–25.25_ E (55); I0 _IX (53); Rel: 3. An underground shock near the western shore of Lemnos island generated a strong tsunami (2, 11, 17, 41, 53, 54, 55).
7.	227 BC: 222 BC (2, 55), 220/222/227 BC (54); SA; ER; 36.6–28.25 (43); I0:(IX); M: (7.5) (45); AA: Rhodes Cyprus, Corinth (2, 10, 11, 21, 41, 53); TI1: 3 (54); Rel: 3. Tsunami associated with a large shock in Rhodes (43); originated on the northern shore of the islands of Rhodes and Tilos; many ships were destroyed (54).
8.	140 BC: 138 BC (11, 54); EM; ER; 33.0N-35.0E (55); I0: VIII (55); Rel: 2–3. Silifke region in Turkey was affected by the tsunami (2, 55); tsunami between Akka and Sur (21, 23, 54).
9.	92 BC: EM; EA; I: Syria III–IV, Egypt III–IV (52); ML: 7.1 (67); Rel: 2. Tsunami hit Levantine coastal cities, mostly Syrian-Lebanese coast (52, 67).
10.	26 BC: 23 BC (23); EM; ER; 34.75N-32.4E (55); I0: VII (55); TI1:3 (11, 23), TI2:5 (23); Rel: 2. Tsunami at Pelusium-Egypt (23); tsunami at Paphos- Cyprus (2, 11, 17, 55).
11.	20±20: 50 (55); BS; EA; 43.0_ N–41.0_ E (33); I0: VIII (55); M_6.5 (33); h: 20 (33); AA: Colchis Shore, Sukhumi Bay, the submersion of the ancient town of Dioscuria on the coast of the Sukhumi Bay, Colchis, can be inferred both from local legend and from the archeological remains at the sea bottom (8, 33, 65); TI1: 4-5 (33), TI2: 4–6 (65); Wr: _2.5 (33); Rel: 3–4. The waves were more than 2.5m high in Sukhumi and were associated with an M= 6.5 earthquake (8).
12.	46: SA; VA; 36.4_ N–25.4_ E (45); I0: VIII (55); M: (6.5) (45); AA: North east of Crete, Santorini Isl. (2, 11, 17, 41, 53, 55), south coast of Crete (11); eruption of Santorini Volcano (41); TI1: 3 (54); Rel: 3. Tsunami observed in Crete (45).

Table A.1 (Cont'd) Tsunamis Occurred on and Near Turkish Coasts (Altinok, 2011)

13.	62: 66 (41, 53), 53/62/66 (2, 24), 46/62/66 (54); at noon (55); SA; ER; 34.8_ N−25.0_ E (45); I0: IX (55); M: (7.0) (45); AA: Southern coasts of Crete, Lebena (2, 11, 17, 54) and northern coast of Crete (55); TI1: 3 (11, 54); Rel: 4. The sea receded about 1300m (45); the sea in Lebena retreated about 100m from the waterline (54).
14.	68: EM; ER; AA: Demre and Patara region of Lycia (2, 24); Rel: 2. The sea retreated along the coast of Alexandria, Egypt and covered the coast of Lycia; the dark waters of the sea spread sand over Patara (24)
15.	76: 77–78 (21), 76/77 (54); EM; ER; I0: X (55); AA: Larnaka, Paphos, Salamis-Cyprus (2, 10, 11, 17, 55, 56); TI1: 4 (54); Rel: 2. The earthquake was accompanied by tsunami waves seen mostly in Kition, Paphos, Salamis (54).
16.	13 December 115: at night (23); EM; ER/EL; 36.25_ N−36.10_ E (55); I0: (IX) (55); ML: 7.4 (67); AA: Antioch region, Mt. Casius (24, 55); probably triggered by an earthquake generated on the Cyprian Arc fault system (49); Rel: 3. Possible landslide (24); tsunami waves hit Caesaria, the Lebanese coast and Yavne (52, 67).
17.	10 October 123: 120 (54, 55), 10 October 120 (45), 120/128 (24); SM; EA; 40.7_ N−29.1_ E (45, 54); I: IX– XI (24); M: (7.2) (45); AA: Kapidaˇg Peninsula (Cyzicus), Iznik and Izmit (24, 55); TI1: 2 (54); Rel: 3. The sea flooded into the Orhaneli (Rhyndacus) River (6, 24).Tsunami in Izmit (54).
18.	142: 144 (55); 148 (41, 43, 44), 142/144 (24); SA; ER; 36.3_ N−28.6_ E (45); I: Rhodes IX (45); M: 7.6 (45); TI1: 3 (11, 41, 44), 3 (43, 54), TI2: 6 (43); Rel: 3–4. A destructive shock caused a strong tsunami in Rhodes, Fethiye Gulf, Kos, Seriphos, Syme, Caria, Lycia (2, 11, 17, 24, 41, 44, 56); destructive sea inundation (43); the sea water penetrated deep into dry land for several miles (54).
19.	262: 261–262 (2, 56); SA; ER; 36.5_ N−27.8_ E (43); I0: IX (55); AA: South coast of Anatolia (2, 11, 17, 24), west Anatolia (54); TI1: 4? (11), 4 (54); 4 (54); Rel: 2. Sea inundation (43); many cities were flooded by the sea, possibly tsunami (54).
20.	300: 293–306 (2, 24); EM; ER; 35.2_ N−33.9_ E (23); I: IX–XI (24); Rel: 1. Great part of Salamis-Cyprus was plunged into the sea by the earthquake (23, 24).
21.	2 April 303: 303/304 (24), 303–304 (52, 67), 306 (55); EM; ER; 33.8_ N−34.3_ E (52); I0: VIII–IX (52); ML: 7.1 (67), MS: 7.1 (52); h: 20 (52); AA: Sidon, Tyre- Syrian (24, 55); Rel: 2. Tsunami in Caesaria in Palestine (52, 67).
22.	342: EM; ER; (34.75_ N−32.4_ E) (55); I: IX–XI (24); AA: Paphos, Famagusta, Salamis, Larnaka-Cyprus (2, 11, 17, 24, 54, 55, 56); TI1: 3 (54); Rel: 4. The harbour of Paphos slid down into sea (54); the tsunami waves were observed on the SW, S and SE shores of Cyprus and in the Bay of Famagusta (54).
23.	344: NA; EA; 40.3_ N−26.5_ E (GITEC); AA: Canakkale region, Thracian coasts (2, 11, 17, 56); TI1: Dardanelles 3, Thrace coasts 4 (11); Rel: 1.
24.	348: 348/349 (24), 348–349 (52, 67); 349 (55); EM; EA/ER; 33.8_ N−33.5_ E (55); I0: (IX) (55); ML: 7.0 (67); AA: Beirut-Leban (24, 55); Rel: 2. Possible tsunami (52); a tsunami was observed on the Arwad island, the Syrian coast and in Beirut (54).
25.	24 August 358: SM; EL; 40.75_ N−29.96_ E (55); I0: (IX) (55); M: 7.4 (15); AA: Izmit Gulf, Iznik, Istanbul (2, 15, 18, 21, 55, 56); Rel: 4. The damaging waves in Izmit could have been generated by coastal landslides (15).
26.	21 July 365: In the morning (24); SA; ER; 35.2_ N− 23.4_ E (45); I: X–XI (24); Mw: 8.5+ (57); AA: East Mediterranean, Crete, Greece, Adriatic coasts, Alexandria, West Anatolia (2, 10, 11, 17, 24, 26, 41, 44, 53, 55); TI1: Methoni, Epidaurus, Crete 4, Adriatic coasts, Alexandria, Sicily 3+ (11), Epidaurus, Crete 4, Alexandria, Albania, Sicily 4 (41), Crete 6, Epidaurus 4+, Methoni 4, Alexandria 3+ (44); Rel: 4. First the sea was driven back and then huge masses of water flowed back (45); shipwrecks were found 2 km off the coastal line on the southwestern shore of Peloponnessus near Methoni (41, 54); tsunami was observed in Asia Minor; the coast of Sicily was flooded (54).

Table A.1 (Cont'd) Tsunamis Occurred on and Near Turkish Coasts (Altinok, 2011)

27.	11 October 368: SM; EA; (40.4_ N–29.7_ E) (55); I: VIII (45); M: (6.4) (45); AA: Iznik and its surroundings (2, 24, 55); Rel: 1–2. Depending on the description given by Guidoboni et al. (1994), the waters of Lake ˙Iznik rose up.
28.	1 April 407: 5 July 408 (55), 20 April 417 (19); at night (24); SM; ER; I: VII–VIII (24); M: (6.6) (45); AA: Istanbul (2, 24); TI1: 3–4 (54); Rel: 2. Many ships were wrecked, many corpses carried out to the coast of Hebdoman (Bakırk¨oy-Istanbul) (24, 45). The Ottoman archives confirm that many ships sunk because of a tsunami caused by an earthquake (19).
29.	6 November 447: November 447 (11, 17, 56), 8 November 447 (2, 54), 8 December 447 (55), 447 (GITEC); 26 January 447 at night (9, 24, 45); SM; ER; (40.7_ N–28.2_ E) (4); I: IX–XI (24); M: 7.2 (15); AA: Istanbul, Gulf of Izmit, Marmara Islands, Sea of Marmara and Canakkale coasts (2, 9, 15, 24, 45); TI1: 4- (11), Istanbul 3 (11, 41, 44), Erdek Gulf 4, Marmara Islands 4- (44); Rel: 4. The sea cast up dead fish; many islands were submerged; ships were stranded by the retreat of waters (9, 15, 24, 54).
30.	25 September 478: 24/25/26 September 477/480 (2, 24); SM; EA; (40.8_ N–29.0_ E) (55); I0: IX (55); M: 7.3 (15); AA: Sea of Marmara, Yalova, Izmit, Hersek, Canakkale Region, Bozcaada (Tenedos), Istanbul (2, 15, 24, 55); Rel: 4. In Istanbul the sea became very wild, rushed right in, engulfed a part of what had formerly been land, and destroyed several houses (15, 24, 45).
31.	26 September 488: SM; EA; (40.8_ N–29.6_ E) (55); I0: VIII (55); AA: Izmit Gulf (2, 56), Istanbul (55); Rel: 1. It might be identical with 25 September 478 (55).
32.	524: 523–525 (24), 524/525 (2); EM; EA; (37.2_ N– 35.9_ E) (55); I0: (VIII) (55); AA: Southern coasts of Anatolia, Anazarba-Adana (2, 55, 56); Rel: 1.
33.	542: 16 August 542 (24, 45), 6 September 542/543 (54), 16 August 541 (55); winter time (54, 56); SM; I: _VIII (24); M: 6.8 (54), M: (6.5) (45); AA: West coasts of Thrace, Bandırma Gulf (2, 56), Edremit Gulf (2, 11, 17); TI1: 4 (11, 54); Rel: 1.
34.	6 September 543: SM; ER; (40.35_ N–27.8_ E) (55); I0: IX (55); M: (6.6) (45); AA: Kapıdag Peninsula, Erdek, Bandırma (2, 6, 10, 21, 24, 41, 53, 55), Gulf of Edremit (56); TI1: 4 (54); Rel: 3. Tsunami waves were reported (6, 24).
35.	August 545: 543±1 (33), 543 (65); BS; ER; I0: IX (33); M: 7.5±0.5 (33); h: 20±10 (33); AA: Thrace, vicinity of Varna (24, 33); TI1: 5 (33); TI2: 8–10 (65); Wr: _2.0–4.0 (33); Rel: 4. Sea covered the territories of Varna and Balchik (33). In the year 544/545, the sea advanced in the territories of Odessa and Thrace, with a maximum inundation of 6 km on Thrace. Many were drowned in Odessa and Balchik (24). Many people were drowned by the waves along the Bosphorus shores (19). The accompanying earthquake may have been related to the one in Balcik-Bulgaria in 544/545 (8, 9).
36.	January 549: SM; ER; AA: Istanbul; Rel: 2–3. Massive waves were created by the earthquake and a huge fish (porphyrion) was thrown on shore (9, 19).
37.	9 July 551: EM; ER+EL; 34.0_ N–35.5_ E (52); I0: IX – X (52); MS: 7.2 (52); h: 28 (52); AA: Lebanese coast (24, 35, 52, 55); TI1: 5 (23), TI2: 8 (23); Rel: 4. Tsunami along Lebanase coast (24, 35, 52, 55, 67); in Botrys Mt. Lithoprosopon broke off and fell in to the sea, and formed a new harbour (24, 35); the sea retreated for a mile and then was restored to its original bed, many ships were destroyed (24, 35); the sea retreating by 1000 m, tsunami waves destroyed many houses (54). Receding distance was 1800m in Botrys (24, 35).
38.	15 August 553: 15 August 554 (24, 45); at night (24); SM; ER; (40.75_ N–29.10_ E) (55); I0: X (55); M: (7.0) (45); AA: Istanbul, Izmit Gulf (2, 24, 55, 56); Rel: 4. Inundation distance about 3000m (56).

Table A.1 (Cont'd) Tsunamis Occurred on and Near Turkish Coasts (Altinok, 2011)

39.	15 August 554: 554–558 (24), 554 (21, 53, 55), 556 (43), 558 (GITEC), August 556 (45); SA; ER; 36.8_ N– 27.3_ E (43, 45); I: X (45); M: (7.0) (45); AA: The southwest coast of Anatolia, Kos Island, Gulf of Gulluk (2, 10, 11, 17, 24, 41, 44, 45, 55, 56); TI1: 4 (54); Rel: 4. The sea rose up to a fantastic height and engulfed all the buildings near shore in the Island of Kos (43, 45); the sea receded at least 2 km and then flooded a 1-km-wide coastal area; many ships were wrecked; many sea animals and fish perished; waves were possibly observed on the Syrian coast (54).
40.	15 August 555: 15/16 August 555 (2, 18, 53, 56), 11 July 555 (24); SM; EA; AA: Istanbul, Izmit Gulf (2, 18, 21, 53, 56); Rel: 1.
41.	14 December 557: 14/23 December 557 (24) towards midnight (24, 55), 11 October/14 December 558 (54); SM; ER; 40.9_ N–28.8_ E (45, 54); I: IX (45); M: (7.0) (45); AA: Lake Iznik region (9), Gulf of Izmit, Istanbul (2, 21, 24, 55, 56); Many houses and churches were destroyed, particularly in the district Kucukcekmece (Regium, Rhegium or Rhegion) which was an outlying port of Istanbul (45); TI1: 4 (54); Rel: 4. Inundation distance about 5000m (56). Depending on recent archaeological findings this place should be the ancient Theodosian Harbor in Yenikapı, Istanbul.
42.	26 October 740: Early afternoon (24); 08.00 (55); SM; ER; 40.7_ N–28.7_ E (15, 16); I: IX–XI (24); MS: 7.1 (16); AA: Sea of Marmara, Istanbul, Izmit, Iznik, southern coasts of Thrace, Mudanya (2, 9, 10, 11, 15, 17, 24, 26, 41, 55, 56); TI1: 3 (54), 4- (44); Rel: 4. In some places, the sea receded from its shores, without returning to flood the coast (15, 24, 45). The sea retreated behind its usual boundaries and was intense enough to change the frontiers of some cities (9, 15).
43.	18 January 747: 18 January 749 (23, 24, 67), 18 January 743/745/746 (54); in the morning (24), 10:00 (23); EM; EA/EL; 32.50_ N–35.60 (52); I0: (IX) (55); MS: 7.2 (52); h: 25 (52); TI1: 5 (23), TI2: 8 (23); Rel: 4. Waves were observed in Lebanon and Egypt (54); the sea boiled and overflowed and it destroyed most of the cities and villages along the coast (24); surface faulting and liquefaction in Mesopotamia, landslide at Mt. Tabor, many ships sank (52); a village near Mt. Tabor moved 6000m from its orginal position; Moab fortress, then situated on the coast when the flood of the sea struck was uprooted from its foundations and set down 4500m away (24).
44.	19 December 803: 803 (47); EM; AA: Gulf of Iskenderun (2, 17, 56); TI1: 3 (11); Rel: 1.
45.	30 December 859: 8 April 859 (55), 8 April 859– 27 March 860 (24), 30 December 859–29 January 860 (52), November 859/861 (54), 859 (47); EM; EA/EL; 35.7_ N–36.4_ E (52); I0: VIII–IX (52); MS: 7.4 (52); h: 33 (52); AA: Syrian coasts, Adana, Antakya, Samandag, Akka (2, 17, 24, 54); Rel: 4. A landslide on Mt. Casius, rocks fell into the sea (24); a part of Jabal Al-Akraa (Mt. Casius) was split and sank into the sea generating high waves (52); in the region of Samandaˇg the sea receded and then flooded the coast (54).
46.	25 October 989: 26 October 989 (24, 45), evening (24); 19:00 (16); SM; ER; 40.8_ N–28.7_ E (15, 16); I: VIII (24); MS: 7.2 (16); AA: Istanbul, coasts of Sea of Marmara, Gulf of Izmit (2, 18, 21, 24, 56); Rel: 4. The earthquake set up waves in the sea between the provinces of Thrace from Bythinia that reached into Istanbul (9, 15, 18).
47.	5 April 991: in the night (24, 52); EM; EA/EL; 33.7_ N–36.4_ E (52); I0: IX (52); MS: 7.1 (52), ML: 6.5 (67); h: 22 (52); AA: Damascus, Baalbek (24, 52, 55); Rel: 2–3. Landslide; tsunami at Syria (52, 67).
48.	5 December 1033: 17 February 1033 (55), 4 January 1034, 6 March 1032, 1039, May 1035 (54); before sunset (25); EM; EA/ER; 32.4_ N–35.5_ E (23); I0: IX (25); M: 6.9 (54); AA: Israel-Palestinian, Syria, Telaviv, Gaza with 70 000 casualties (25, 55); TI1: 3 (23, 54), TI2: 5 (23); Rel: 4. Tsunami and subsidence, a tsunami on the coast of Palestine, causing the water of Akka to recede at night (23, 25); tsunami at Balash (55); the sea port of Akka went dry for a long time, and then it was half destroyed by a wave (54).
49.	12 March 1036/11 March 1037: EM; EA/ER; AA: Cilicia (?), Southern Turkey; mountains were severely shaken and some landslides (25, 67); Rel: 2–3. There was a strong tsunami in relation to this earthquake (25, 67).

Table A.1 (Cont'd) Tsunamis Occurred on and Near Turkish Coasts (Altinok, 2011)

50.	2 February 1039: January 1039 (11, 17, 56), 2 January/ February 1039 (54), 1 September 1038–31 August 1039 (25); SM; EA; 41.02_ N–28.5_ E (25); AA: Istanbul and other coastal region of the Sea of Marmara (2, 11, 17, 41, 56); TI1: 4 (54); Rel: 1.
51.	23 September 1064: 23 September 1063 (16, 25, 45), 23 September 1065 (54); at night (25); 22:00 (16); SM; ER; 40.8_ N–27.4_ E (16); I0: (IX) (55); MS: 7.4 (16); AA: Iznik, Bandırma, M¨urefte and Istanbul (2, 21, 55, 56); Rel: 1.
52.	29 May 1068: 18 March 1068/1067/1069 (54); 08:30 (23); EM; EA/ER; 32.0_ N–34.83_ E (23); I0: IX (25); M: 7.0 (23); AA: Yavne-South Israel, Jerusalem, coast of Palestine (23, 25, 54); TI1: 4 (54), 5 (23), TI2: 8 (23); Rel: 3–4. Tsunami in Holon, Ashdod and Yavne (23, 54); the sea retreated from the coast of Palestine, and then flowed back, engulfing many people, the banks of the river Euphrates overflowed (25, 54).
53.	20 November 1114: 1114 (54), 10 August 1114 (55), November 1114 (52, 67); EM; ER; 36.5_ N–36.0_ E (54); I0: VIII–IX (52); MS: 7.4 (52); h: 40 (52); AA: Ceyhan, Antakya, Maras¸, Samandag (2, 29, 47, 54, 55);TI1: 3 (54); Rel: 2–3.Landslide (52, 67); tsunami in Palestine (67).
54.	12 August 1157: 15 July 1157 (2, 55); EM; EA; 35.4_ N–36.6_ E (52); I0: IX–X (52); MS: 7.4 (52); h: 15 (52); AA: Hama-Homs, Shaizar region (2, 55),Western Syria including Damascus (52); Rel: 1.
55.	29 June 1170: 03:45 (25); EM; ER; 34.4_ N–35.8_ E (55); I0: X (25); MS: 7.7 (52); h: 35 (52); AA: Trablus, Antakya, Aleppo, Damascus region (52, 55), felt in Cyprus (55); Rel: 2.Tsunami is reported without any location (52, 67).
56.	20 May 1202: 2 June 1201 (47), 21 May 1201 (23), early morning (52), 22 May 1202/1222 (54); EM; EA/ER; 33:43_ N–35.72_ E (25); I0: X (25); MS: 7.6 (52); h: 30 (52); AA: Cyprus, Syrian coasts, Egypt, Nablus, Lebanon (2, 11, 17, 29, 47, 55, 67); TI1: 5 (54), 4 (23), TI2: 7 (23); Rel: 4.Damaging sea wave on Levantine coast (23); the sea withdrew from the coast, ships were hurled onto the eastern coast of Cyprus, fish were thrown onto the shore, and lighthouses were severely damaged (67); Paphos harbour in Cyprus dried (54).
57.	11 May 1222: 25 December 1222, 06:15 (10, 21), May 1222 (2, 10, 11, 17); EM; ER; 34.7_ N–32.8_ E (67); I0: IX (25, 55); M: 7.0–7.5 (67); AA: Baf, Limassol - Cyprus, Nicosia (2, 23, 55, 56, 67); TI1: 3 (23), TI2: 5 (23); Rel: 4.Tsunami flooding in Paphos and Limasol (23); the harbour at Paphos was left completely without water (25, 67).
58.	11 August 1265: 10/11/12 August 1265, at midnight (6); SM; EL; 40.7_ N–27.4_ E (6, 45); I: VIII (13); M:(A big piece of mountain breaks off and tumbles into the sea at Cınarlı, Marmara Island, creating huge waves that hit the shore and swallow up the area (6, 25, 45).
59.	8 August 1303: 8/12 August 1303/1304 (54), August 1304 (44), 8 August 1304 (2, 41, 55); 03:30 (25), at 6 a.m. (43); SA; ER; 35.0_ N–27.0_ E (43); I0: X (25, 43, 55, 67); M: 8.0 (43, 45, 54); AA: Crete, Peloponnesus,Dodecannesse Island, Rhodes, Antalya, Cyprus, Akka, Alexandria – Nile Delta, Lebanon, Palastine,Syria (23, 54, 67); TI1: 4 (54), 5 (43), TI2: 10 (43); Rel: 4.Destructive inundation (43); the sea wave drowned many people and threw European ships on land (45); tsunami (25); landslide, the tsunami struck Crete, the coast of Egypt and part of Palestine, and fewer effects were observed in the Adriatic (67); in Egypt, ships sailing in the middle of the Nile and lying at anchor were thrown up into the banks 15m inland (54).
60.	12 February 1332: 16 January 1332 (9, 19, 51), 12 February 1332/1331 (54), 17 January 1332 (25), 12February 1331 (45); SM; ER; 40.9_ N–28.9_ E (45, 54); I0: VIII (45); M: (6.8) (45, 54); AA: Marmara Sea, Istanbul (2, 9, 11, 17, 54, 56); TI1: 3+ (54); Rel: 3.The waves beat the city walls of Istanbul, seriously damaging many of the dwellings therein (9); huge waves not necessarily of a tsunami but a by the product of the storm in Istanbul (54); a large sea wave covered and destroyed the coastal walls of Byzantium up to their foundation (45).

61.	18 October 1343: 12 February 1331/1332/1334/ 1342/1343/1344 (54), 14 October 1344 (2, 10, 11, 17, 26, 41, 55, 56), 1343.10.18 at 21:00 (16), 16:15 (25, 67); SM; ER; 40.9_ N–28.0_ E (16); I: VIII (45, 67); MS: 7.0 (16); AA: Sea of Marmara, Istanbul, Marmara Ereglisi (Heraclea), Gelibolu (2, 15, 16, 45, 54, 55); TI1: 4 (54); Rel: 4.Huge waves flooded the shore of Thrace at a great distance, for a mile in some place (54). The sea rushed on land and plains, reaching up to 2000 m. In some places it took off some ships at harbour and crushed them (9, 11, 36, 41, 45); the large sea wave caused great destructions in Istanbul and in several other cities of Thrace in the Marmara (45); the sea receded, leaving mud and dead fish on land behind (9, 25, 36, 67); tsunami waves reached the Strait of Istanbul and affected Beylerbeyi (9, 36).
62.	20 March 1389: 12:30 (25); CA; ER; 38.4N-26.3E (45, 54); I0: VIII-IX (25, 67); M: 6.8 (54); AA: Izmir, Chios (2, 5, 10, 11, 17, 41, 44, 53, 55, 56, 67); TI1: 3 (54); Rel: 4.Tsunami penetrated as far as the market place in Chios (25, 45). The waves caused destruction in ˙Izmir and Yeni Foc¸a (54).
63.	16 November 1403: 1402 (21, 26, 55), 16 November 1402/1403 (54), 18 December 1403 (25, 52); EM; ER; I0: (VIII) (55); AA: Aleppo (25, 52), southern coasts of Anatolia, Syrian coasts (2, 11, 17, 54, 56); mountains collapsed (54); TI1: 3 (54); Rel: 4.Near the shore of Syria and Palestine, the sea receded by more than one mile and then returned to its usual limits (54).
64.	20 February 1404: EM; EA+EL; 35.7_ N–36.2_ E (52); I0: VIII–IX (52); MS: 7.4 (52); h: 30 (52); AA: Aleppo (52, 67); Rel: 2–3.Landslide with damage in a few cities and tsunami in the Syrian coast (52).
65.	29 December 1408: 30 December 1408 (47), 1408 (23); EM; EA+EL; 35.8_ N–36.1_ E (52); Imax: X (25);MS: 7.4 (52); h: 25 (52); AA: Western Syria-Cyprus (67); TI1:3 (23), TI2: 5 (23); Rel: 3–4.Landslide in Sfuhen and tsunami in Lattakia (52); tsunami threw the boats onto the shore (25, 67); strong tsunami in Syrian coasts (23); faulting between Sfuhen and Al-Quseir (52); faulting along at least 20 km from Quasr along Dead Sea Fault (25, 67).
66.	18 December 1419: 25 May 1419 (45), 19 December 1419/16 January 1420 (67); SM; ER; 40.9_ N–28.9_ E(45); M: (6.6) (45); AA: Istanbul (45); Rel: 2.The earthquake caused tsunami (45); the sea became very rough and flooded the land, which was unusual (15).
67.	3 May 1481: 06:30 (25); SA; ER; 36.2_ N–28.5_ E (54); I: IX (45); M: 7.2 (45); AA: Rhodes, southwesterncoasts of Anatolia, Crete (2, 25, 56); TI1:3 (54), TI2:8 (43); Wr: 1.8 (11, 41); Rp: 3 (43, 60); Rel: 4.The largest shock accompanied by a sea wave of 3 m height (43, 45, 54, 60); the wave flooded the land and a hip in the harbour was whisked away, the damage done by the tsunami waves was greater than the damage caused by the earthquake (45, 54). In Rhodes the inundation distance was 60m (11, 41).
68.	1489: 1481/1505–1510 (30); SA; ER; AA: Southern coasts of Anatolia, Antalya (2, 56); Rel: 2–3.Submarine earthquake and strong withdrawal (43); the sea receded for three hours in Antalya (30); a tsunamiwas described by Leonardo da Vinci to have occured in 1489 in the sea of Antalya (17, 43)
69.	1 July 1494: Evening time (41, 55); 10:10 (25); SA; ER; 35.5 N–25.5 E (54, 55); Imax: VIII–IX (25); M: 7.2 (54); AA: Heraklion-Crete (2, 11, 17, 25, 44, 55); TI1: 2+ (54); Rel: 4.In the Candia (Heraklion) harbour, large waves caused violent collisions of anchored ships (25, 45, 54); a withdrawal of the sea was observed in Israel (45).
70.	10 September 1509: 22:00 (14, 16); SM; ER; 40.75 N–29.0 E (55); I0: IX (55); MS: 7.2 (16); AA: Istanbul and coasts of the Sea of Marmara (2, 10, 11, 17, 21, 26, 38, 41, 44, 53, 55, 56), felt over a large area from Bolu to Edirne with 4000–5000 casualties (9, 14); TI1: 3+ (44), 3- (54); Rp: 6.0 (38); Rel: 4.The shipyard in Izmit collapsed and waves flooded the dockyard (9, 14, 38); In Istanbul tsunami waves overtopped the walls in Galata and flooded the districts of Yenikapı and Aksaray (2, 9, 38); depending on recentarkeological findings in Yenikapı the inundation distance in this region can be estimated as 500–600m along the paleo-Lycus (Bayrampaş¸a) stream valley.

71.	29 September 1546: 14 January 1546 (23, 54); EM; EA; 32.0 N–35.1 E (23); I: VIII (23); M: 6.0 (23); AA: Nablus, Damascus, Jarusalem, Yafa, Tripoli, Famagusta (52); Israel and Palestine (23); Jerusalem, Damascus, Yafa, Sisem (61); TI1: 3+ (54), 5 (23), TI2: 8(23); Rel: 4.Tsunami at Cyprus (52); tsunami from Yafa to Gaza (23); many people were killed (61); after the storming sea had returned and rolled onto the coast, over 12,000 inhabitants of Gaza and Yafa were drowned (54); tsunami on the coasts of Cyprus and of Asia Minor (54).
72.	717 July 1577: 18:00 (14); SM; ER; AA: Istanbul (2, 14); Rel: 1.Tremors in the sea, causing the sea to swell and engulf the galleys harboured therein (14).
73.	1598: BS; EA; (40.4) N–35.4 E (55); I0: (IX) (55); AA: Amasya, C̦ orum (14); TI1: (4–5) (34), TI2: 2–4(65); Wr: 1.0 (34); Rel: 4.Tsunami waves at the coastal area between Sinop and Samsun 8, 34). The waves inundated about 1.6 km landward drowning a few thousand people living in the towns and villages (14).due to the Amasya and C̦ orum earthquake (2,)
74.	April 1609: SA; ER; 36.4 N–28.4 E (45, 54); I0: IX (43); MS: 7.2 (43); AA: Rhodes, Eastern Mediterranean,SE Aegean Sea (2, 14, 67); TI1: 4 (54), TI2: 8 (43); Rel: 4.Over 10 000 people were drowned by the waves (14); tsunami on the eastern part of Rhodes (54). Very strong waves observed in Rhodes and Dalaman (43, 67).
75.	8 November 1612: SA; ER; 35.5 N–25.5 E (54, 55); I0: VIII (55, 67); MS: 7.0 (67); AA: Northern Crete (2,10, 11, 17, 41, 44, 55, 67); TI1: 5- (54); Rel: 4.Many ships sank in the harbour of Heraklion (45, 54).
76.	28 June 1648: 5 April 1641 (56), 5 April 1646 (2, 9, 54), 1646 (44), 21 June 1648 (14, 45), 28 June 1648, just before sunset (51); afternoon (55); SM; ER; I0: (VIII) (55); M: (6.4) (45); AA: Istanbul (2, 9, 10, 11, 14, 26, 44, 55); TI1: 3 (54), 4- (44); Rel: 4.The sea rushed onto the dry land destroying 136 ships (54, 56).
77.	29 September 1650: 9 October 1650 (11, 17, 45), 29 September 1650 (41, 44); SA; VO; 36.4 N–25.4 (44, 54); I: Santorini VIII; M: (7.0) (45); AA: Santorini, Patmos, Sikinos Islands, Northern Crete (2, 10, 11, 17, 41,44); a strong underground volcanic eruption (45, 54); TI1; Sikinos 4+ (44), Heraklion 4 (41, 44); Wr: Western Patmos 30, Eastern Patmos 27, Ios 18 (11), Eastern Santorini 19, Patmos 30, Ios 18 (41); Rp:50 (GITEC); Rel: 4.Inundation distances 200 and 100min Eastern Santorini and Sikinos, respectively (41). The generated sea wave reached a height of 30m in the west coast of Patmos and 27m in the east coast. In Sikinos, the sea entered 180 m inland. In Kea, ships drifted onto land and in Crete many ships broke from their anchorage (45).
78.	30 November 1667: 30 November 1667/10 July 1668 (54), 10 July 1668 (18, 21, 41, 56), November 1667 (55); CA; 38.4 N–27.1 E (54); I0: (VIII) (55); M: 6.6 (54); AA: Izmir Gulf (2, 11, 14, 17, 54, 55, 56); TI1: 2 (11, 41, 54); Rel: 1. The sea was stormy in Izmir (54).
79.	14 February 1672: April 1672 (53, 55), 1672 (17), 1672/1673 the middle of April (54); NA; ER; 40.0 N–26.0 E (54, 55); I: IX (54); MS: 6.8 (67); AA: NE Aegean Sea, SE Aegean Sea (43, 67), Santorini, Cyclades, Bozcaada and Kos islands (2, 14, 17, 41, 43, 55), Cyclades and Santorini (17); Rel: 2. Some houses in Bozcaada disappeared in waves (54); abnormal waves in Kos Island (43, 67); the island sank, no tsunami (11).
80.	10 July 1688: 11.00 (55), 11.45 (14, GITEC); CA; ER; 38.4 N–26.9 E (54); I0: X (55); M: 7.0 (54); AA: Izmir Gulf (2, 11, 14, 17, 44, 55); TI1: 3 (44), 2 (54); Rel: 2. A weak tsunami was noted in Izmir (54). Ships in the harbour were disturbed (45).
81.	31 January 1741: 01:15 (14, 43, 45); SA; ER; 36.2 N – 28.5 E (43, 45, 54, 67); I: Rhodes VIII (45); M: 7.3 (43, 45, 54); AA: Rhodes (2, 14, 43, 45, 54); TI1: 5 (43), TI2: 8 (43); Rel: 4. The sea retreated then flooded the coast of Rhodes 12 times with great violence (2, 14, 43, 45, 67); the upper tsunami sediment layer found in Dalaman could be attributed to the 1741 tsunami (43, 67).
82.	14 March 1743: 8–20 March 1743 (14, 43); EM; ER; AA: Antalya, Rel: 2–3. Sea withdrawal in Antalya (43, 67); the port dried up for some time (14, 43).

Table A.1 (Cont'd) Tsunamis Occurred on and Near Turkish Coasts (Altinok, 2011)

83.	15 August 1751: SM; ER; AA: Istanbul (2, 14); Rel: 1–2. An earthquake during a thunderstorm; ensuing flood caused considerable damage, carrying away 15 houses; might have been a minor submarine event causing abnormal waves (14).
84.	21 July 1752: EM; ER; (35.6 N–35.75 E) (55); I: X (23); ML: 7.0 (67); AA: Syrian coast (54); TI1: 3? (54), 2 (23), TI2: 3 (23); Rel: 3. Tsunami at Syrian coasts (2, 11, 17, 21, 23, 52, 55, 67); harbour constructions in Syria suffered, possibly from the attack of tsunami waves (54).
85.	2 September 1754: 21:45 (55), 21:30 (16); SM; ER; 40.8 N–29.2 E (15, 16); I0: IX (55); MS: 6.8 (16); AA: Izmit Gulf and Istanbul (2, 14, 15, 55); Rel: 2–3. In places the sea receded from the shore, presumably in Istanbul (15).
86.	30 October 1759: 03:45 (23, 52); EM; EA/EL; 33.1 N–35.6 E (23, 52); I0: VIII–IX (52); MS: 6.6 (23, 52); h: 20 (52); AA: Palestine and Lebanon (54); TI1: 3 (23), TI2: 5 (23); Rp: 2.5 (23); Rel: 4. Landslides at the west of Damascus and Tabariya (52). Tsunami at Akka and Tripoli (23, 52).
87.	25 November 1759: 19:23 (23, 52); EM; EA/EL; 33.7 N–35.9 E (23, 52); I: X (23); MS: 7.4 (23, 52); h: 30 (52); AA: Bekaa-Syria, Antakya (23, 55), faulting along the Bekaa Valley (52); TI1: 4 (23), TI2: 7 (23); Rel: 4. Landslides near Mukhtara and Deir Marjrjos (52); tsunami in Akka (23, 52).
88.	22 May 1766: 05:30 (14, 41, 55), 06:00 (51); SM; ER; 40.8 N–29.0 E (15, 16, 54); I0: IX (55); MS: 7.1 (16); AA: Istanbul and Sea of Marmara (2, 11, 14, 17, 41, 53, 54, 55, 56) causing 4000–5000 casualties and heavy damage extended over a large area from Izmit to Tekirdag (14); TI1: 2 (11, 41, 54); Rel: 4.Tsunami waves were recognized in the coastal village Besiktas-Istanbul and the inner parts of the Straits of Istanbul; uninhabited islets in the Sea of Marmara were said to have half-sunk into the sea. Izmit coasts were badly damaged by sea waves (9, 14, 15); strong waves were particularly effective along the Bosphorus and in the Gulf of Mudanya (14).
89.	24 November 1772: 07:45 (2, 5, 14); CA; ER; 38.8 N – 26.7 E (45); I: Foc̦a (VIII) (45); M: (6.4) (45); AA: Chios Island and Foc̦a (2, 5, 14); Rel: 3. The gates of Foc̦a Castle, which were on the edge of the sea, were completely destroyed by the earthquake and tsunami (14).
90.	13 August 1822: 21:50 (52), 20:00 (28); EM; EA; 36.1 N–36.75 E (52); I0: IX (52); MS: 7.0 (52); h: 18 (52); AA: Antakya, Iskenderun, Kilis and Latakia (28, 55) with 20 000 casualties (52, 55); TI1: 3 (54); Rel: 4. Faulting and tsunami in Beirut (52); tsunami in Beirut, Iskenderun, Cyprus and Jerussalem (54, 67).
91.	23 May 1829: 5 May 1829, 09:00 (45); SM; ER/EA; I: Drama X (45); M: 7.3 (45, 54); AA: AA: Istanbul, Gelibolu (2, 55, 56); TI1: 2 (11, 54); Rel: 1. Tsunami in Istanbul (2, 10, 17, 28, 55, 56); a spurious event (15); two shocks in Istanbul, buildings damaged on the Asiatic coast (28). An unusual roughness in the sea was observed (54).
92.	1 January 1837: 03:00 (28, 55), 16:00 (52); EM; EA/ER; (32.9 N–35.4 E) (55); I0: VIII (52); MS:>7.0 (52); AA: Israel and Syria (23) with 5000 casualties (28, 55); Rel: 3. Tsunami on the coasts of Israel and Syria (23); tsunami in Lake Tabariya (28, 52).
93.	18 October 1843: SA; ER; 36.3 N–27.7 E (45); I0: IX (55); M: 6.5 (44, 54); AA: Chalki and Rhodes Islands, 6000 dead (55); Rel: 3. Chalki, tsunami was observed (54). Ships overturned and a mountain collapsed (45).
94.	25 July 1846: 17:30: CA; ER; AA: Izmir, Aegean Sea (54); TI1: 3? (54); Rel: 1. The sea was very turbulant during fine weather (54).
95.	28 February 1851: 15:00 (43, 45, GITEC), 02:58 (54); SA; ER; 36.4 N–28.7 E (67); I0: IX (55, 67); MS: 7.1 (67); AA: Fethiye, Kaya-Mu¢gla, Rhodes (2, 11, 17, 28, 41, 44, 53, 55, 56, 67); TI1: 3 (11, 41, 54); Rp: 0.6; Rel:4. Tsunami in Fethiye (43, 67); a subsidence on the Fethiye coast and landslides from the Mu¢gla mountainsides (45). The sea in Fethiye rose approximately 34 cm. The shore in Fethiye sunk 0.5m (54); the coast was flooded about 0.6m above the normal sea level at Fethiye (43, 67).

96.	3 April 1851: 3/23 April/May 1851 (54); 17:00 (54); SA; ER; 36.4 N–28.7 E (43, 67); AA: Gulf of Fethiye (2, 11, 17, 41, 56, 67), Rhodes (54); TI1: 3 (54); Rp: 1.8; Rel: 4. Tsunami in Fethiye (43, 67). The sea rose many meters higher than its level and flooded the coast (54). This event was possibly an aftershock of the 1851.02.28 earthquake; the run-up was 1.8m in the Fethiye region (43, 67).
97.	23 May 1851: 23 April/May 1851 (54); SA; ER; 36.4 N–28.7 E (43, 67); AA: AA: Rhodes, Dodecanese Islands and Chalki (2, 11, 17, 41, 43, 54, 56, 67); possibly an aftershock of the event of 28 February 1851; TI1: 2 (11, 41, 54); Rel: 2. Tsunami waves observed in Rhodes and Chalki, but the reported inundation distances are doubtful (43, 67).
98.	12 May 1852: 5/12 May 1852, 02:00 (54); CA; ES; TI1: 2–3 (54), 3 (11, 41); Rel: 1–2. The day before the earthquake occurred in Izmir (2, 11, 17, 28, 41, 54) the sea receded leaving the sea bottom dry for a distance of many yards (54). Rather strong tsunami at Izmir (28).
99.	8 September 1852: 22:30 (54); CA; AA:Izmir (2, 11, 17, 28, 41, 56), Fethiye Gulf (56); TI1: 3 (54); Rel: 1-2. Rather strong tsunami at Izmir (28); the sea rose, though no slightest breath of wind was to be felt before (54).
100.	13 February 1855: 9/10/13 February 1855 (21, 29), 2 March 1855 (28, 55), 9–13 February 1855 (56); EM; ER; AA: Chios Island (56), Fethiye Gulf (2, 11, 17, 21, 29, 41); Rel: 2. Tsunami waves in Fethiye with doubtful inundation (43, 67). Depending on the definitions given by Karnik (1971), a 32-m-wide coastal strip in Fethiye sank into the sea.
101.	12 October 1856: 00:45 (55), 02:45 (45); CA/SA; ER;(35.5 N–26.0 E) (28, 54); I: Heraklion IX (45); M: 8.2 (45); AA: Crete and Heraklion (45, 54), Rhodes, Crete, Chios, Karpatos (55); TI1: 3+ (54); Rel: 2–3. A tsunami was generated (54).
102.	13 November 1856: 13 December 1856 (56); CA; ER; 38.25 N–26.25 E (55); I0: VIII (5); M: 6.6 (44, 54); AA: Chios Island (2, 5, 11, 17, 28, 41, 44, 45, 53, 54), Rhodes (55); TI1: 3+ (54); Rel: 4. A large tsunami wave was observed (54); the sea rushed on the land and some people were lost in Chios (5, 45).
103.	17 September 1857: 22:00 (28, 54); SM; ER+EL; AA: Istanbul (54); Rel: 1. Houses on the seashore and the cellar of a brewery at Kuruc̦eșme, Bosphorus, were flooded by seawater, a consequence of local land subsidence (54).
104.	21 August 1859: 02:00 (45, 55), 11:55 (28, 54), 11:30 (16); NA; ER; 40.3 N–26.1 E (15, 16); I0: IX (55); MS: 6.8 (15, 16); AA: Gokceada (Imbros) Island (45, 54, 55), felt at Enez, Edirne, Istanbul and Gelibolu (28); TI1:3 (54); Rel: 1–2. Some sailors at sea reported the disappearance of Gokceada for a moment. The sea waves observed at the northern approaches of the Strait of Istanbul could not be related with this event (15).
105.	22 March 1863: 22 April 1863, 20:30 (28, 55), 22 April 1863, 21:30 (45); 22:15 (54); SA; ER; 36.5 N – 28.0 E (28, 54, 55); I: Rhodes X (45); M: 7.8 (45); AA: Rhodes (45, 54); Rel: 2–3. The earthquake gave rise to a terrible storm at the sea which resulted in many accidents, several calamities occurred on the Mersin roadstead, the sea near Tripoli (Lebanon) was furrowed by huge waves at midday of 22 March (54).
106.	19 January 1866: 12:30 (5, 54); CA; ER; 38.25 N – 26.2 E (55); I0: VII (54, 55); M: 6.8 (54); AA: Chiosisland (5, 54); Rel: 2. Intensive boiling of the sea water was noticed approximately in the middle of the Cesme strait, oscillations of the level were observed (54).
107.	31 January 1866: 28/31 January 1866 (54); at night (45); SA; ER; 36.4 N–25.4 E (44, 45); I0: (VIII) (55); M: 6.1 (28); AA: Santorini Island (2, 28, 44, 45, 54, 55); TI1: Santorini 4, Kythera 3, Chios 3 (44); Rel: 1–2. The sea started to hit the coastal houses causing cracks and submersions (45); some other sources indicate that no tsunami occurred (54).
108.	2 February 1866: CA; ER; 38.25 N–26.25 E (28, 55); I0: VIII (55); M: (6.4) (45); AA: Chios Island (2, 11, 17, 21, 28, 55); TI1: 3 (11, 54); Rel: 2. Tsunami in Chios (28, 54, GITEC). This earthquake was preceded by a strong shock on 19 January (45).

109.	7 March 1867: 06:00 (55), 16:00 (28), 18:00 (45, 54); CA; ER; 39.1 N.- 26.6 E (54); I: (X) (45); M: 6.8 (45); AA: Lesvos Island (45, 54, 55), at Mitilini more than 500 casualties (28, 55); TI1: 2 (54); Rel: 4. After the earthquake dead fish were found inside a boat in the Mitilini harbour, the low-lying lands of Mitilini were flooded after the earthquake (45, 54).
110.	3 April 1872: 2 April 1872, 07:45 (55), 07:40 (23); EM; EA; 36.25 N.(36.10) E (55); I0: (IX) (55); MS:7.2 (23, 67), MS:5.9 (52); h: 10 (52); AA: Antakya, Samandag (55), Amik Lake (23); faulting at Baghras, liquefaction (52); TI1: 3 (23), TI2: 6 (23); Rel: 4. Tsunami waves flooded the Samandag (Suaidiya) coast (23).
111.	19 April 1878: 09.00 (55); SM; EA/ER; 40.7 N - 30.2 E (15); I: IX (54); M: 5.9 (15); AA: Izmit (2, 10, 11, 15, 17, 28, 55, 56), Istanbul, Bursa, Sapanca (55); TI1: 3 (11, 54); Rel: 4. In the Gulf of Izmit the shock set up a small tsunami which propagated into the west of the Gulf where the earthquake was also felt on board of ships, causing some concern (15). A rather strong tsunami was supposedly observed in Izmit (54).
112.	3 April 1881: 11:30 (28, 55); CA; ER; 38.3 N - 26.2 E (5); I: Chios IX (5, 45); M: 6.5 (5, 45); AA: Chios Island and C□C esme (5, 55) with 4000 casualties; TI1: 2+ (54); Rel: 3. On 5 April at 03:10 a.m. a strong vertical shock demolished some city walls. The sea became wavy right away and a mass of smoke was seen rising from sea surface. The aftershocks created waves on the sea surface (5).
113.	9 February 1893: 28 January 1893 (21, 55), 9 February 1893/28 January 1893 (54); 18:00 (41, 45, 55), 17:16 (16); NA; ER; 40.5 N-26.2 E (15; 16); I0: IX (55); MS: 6.9 (15, 16); AA: Northern Aegean Sea, Samothrace Island, Thracian coasts, Alexandroupolis (2, 10, 11, 17, 21, 28, 41, 44, 55); TI1: Alexandroupolis 3 (11, 41, 44); Wr: Samothrace 0.9 (11, 41), Alexandroupolis 0.9 (41), Islet Aghistro and Alexandroupolis 1.0 (28, 54); Rp: 1.0, Saros (15); Rel: 4. Tsunami at Thracian coasts (55); the water rose by 1m near Islet Aghistro and entered the land in a distance of 25.30m and 40m in Aghistro and Alexandroupolis, respectively (28, 41, 45, 54); tsunami flooded the coast on Samothrace and the mainland in Thrace about 15 min after the main shock (15).
114.	10 July 1894: 12:24 (16), 12:30 (55), 12:33 (28, GITEC); SM; ER; 40.6 N - 28.7 E (28, 54); I0: (X) (55); MS: 7.3 (16); AA: Istanbul (2, 11, 17, 22, 28, 29, 38, 39, 41, 44, 55), Izmit (15), Karamursel, Adapazari, Prince Islands off the coast of Istanbul (55); 474 casualties in Istanbul (9, 39); TI1: 3 (54); Wr: ≤6.0 (38); Rp: 1.5m in Yesilkoy (San Stefano), 4.5m at the Azapkapi Bridge (9, 15); Rel: 4. Tsunami occurred with a receding distance of 50m and a maximum inundation distance of 200m between Buyukcekmece and Kartal (2, 39).
115.	31 March 1901: BS; EL; 43.4 N-28.5 E (GITEC); I0: X (GITEC); AA: Balchik, Bulgaria (27); Wr: 3.0 (20); Rel: 4. At Balchik boats uplifted (GITEC) and landslide occurred (27). The coastal area (0.2 km2) at Kecikaya District subsided (27). A three-meter-high tsunami washed away the port of Balchik (20).
116.	9 August 1912: 01:29 UTH (4), 01:28 (16); SM; ES; 40.75 N - 27.2 E (EMSC) I: X (12); MS: 7.3 (12, 15, 16, KOERI); h: 16 (4); AA: Sarkoy, Murefte, Istanbul (4), Ganos (15) with 2800 casualties (12); TI1: 3.4; Rp:Yesilkoy 2.7 (4); Rel: 4. A high water occurred within the Bosphorus, demolishing a yacht named "Mahrussa" anchored at Pasabahce (4); the sea receded along the Tekirdag shores (12). The ships anchored offshore Yesilkoy were aground with the recede of the sea after the earthquake and then the sea lifted the fishery boats up to a height of 2.7m (4).
117.	31 March 1928: 00:29:47 (2, 28, 41): CA; EA; (38.2 N - 27.4 E) (EMSC); I0: IX (28); MS: 6.5 (54, KOERI); AA: Izmir (2, 11, 17, 28, 41, 54); TI1: 2 (54); Wr: 0.5 (54); Rel: 2. A weak tsunami (54).
118.	23 April 1933: 05:57:37 (45), 05:58 (54); SA; ER; 36.8 N - 27.3 E (45); I0: IX (28); M: 6.6 (45); h: 50 (28, 54); AA: Kos Island and Nisyros (45, 54); TI1: 2 (54); Rel: 2. An earthquake and tsunami took place (54).

Table A.1 (Cont'd) Tsunamis Occurred on and Near Turkish Coasts (Altinok, 2011)

119. 4 January 1935: 14:41:29UTH (6), 14:41:30.4 (KOERI), 16:41:29 (6); SM; ER+EL; 40.64 N - 27.51E (6); I0: IX (6); MS: 6.4 (6); h: 30 (KOERI); AA: The villages of Marmara Island were totally destroyed; strongly felt in Istanbul, Tekirda.g, Edirne, Izmir and Bursa (6); TI1: 2.3; Rel: 4. The Hayırsız Island collapsed on three sides causing a local tsunami (6).
120. 26 December 1939: 23:57:16 (2); BS; EA; 39.7 N – 39.7 E (2); I: XI (2); MS: 8.0 (2); h: 20 (KOERI); AA: Erzincan (33, 65); TI1: 4 (33), TI2: 3.5 (65); Wr: 1.0 (33); Rel: 4. Fatsa; extraordinary sea disturbances were seen at the time of the Ms = 8.0 Erzincan earthquake (2, 8, 33, 46, 65). The sea receded in Fatsa about 50m and then advanced 20m. In Unye the sea receded about 100m causing some sunken rocks to appear for the first time. The sea also receded in Ordu by about 15m and then returned back. The initial rise of the sea level was recorded at 6 tidal stations (Tuapse, Novorossiyk, Kerch, Feodosia, Yalta, and Sevastopol) on the northern coast of the Black Sea (32).
121. 20 January 1941: 03:37 (23); EM; ER; 35.0 N–34.0 E (28); Imax: IX (28); MS: 5.9 (23); AA: Cyprus and Ammochostos (23); TI1: 2 (23), TI2: 3 (23); Rel: 2. Small tsunami on Palestine coast (23).
122. 6 October 1944: 02:34:48.7 (7); CA; ER; 39.48 N–26.56 E (7); I0: IX (7); MS: 6.8 (7); h: 20 (EMSC); AA: Earthquake in Ayvacık and Edremit Gulf with 30 casualties and 5500 damaged/destroyed houses (7); TI1: 4; Rel: 4. Numerous surface cracks and water gushes reported; coastal neighborhoods of the town of Ayvalık were flooded; inundation distance was 200 m in Ayvalık (7).
123. 9 February 1948: 12:58:13 (2, 41, 43, 45, 67); SA; ER; 35.51 N–27.21 E; I0: IX (67); MS: 7.1 (67); h: 40 (EMSC); AA: Karpathos-Dodecanese (2, 11, 17, 31, 41, 42, 44); TI1: 4 (43, 54), TI2: 7 (43); Rp: 2.5; Rel: 4. Damaging waves in Karpathos (43, 67, GITEC); a destructive tsunami originated and rolled along the eastern shore of the Island of Karpathos (54); tsunami caused damage n the southwest coast of Rhodes (45); the first tsunami wave followed about 5–10 min after the earthquake, many vessels were cast ashore and destroyed (43, 67); the 1948 wave pentrated inland about 250m leaving scores of fish behind to a distance of about 200m from the shore line (43); the first motion of the sea was withdrawal (43, 67); inundation distance of 900m (11, 41, 42); inundation distance of 1000m near Pigadia (45, 54).
124. 23 July 1949: 15:03:30 (42), 15:03:33.2 (KOERI); CA; ER; 38.58 N–26.23 E (5, 45); I0: IX (5, 45); M: 6.7 (5, 45); h: 10 (KOERI); AA: East Aegean Sea, North Chios Island (2, 42, GITEC); TI1: 2 (54); Wr: 0.7/2.0(2, 42); Rel: 4. In Chios, the port sank 0.35 m; the sea attacked the coast of Cesme town, leaving many dead fish behind after it retreated (5).
125. 10 September 1953: 04:06 (54), 04:06:09 (23); EM; ER; 34.76 N–32.41 E; I: X (54); M: 6.2 (40); h: 30 (KOERI); AA: South coasts of Turkey (2, 31) and Paphos (23); TI1: 2–3 (54), 2 (23), TI2: 3 (23); Rel: 3–4.Series of tsunami waves were noted on the Island of Cyprus (54); small tsunami wave along the coast of Paphos (23).
126. 9 July 1956: 03:11:40 (41, 42, 45, 67); SA; ER; 36.69 N–25.92 E (KOERI); I0: IX (67); MS: 7.5 (67); h:10 (KOERI); AA: Greek Archipelago, Amargos, Astypalaea Islands, Fethiye (2, 11, 17, 31, 41, 42, 66); 03:12 and 05:24, event associated with two shocks (54); TI1: Amargos 6 (41), Astypalaea 6 (42); Wr: Amorgos 30 (11), 20–25 (41, 42); 30 (11), Astypalaea 20 (11, 41, 42), Pholegandros 10 (11, 41), Patmos 4, Kalimnos 3.6, Crete 3, Tinos 3 (11), 5 (41), Fethiye 1 (66); Rel: 4.Huge waves flooded the fields in the islands. The sea rose up 1m and a recorded inundation distance of 250m in Fethiye (66); inundation distance at Amargos 80–100m (41, 42); at Astypalaea 400m (41, 42); at Pholegandros 8m (41), at Tinos ≥700m (41).
127. 23 May 1961: 02:45:20 (45), 02:45:22 (KOERI); SA; ER; 36.6 N–28.3 E (EMSC); I: Rhodes (VII) (45); h: 72 (EMSC); AA: Marmaris, Fethiye, Rhodes, Izmir, Aegean Sea (45, 54, 59); TI1: 3 (54); Rel: 2. A weak wave, the color of the water in the Gulf of Izmir changed after the earthquake and it was filled with algae (54); the sea colour turned red in Fethiye and Izmir after the earthquake (59).

Table A.1 (Cont'd) Tsunamis Occurred on and Near Turkish Coasts (Altinok, 2011)

128.	18 September 1963: 16:58:14.8 (2, 37); SM; ER; 40.64 N–29.13 E; I0: VIII (37); MS: 6.3 (2, KOERI); h: 40 (EMSC); AA: Eastern Marmara, Yalova-Cınarcık, Karamursel, Kılıc, Armutlu, Mudanya, Gemlik Gulf (2, 29, 37); Rp: 1.0 (2, 29); Rel: 4. Along the coast of Mudanya a strip of sea shells and molluscs was observed and waves reached a height of 1m (2, 29, 37).
129.	19 February 1968: 22:45:42 (41, 45), 22:57:47 (42); NA; ER; 39.4 N–24.9 E (54); I: Aghios Eustrations IX (45); M: 7.1 (45); AA: North Aegean Sea (2, 17, 31); TI1: 2 (41), 3 (54); Wr: 1.2 in Mirina (41, 45, 54); Rel: 4. A small tsunami originated on the western (54) and southern (45) shore of the Island of Lemnos; the sea penetrated on land by 20m in Moudros and 4m in Kaspakas (45, 54).
130.	3 September 1968: 08:19:52.6 (2); BS; ER; 41.78 N–32.43 E (1); I0: VIII (1); MS: 6.6 (1); h: 4 (1); AA: Bartın and Amasra (1); TI1: 3+ (33), TI2: 3–5 (65); Wr: 3.0 (48); Rel: 4. The Bartın earthquake exhibited the first known seismological evidence of thrust faulting along the southern margin of the Black Sea (1). The coastal hills between Çakraz and Amasra were uplifted. The sea receded 12– 15m in Çakraz and never returned entirely to its original level (29). The sea inundated 100m in Amasra and after 14 min the second wave inundated the shore about 50–60m (62). The reason for this progression was most probably the uplifting around Çakraz (2, 8, 65). The sea rose about 3m in Amasra (48).
131.	6 August 1983: 15:43:51.9 (KOERI); 15:43 (45); NA; ER; 40.0 N–24.7 E (45); I: Aghios Dimitrios VI (45); M: 6.8 (45); h: 10 (EMSC); AA: Lemnos Island (45); TI1: 2+ (54); Rel: 3–4. Tsunami on Lemnos Island (54); light tsunami waves in Mirina of Lemnos (54).
132.	4 January 1991: CA; ER; 37.7 N–26.3 E; AA: Ikaria Island (54); TI1: 2; Rel: 1. Weak local sea waves in Ikaria Island; possibly of meteorological origin (54).
133.	7 May 1991: CA; ER; 37.1N-26.8E; AA: Leros Island (54); TI1: 3; Wr: 0.5; Rel: 1. Sudden and intense rise of the sea level by 0.5 m in Leros Island; possibly of meteorological origin (54).
134.	17 August 1999: 00:01:38.6 (KOERI); SM; EA+EL; 40.73 N–29.88 E; MW: 7.4 (2, 3, 50, 58, 63, 64); h: 18 (2); AA: A very strong earthquake with at least 18850 casualties in the Gulf of Izmit was felt over a very large area (9). The earthquake produced at least 120 km of surface rupture and right lateral offsets as large as 4.2m with an average of 2.7m (3, 9); TI1: 3; Wr: Degirmendere≥12 (3); Rp: Degirmendere 4m (50), Yarımca 3.2m (58), generally between 1–2.5m (2, 3); Rel: 4. The runups are more complex along the south coast due to the presence of coastal landslides (2, 3, 9, 50, 63, 64). The period of tsunami was less than 1 min (63). The inundation distance in Kavaklı was more than 300m(3).